Principles of Optical Emission Spectroscopy and Laser Induced Plasma/Breakdown Spectroscopy

Salvatore Amoruso

Lectures for the course of Atomic and Molecular Physics and Laser Spectroscopy

Basic idea of Optical Emission Spectroscopy (OES)

Atoms and molecules in excited states emit characteristics radiation related to their energy level structure

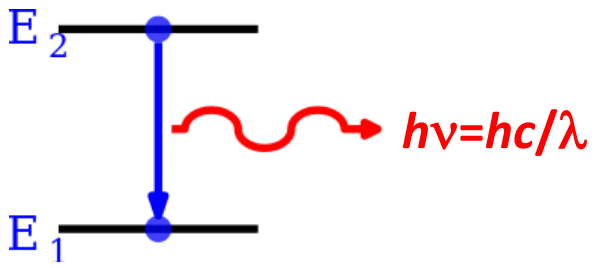

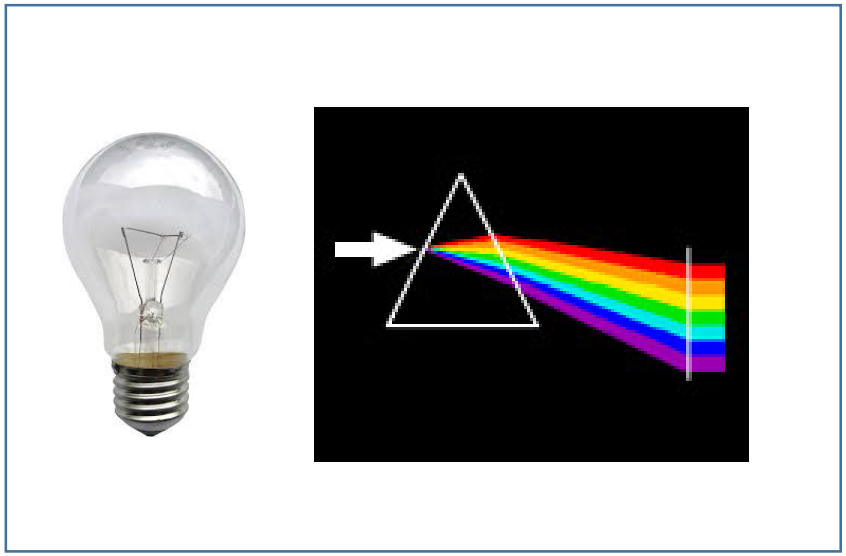

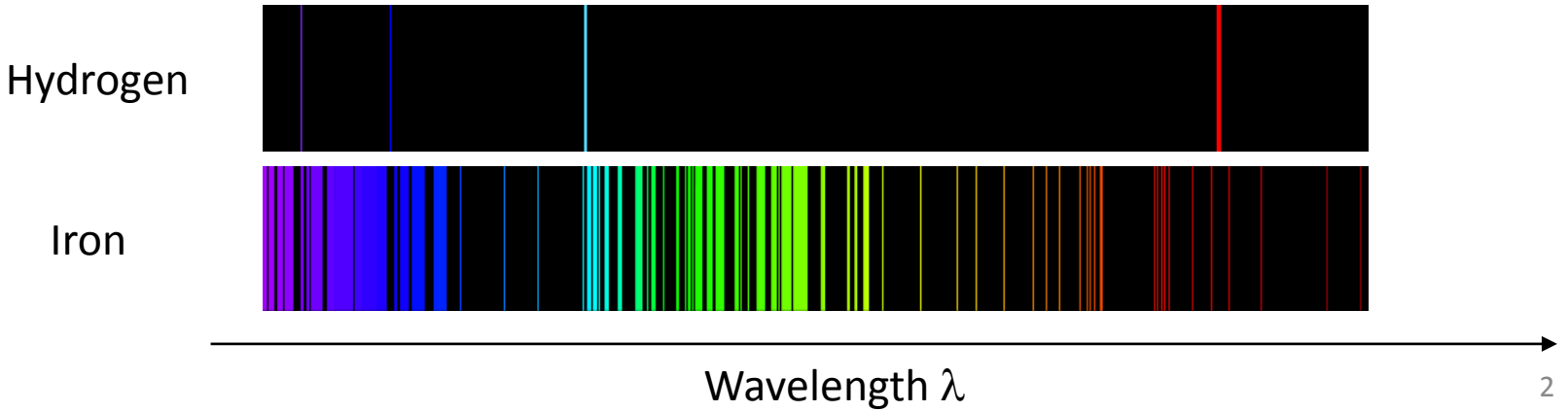

Optical Emission Spectroscopy (OES)

Analysis of the an excited source emission

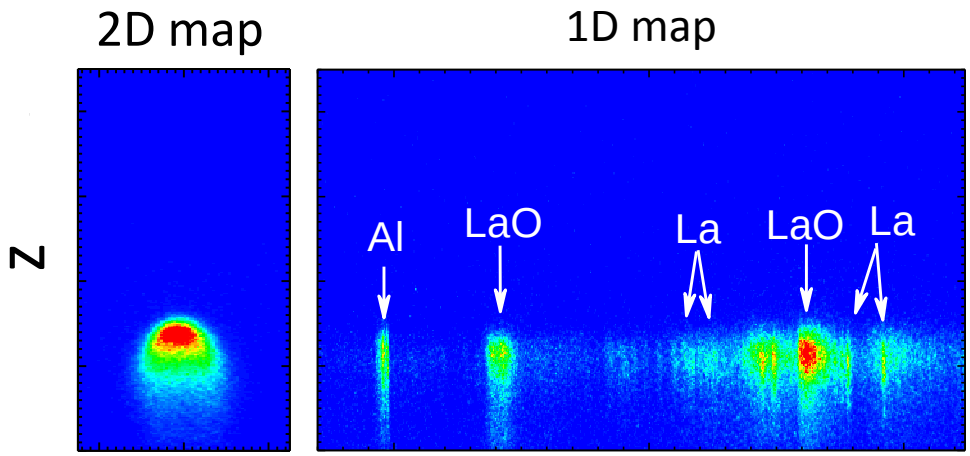

Source composition
(e.g. oxidation, excitation degree, chemical reacctions, etc.)

Species propagation dynamics
(e.g. position, specie dynamics KE, etc.)

Source parameters and evolution
(e.g. Temperature, Electron density,, etc.)

OES can be an effective and useful methods to analyze physical processes and underlying mechanisms through the investigation of atomic and molecular species and their spatial and temporal evolution or to setup diagnostics techniques of applicative interest

Typical transitions in an atom or ion

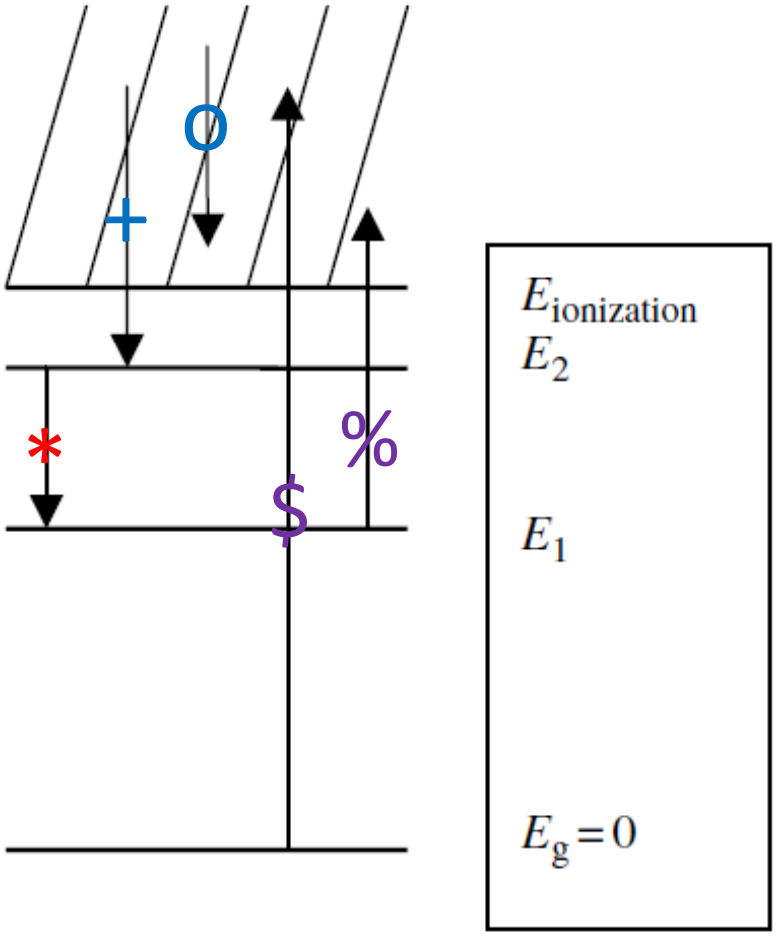

De-excitation and emission of photons

* bound-bound
+ free – bound
o free-free

Ionization
$ from ground state
% from excited state

All these phenomena have characteristic rates and can be related to the level populations and temperature via rate equations

Illustration of a transition between two levels
and corresponding spectral line emission intensity

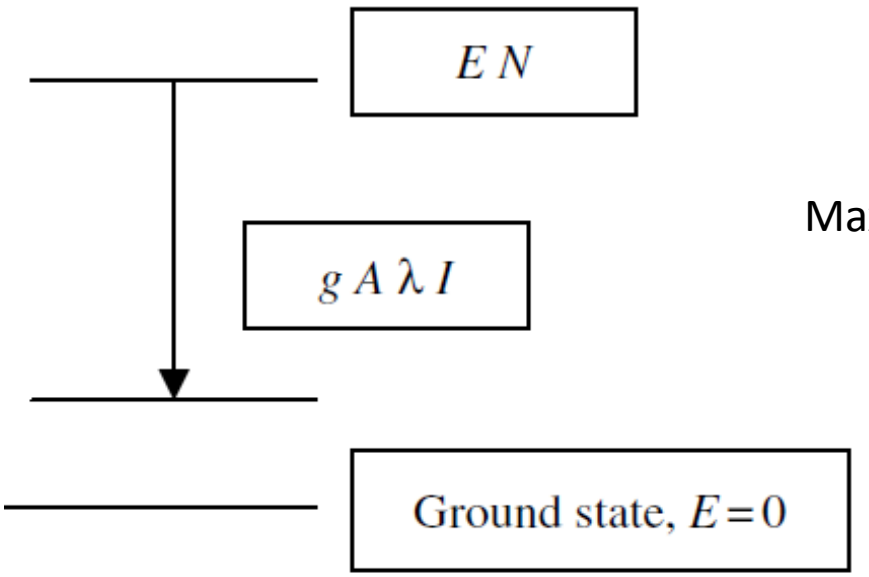

Equilibrium – Boltzmann distribution

the distribution of several quantities (e.g. electron speed, level populations, ..) depend on temperature T

Maxwell velocity distribution function of electrons

$$f_{\mathrm{M}} = (m/2\pi kT)^{3/2} \exp(-mv^2/2kT)$$

Relative populations of levels

$$N_j/N_{\mathrm{o}} = (g_j/Z) \exp(-E_j/kT)$$

$$N_j/N_i = (g_j/g_i) \exp[-(E_j - E_i)/kT]$$

Spectral line radiant intensity *I* (W/sr)

$$I = h\nu\, gA\, N/4\pi = (hcN_{\mathrm{o}}gA/4\pi\, \lambda Z) \exp(-E/kT)$$

Principle of LIPS and LIBS

We need a source, a detection system and methods to analyze the data

Use laser pulses to

- vaporize/ablate a solid sample
- cause breakdown in a gas or a liquid

→ Laser produced plasma

Use a diagnostic system to collect and analyze optical emission

→ Optics and Atomic/Molecular Physics

Elaborate methods to analyze data and gain information on the system under study: composition; temperature; electron density; physics and mechanisms, etc…

It can seem that everything is simple and straightforward
BUT this is not the case

LIBS is still a field of intense research, even if
commercial systems for elemental analysis through LIBS are available on the market

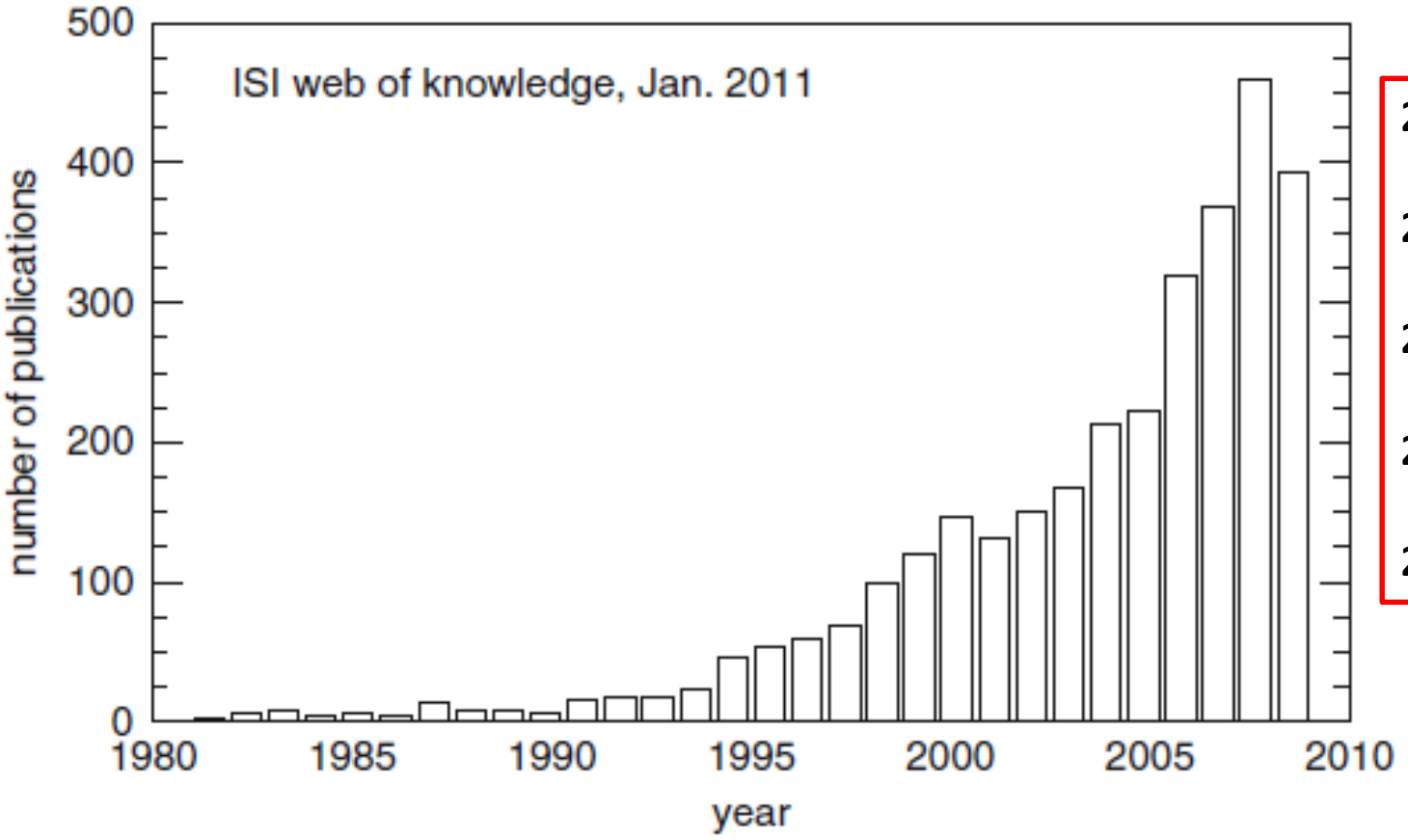

2015*: 334

2014: 988

2013: 752

2012: 599

2011: 499

Fig. 1.1 Number of publications in the field of laser-induced breakdown spectroscopy or LIBS in the years 1980–2010 from a database search in ISI Web of Knowledge

Example of two very recent articles

Analysis of bakery products by laser-induced breakdown spectroscopy.

By: Bilge, Gonca; Boyaci, Ismail Hakki; Eseller, Kemal Efe; Tamer, Ugur; Cakir, Serhat

Food chemistry
Volume: 181 **Pages:** 186-90
DOI: 10.1016/j.foodchem.2015.02.090
Published: 2015-Aug-15 (Epub 2015 Feb 24)

Abstract

In this study, we focused on the detection of Na in bakery products by using laser-induced breakdown spectroscopy (LIBS) as a quick and simple method. LIBS experiments were performed to examine the Na at 589nm to quantify NaCl. A series of standard bread sample pellets containing various concentrations of NaCl (0.025-3.5%) were used to construct the calibration curves and to determine the detection limits of the measurements. Calibration graphs were drawn to indicate functions of NaCl and Na concentrations, which showed good linearity in the range of 0.025-3.5% NaCl and 0.01-1.4% Na concentrations with correlation coefficients (R(2)) values greater than 0.98 and 0.96. The obtained detection limits for NaCl and Na were 175 and 69ppm, respectively. Performed experimental studies showed that LIBS is a convenient method for commercial bakery products to quantify NaCl concentrations as a rapid and in situ technique.

Elemental analysis of materials in an underwater archeological shipwreck using a novel remote laser-induced breakdown spectroscopy system

By: Guirado, S (Guirado, Salvador)[1]; Fortes, FJ (Fortes, Francisco J.)[1]; Laserna, JJ (Javier Laserna, J.)[1]

TALANTA
Volume: 137 **Pages:** 182-188
DOI: 10.1016/j.talanta.2015.01.033
Published: MAY 15 2015
View Journal Information

Abstract

LIBS analysis of submerged materials in an underwater archeological site has been performed for the first time. A fiber-optics-based remote instrument was designed for the recognition and identification of archeological assets in the wreck of the Bucentaure (Bay of Cadiz, South of Spain). The LIBS prototype featured both single-pulse (SP-LIBS) and multi-pulse excitation (MP-LIBS). The use of multi-pulse excitation allowed an increased laser beam energy (up to 95 mJ) transmitted through the optical fiber. This excitation mode results in an improved performance of the equipment in terms of extended range of analysis (to a depth of 50 m) and a broader variety of samples to be analyzed (i.e., rocks, marble, ceramics and concrete). Compared to single-pulse, an intensity

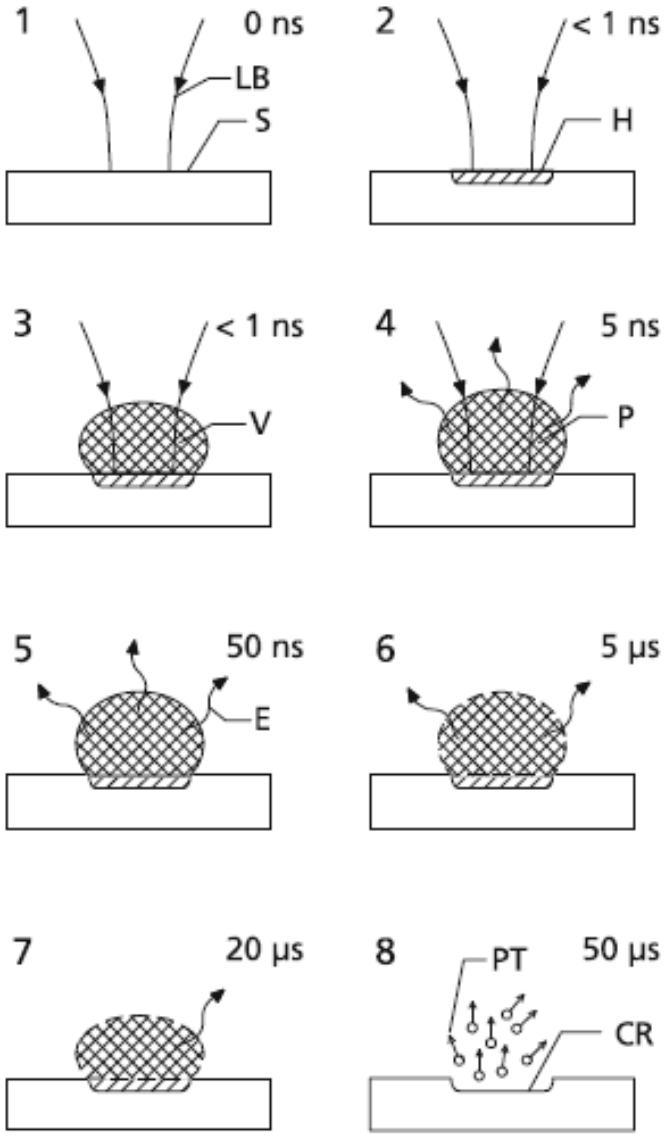

Let's look in more detail!

*The laser interaction with a sample produces a **transient plasma**, therefore one must ascertain if and when thermodynamic equilibrium does exist!*

Typically for fs and ns laser pulse excitation the plasma lifetime lies in a range of 0.1-10 µs due to typical emission lifetimes and electron collisional re-excitation processes

Fig. 2.1 Principle of laser-induced breakdown spectroscopy shown in phases 1–8; LB = incoming laser beam, S = sample, H = region of energy deposition, V = material vapor, P = plasma, E = element-specific emission, CR = crater, PT = particles . The times given depict the temporal evolution after start of irradiation of the laser pulse

What we want to measure?

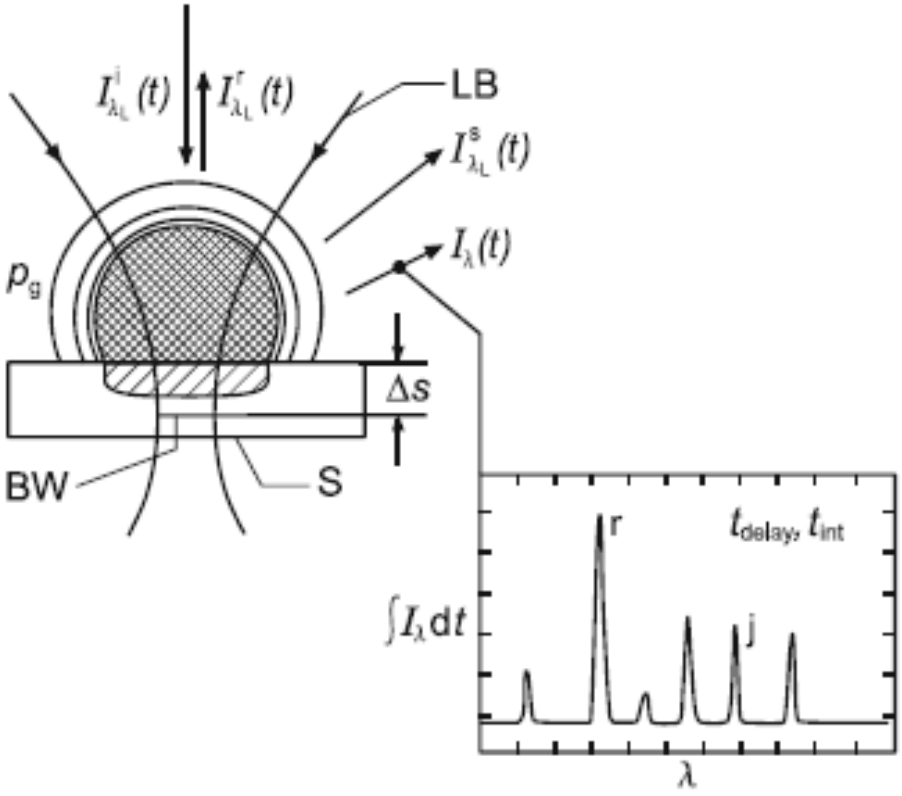

Fig. 2.2 Schematic illustration of some measuring parameters and the emitted spectrum; LB = incident laser beam, S = sample, BW = beam waist, $I^{i}_{\lambda_L}(t)$ = irradiance of the incident laser beam, $I^{r}_{\lambda_L}(t)$ = reflected laser irradiance, $I^{s}_{\lambda_L}(t)$ = scattered laser irradiance, p_g = ambient gas pressure, Δs = beam waist position, j = emission line of an analyte, r = emission line of a reference line, t_{delay} = delay time between the laser pulse and the start of the integration window to record the spectrum, t_{int} = width of the integration window

Plasma emission vs temporal delay with respect to laser pulse

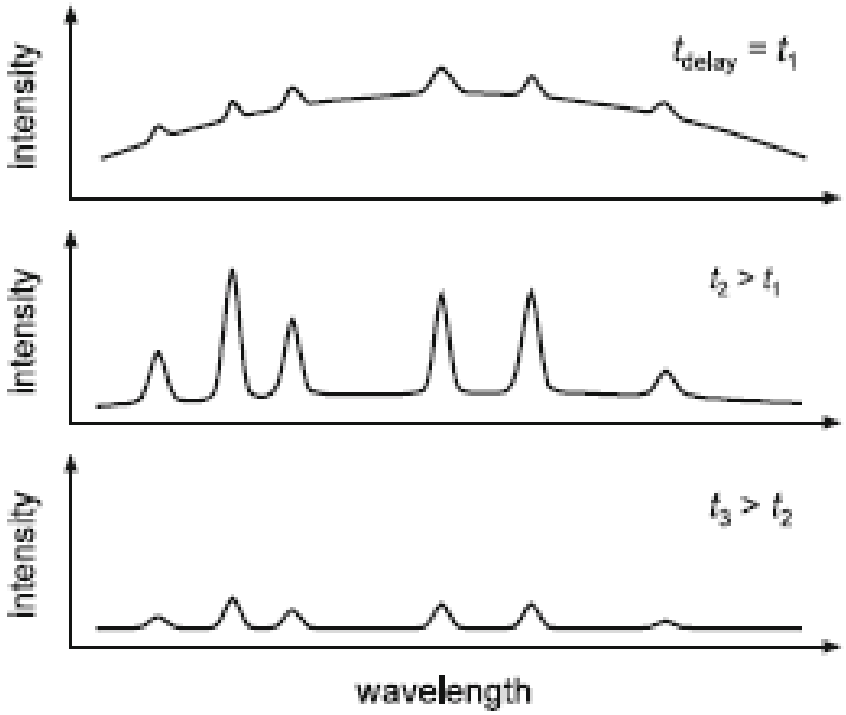

Fig. 2.3 Schematic illustration of the emission spectra of the laser-induced plasma for different time delays with respect to the irradiation of the laser pulse

Early delay: free-free and free-bound transitions
Intense continuum emission

Intermediate delay:mainly bound-bound transitions

Long delay: plasma cooling and reduction of intensity

Appropriate timing for recording the emitted light can optimize the collected signal characteristics

Specific line emission vs temporal delay

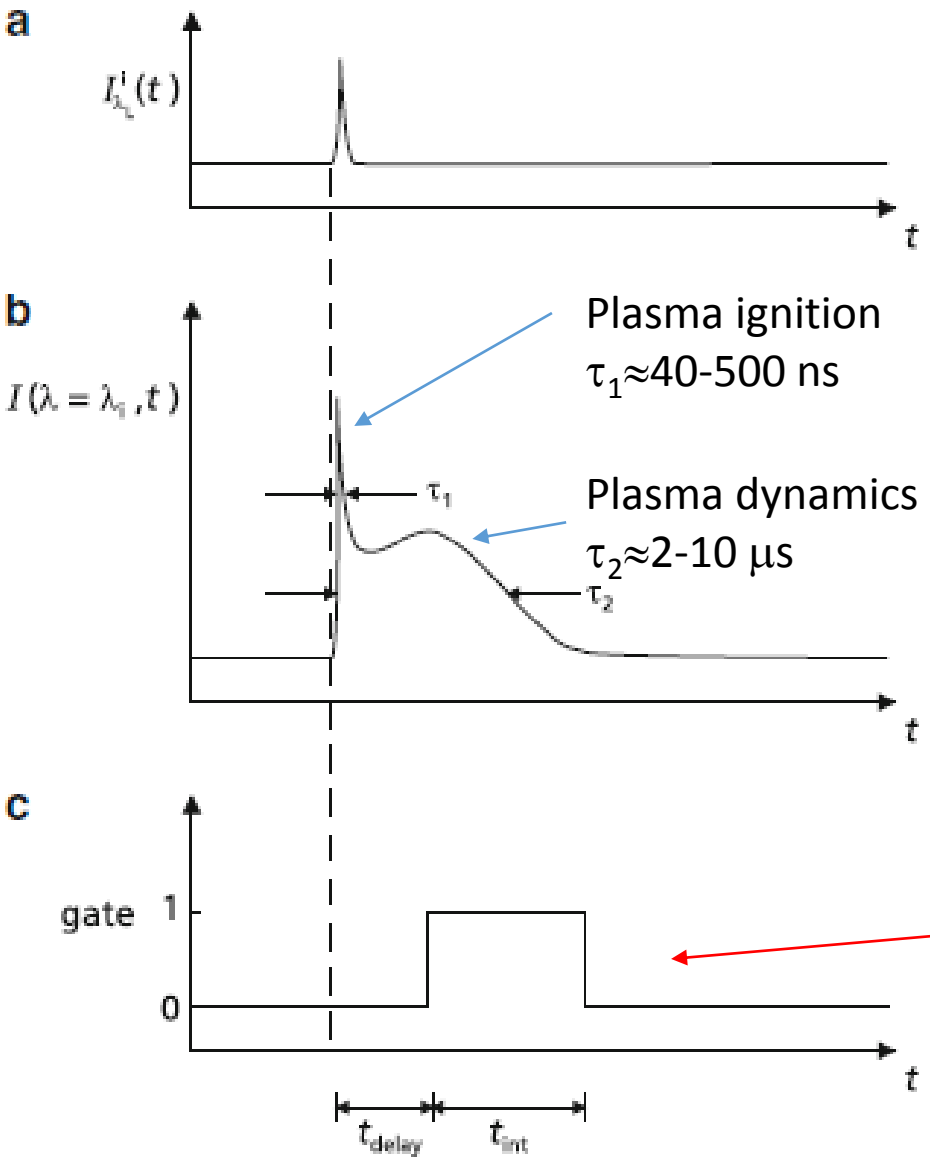

Fig. 2.4 Schematic illustration of the temporal variation of: (a) laser pulse, (b) plasma emission at an element-specific wavelength λ_i. $I(\lambda = \lambda_i, t)$ = intensity of the plasma emission at the wavelength λ_i; τ_1, τ_2 = FWHM times of the two signal components. (c) Gate signal defining the position and duration of the integration window; t_{delay}, t_{int} = cf. Fig. 2.2

Appropriate timing (delay and integration) for recording the emitted light can optimize the collected signal characteristics

Looked again directly with log time scale

Appropriate timing (delay and integration) for recording the emitted light can optimize the collected signal characteristics

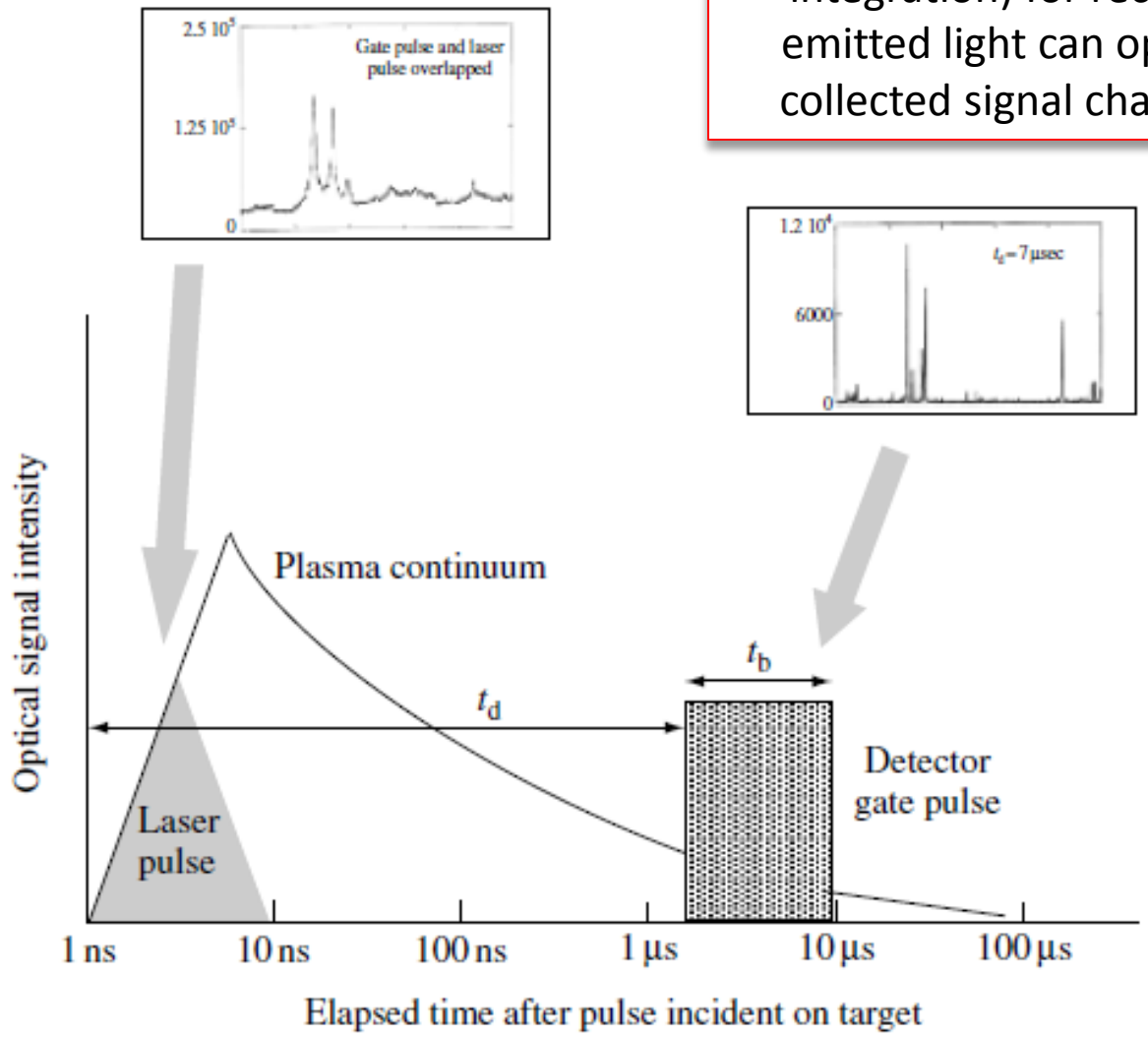

Figure 2.1 A schematic overview of the temporal history of a LIBS plasma. The delay and window are shown. Inserts illustrate the kind of spectra one might observe at the different times

The following measurands are used for LIBS:

(a) The intensity of the plasma emission at discrete wavelengths as a function of time is: $I(\lambda = \lambda_i, t)$, where λ_i denotes a set of wavelengths of element-specific lines (for simplicity of notation the index λ at the quantity I to denote the spectral intensity is omitted). Usually this signal is integrated over a time interval $[t_{\text{delay}}, t_{\text{delay}} + t_{\text{int}}]$.

(b) A spectrum, which is integrated over a time interval $[t_{\text{delay}}, t_{\text{delay}} + t_{\text{int}}]$: $S(\lambda) = \int_{t_{\text{delay}}}^{t_{\text{delay}}+t_{\text{int}}} I(\lambda, t)\mathrm{d}t$ with t_{delay} = start of integration interval with respect to the start of the laser pulse and t_{int} = temporal width of the integration window.

The measurands (a) and (b) are used for the quantitative determination of the chemical composition of a substance. As a rule this composition is described by the concentrations of the chemical elements expressed as the mass of the analyte in relation to the total mass using the unit g/g or µg/g for traces. For higher concentrations, the unit m.-% is used in the following expressing the mass percentage of an analyte. For quantitative measurements, the method has to be calibrated using reference samples to determine the functional dependence between the measurands and resultant quantities on the known concentrations of a set of reference samples, cf. Sect. 11.2.

Spectral position → Elemental specie

Emission intensity → Specie concentration in the sample

BUT the line intensity can depend on a number of factors, like: laser pulse energy, plasma temperature, plasma size, atomic parameters of the line transition, sample surface, detector response function

RELATIVE MEASUREMENT WITH RESPECT TO A REFERENCE

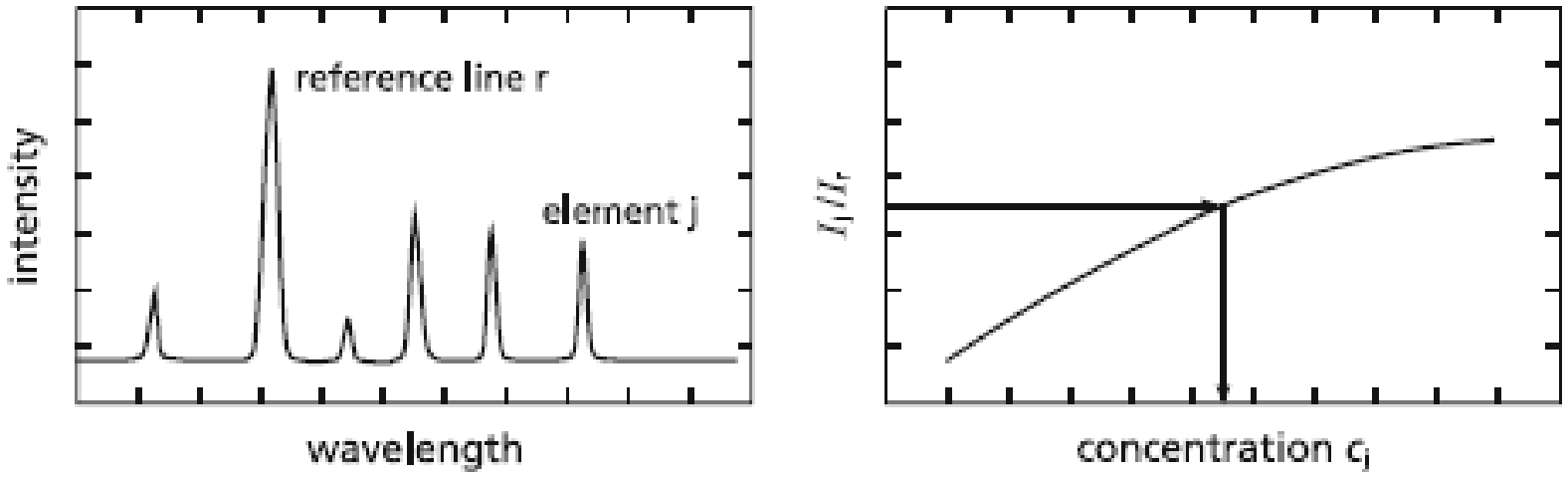

Fig. 2.5 *Left*: emission spectrum of laser-induced plasma with analyte and reference line. *Right*: calibration curve

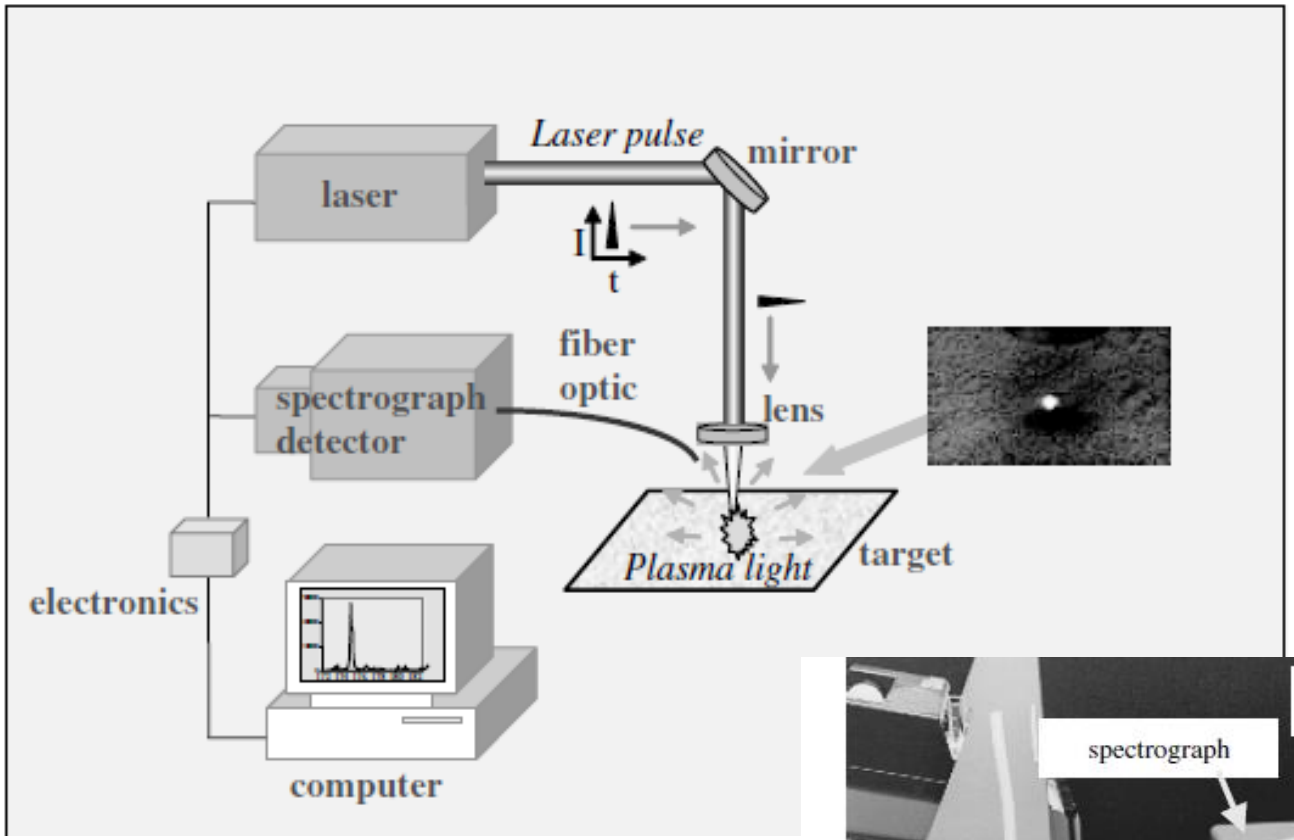

Schematic of a typical LIBS setup

Photo of a LIBS setup

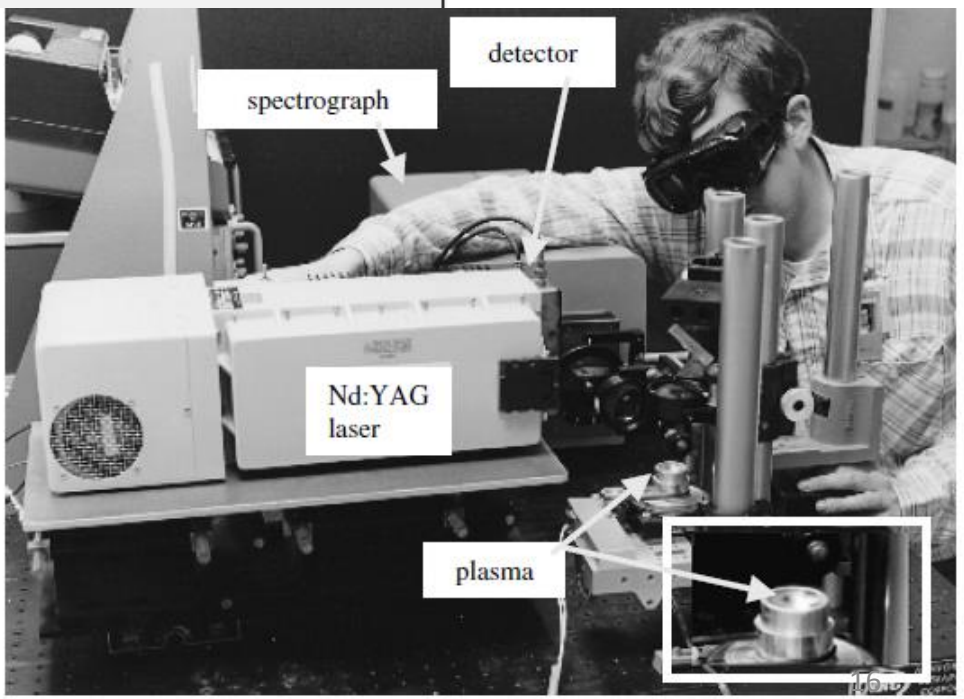

LIBS vs other methods

Table 1.1 Comparative survey of laser spectroscopic methods with exemplary data of the used laser sources and measuring quantities

Method	LIBS	LIF	Raman	CARS	LAS
λ_{exc} (nm)	266, 532, 1,064	200–800; 337	347, 694; 488, 515, 532; 266	532, 607–609	760, 1,570, 1,800; 3,160–3,670; 10,600
$\Delta\tilde{\nu}(cm^{-1})$	1	0.5; 1.2	<1	0.8; 180	<0.05
t_{exc} (ns)	5–100	10–cw	10–cw	10	6–cw
$I(W/cm^2)$	10^8–10^{11}	10^3–10^6	10^3–10^6	10^9–10^{11}	
Measuring species	g, l, s, atoms	g, l, atoms, molecules	g, l, s, molecules	g, l, s, molecules	g, molecules
Measuring quantity	c_i	c_i	c_i, T	T, c_i	c_i
Measuring range	>1 µg/g	>0.01 µg/g	>10 µg/g, 300–3,500 K	300–3,500 K, 1 mbar–100 bar	>1 ng/g
Measuring distance (mm)	10–1,500	10–1,000	10–1,000	50–1,000	500–4,000
Spatial resolution	>1 µm	>1 µm	>1 µm	>1 mm^3	./.
Minimum measuring time	~10 µs	<10 µs	~10 ns	~10 ns	~100 ms
References	[1.13], [1.17], [1.18]	[1.19], [1.20], [1.21]	[1.22], [1.23], [1.24]	[1.25], [1.26]	[1.7], [1.27], [1.28]

LIBS laser-induced breakdown spectroscopy, *LIF* laser-induced fluorescence, *CARS* coherent anti-Stokes Raman spectroscopy, *LAS* laser absorption spectroscopy, λ_{exc} wavelength of the laser used for excitation, $\Delta\tilde{\nu}$ bandwidth of the laser, t_{exc} pulse duration of the laser beam, I irradiance at the location of interaction, g gaseous, l liquid, s solid, c_i concentration of species i, T temperature, *cw* continuous wave

LIBS is the only method which allows for a **simultaneous multispecies analysis** in all states of aggregation

LASER INDUCED BREAKDOWN and/or PLASMA FORMATION

Breakdown in a gas

$$M + mh\nu \longrightarrow M^+ + e^-$$

Multi-photon ionization
(small cross section, needs high intensity)

$$e^- + M \longrightarrow 2e^- + M^+$$

Electron Impact ionization
(high energy electrons can ionize atoms, molecules)

Ionization energies of air molecules, e.g.: Oxygen (12.2 eV), Nitrogen (15.6 eV)

Laser photons energies for Nd:YAG

1064 nm → 1.25 eV
532 nm → 2.33 eV
355 nm → 3.5 eV
266 nm → 4.7 eV

For ns pulses $I \approx 10^{10}$ W/cm^2 produces weak MPI

Breakdown in a gas

Table 2.3 Measured breakdown thresholds for several lasers and gases

Laser, wavelength, pulse length, other	Gas and pressure	Breakdown threshold irradiance (W/cm^2)	Reference
Nd:YAG, 1064 nm, 10 ns	Laboratory air, 1 atm	8.2×10^{10}	Stricker and Parker, 1982
Nd:YAG, 1064 nm, 8 ns	Laboratory air, 1 atm	2.0×10^{10}	Simeonsson and Miziolek, 1994
Nd:YAG, 1064 nm, 8 ns, spot diameter 5×10^{-3} cm	Laboratory air, 1 atm	5.0×10^{11}	Tambay and Thareja, 1991
Nd:YAG, 1064 nm, 7 ps	Nitrogen, 760 Torr	8×10^{14}	Dewhurst, 1978
Nd:YAG, 532 nm, 7 ns	Laboratory air, 1 atm	1.5×10^{10}	Simeonsson and Miziolek, 1994
Nd:YAG, 532 nm, 6 ns, spot diameter 5×10^{-3} cm	Laboratory air, 1 atm	1.0×10^{11}	Tambay and Thareja, 1991
Nd:YAG, 532 nm, 8 ns	Laboratory air, 1 atm	2.5×10^{12}	Bindhu *et al.*, 2004
Nd:YAG, 532 nm, 80 ps	Laboratory air, 1 atm	1.8×10^{13}	Williams *et al.*, 1983
Nd:YAG, 532 nm, 25 ps	Nitrogen, 760 Torr	4×10^{13}	Dewhurst, 1978
Nd:YAG, 355 nm, 7 ns	Laboratory air, 1 atm	2.7×10^{10}	Simeonsson and Miziolek, 1994
Nd:YAG, 355 nm, 4 ns, spot diameter 5×10^{-3} cm	Laboratory air, 1 atm	1.05×10^{11}	Tambay and Thareja, 1991
Nd:YAG, 266 nm, 7 ns	Laboratory air, 1 atm	1.7×10^{10}	Simeonsson and Miziolek, 1994
Nd:YAG, 266 nm, 4 ns, spot diameter 5×10^{-3} cm	Laboratory air, 1 atm	1.06×10^{11}	Tambay and Thareja, 1991
ArF, 193 nm, 10 ns	Laboratory air, 1 atm	9.7×10^{9}	Simeonsson and Miziolek, 1994

Laser breakdown in a liquid

Table 2.5 Recent measured breakdown thresholds for some laser pulses in liquids

Laser, wavelength, pulse length	Medium	Breakdown threshold irradiance (W/cm^2)	Reference
Nd:YAG, 1064 nm, 7 ns	Tap water	5.6×10^9	Kennedy *et al.*, 1995
	Ultra pure water	1.82×10^{10}	
	Vitreous	1.27×10^{10}	
	Saline	8.31×10^9	
Nd:YAG, 532 nm, 3 ns	Tap water	9.35×10^9	Kennedy *et al.*, 1995
Nd:YAG, 1064 nm, 80 ps	Tap water	1.91×10^{11}	Kennedy *et al.*, 1995
Dye laser, 580 nm, 100 fs	Tap water	5.6×10^{12}	Kennedy *et al.*, 1995
Nd:YAG, 1064 nm, 6 ns	Distilled water	7.6×10^{10}	Vogel *et al.*, 1996
Nd:YAG, 1064 nm, 30 ps	Distilled water	4.5×10^{11}	Vogel *et al.*, 1996

Laser breakdown in solids

LASER ABLATION

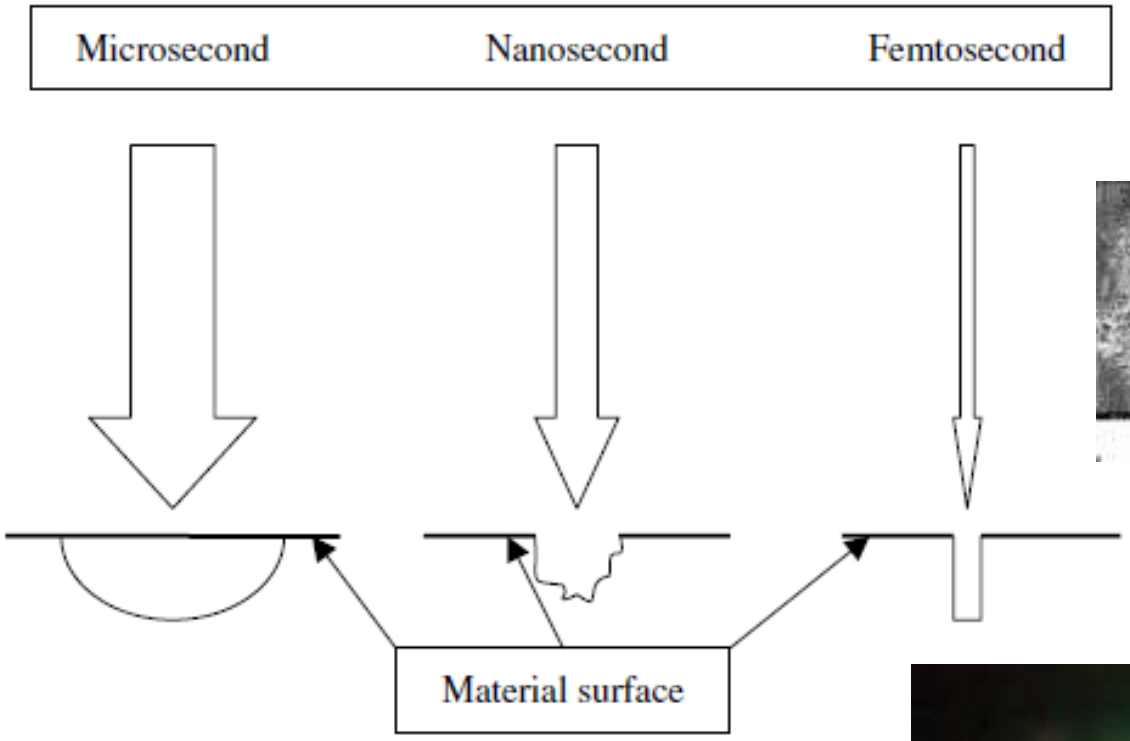

craters

Laser ablation plasma plumes

in a vacuum

Table 2.4 Recent measured breakdown thresholds for some laser pulses on solids

Laser, wavelength, pulse length	Surface, gas and pressure	Breakdown threshold irradiance (W/cm^2)	Reference
Nd:YAG, 532 nm, 6 ns	Cu, atm air	1.67×10^9	Semerok *et al.*, 2002
Ti:sapphire, 800 nm, 5 ps	Cu, atm air	9×10^{10}	Hashida *et al.*, 2002
Ti:sapphire, 800 nm, 70 fs	Cu, atm air	2.5×10^{11}	Hashida *et al.*, 2002
Colliding-pulse laser, 620 nm, 90 fs	$BaTiO_3$, vacuum	5×10^{11}	Millon *et al.*, 2003
Colliding-pulse laser, 620 nm, 120 fs	Fused silica, atm air	1×10^{13}	von der Linde and Schűler, 1996 (also investigated were glass, sapphire and magnesium fluoride)
Nd:YAG, 1064 nm, 6.4 ns	Fused silica, argon	5.5×10^{10}	Galt *et al.*, 2003

Typical ablated mass for ns pulses

Table 2.6 Averaged ablation rate values in μm/pulse for some pure metals, at atmospheric pressure in air, as a function of fluence

Fluence (J/cm²)	1.3	5.3	7.7	16.7
	Depth/pulse (μm)			
Aluminum	1.3	2.5	4.2	5.0
Copper	0.11	0.50	0.38	0.50
Tungsten	0.04	0.20	0.23	0.15

Data from Vadillo *et al.* (1999), with permission from John Wiley & Sons, Ltd

Non-linear over a large fluence range!

At low fluence

nanosecond

$$\Delta z_v \approx \frac{A(F_L - F_{th})}{\rho L_v}$$

femtosecond

$$\Delta z_v \approx \alpha^{-1} \ln\left(\frac{F_L}{F_{th}}\right)$$

$\alpha^{-1} \approx 10$ nm

The ablated mass decreases going from ns to fs

The environmental gas can confine the plasma plume and influence its emission lifetime

An example for a LIBS plasma at two pressures in CO_2

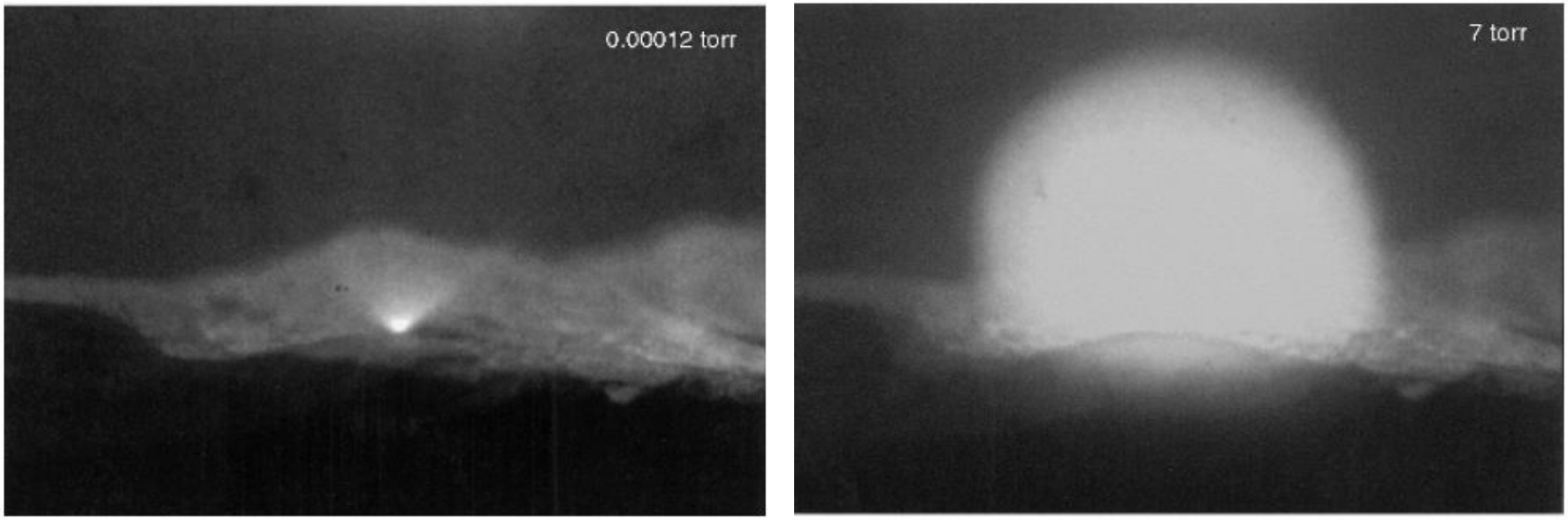

Figure 2.13 Size variation of a LIBS plasma at 7 Torr and 0.00012 Torr of CO_2. (Reproduced from Radziemski *et al.*, 2005, with permission from Elsevier)

Examples of different applications

LIBS/LIPS is a versatile tool to analyze solid, liquid or gaseous substrances

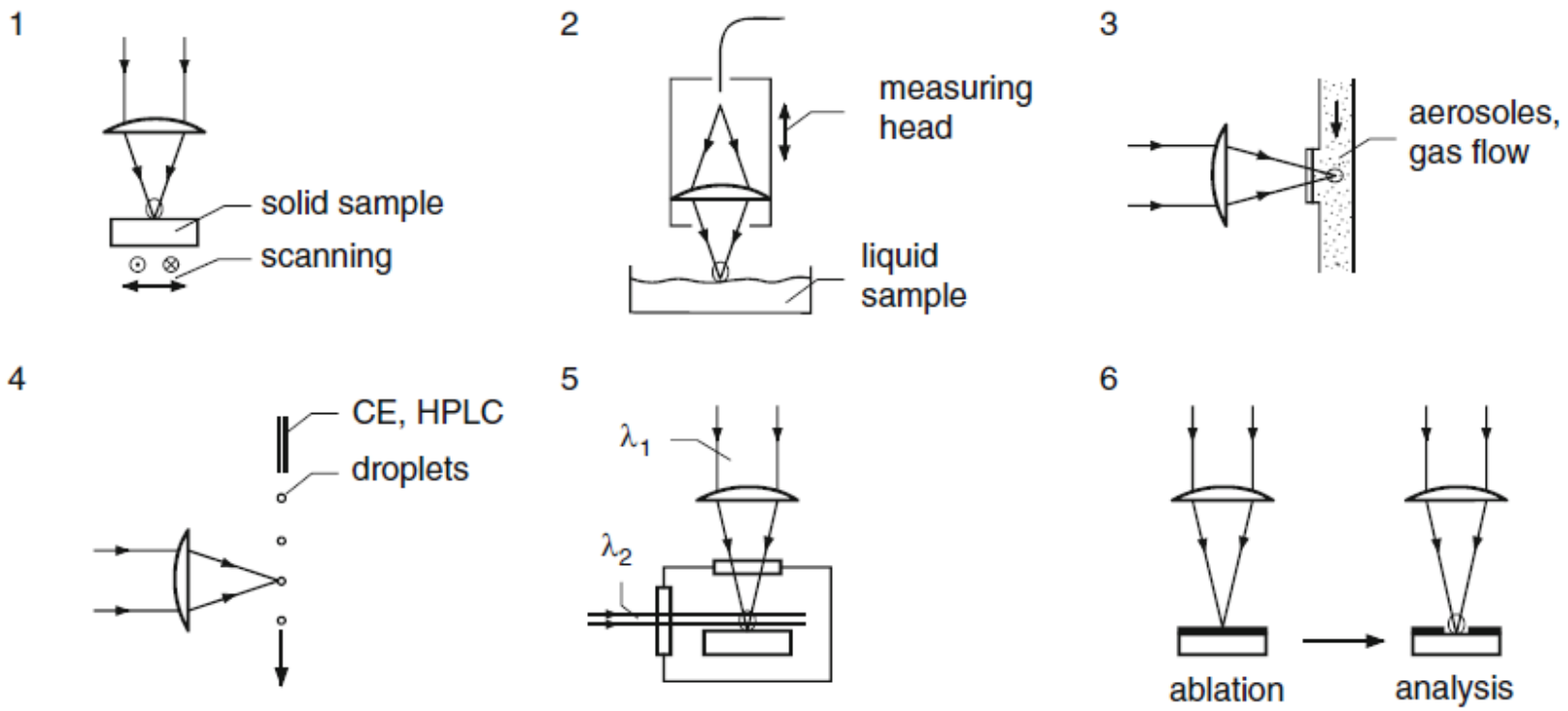

Fig. 2.9 Applications and methodical extensions of LIBS: *1* = element mapping of sample surfaces by scanning, *2* = analysis of liquids, *3* = analysis of aerosoles and gases excited through an optical window, *4* = combination of molecule-specific separation techniques with LIBS (CE = capillary electrophoresis, HPLC = high-pressure liquid chromatography), *5* = LIBS combined with laser-induced fluorescence (LIF), *6* = laser ablation of surface layers and subsequent analysis of the bulk material

Measuring Procedure

A measuring procedure comprises the following steps:

1. Definition of a measuring method or retrieval of a measuring method which was already defined. Putting the sample on the sample stand
2. Start of the measurement
3. Evaluation of the spectral signals
4. Display of the measuring results

A measuring method is defined in particular by the selection of measuring parameters and their temporal sequence, cf. Sect. 11.1. Measuring parameters are, e.g., the laser pulse energy, the number of prepulses and measuring pulses, and the gas flow in the measuring chamber. These various parameters influencing the measuring process will be discussed in more detail in Chap. 3.

A typical measuring sequence for a quantitative analysis of a sample including data evaluation takes about 30 s–2 min. For an identification testing of work pieces, inspection times of a few seconds or even fractions of a second are achievable, cf.

The measuring procedure cannot prescind from the physics of the processes involved

ACCURATE LIBS/LIPS MEASUREMENTS

REQUIRES A LOT OF ATTENTION TO BE VERY QUANTITATIVE

WHICH EXPLAINS WHY IT IS STILL SUBJECT OF MANY REASERCHES AND CONFERENCES

- CALIBRATION PROBLEMS CAN ARISE IN SPECIFIC CONDITIONS
- SEARCH FOR CALIBRATION-FREE APPROACHES
- IMPROVEMENT OF SENSITIVITY
- DEVELOPMENT OF SPECIFIC INSTRUMENTS (PORTABILITY, EXTREME AMBIENTAL CONDITIONS, SPACE, DANGEROUS SUBSTANCES,……)

Handbook of Laser-Induced Breakdown Spectroscopy

Handbook of Laser-Induced Breakdown Spectroscopy D. A. Cremers and L. J. Radziemski
 ISBN: 0-470-09299-8

Laser-Induced Breakdown Spectroscopy

Fundamentals and Applications

Reinhard Noll

Springer-Verlag Berlin Heidelberg 2012

There are a number of books and reviews to which one can refer

Let's continue with some principles

WE HAVE TO DEAL WITH SPECTRAL LINE MEASUREMENT AND ANALYSIS

Spectral lines profiles in a plasma: what does matter?

Line widths and shapes are related to plasma temperature and electron density, besides the other basic lineshape influencing factors (natural width, doppler, etc..)

Spectral line profiles are determined by the dominant broadening mechanism

1. DOPPLER BRADENING → GAUSSIAN PROFILE

$$I(\sigma) = (4\ln 2/\pi\Gamma^2)^{1/2} \exp[-4\ln 2(\sigma-\sigma_0)^2/\Gamma^2]$$

where Γ is the full-width at half-maximum (FWHM),

$$\Gamma = (8kT\ln 2/Mc^2)^{1/2}\sigma_0 \qquad (2.3)$$

where M is the species mass and σ_0 the central wave number of the transition.

$\sigma=2\pi/\lambda$ is the wavenumber (typically also indicated as *k*) [from R&C]

2. NATURAL and COLLISIONAL BROADENING→ LORENTIAN PROFILE

$$I(\sigma) = (\Gamma/2\pi)/[(\sigma - \sigma_0)^2 + (\Gamma/2)^2]$$

Voigt profile

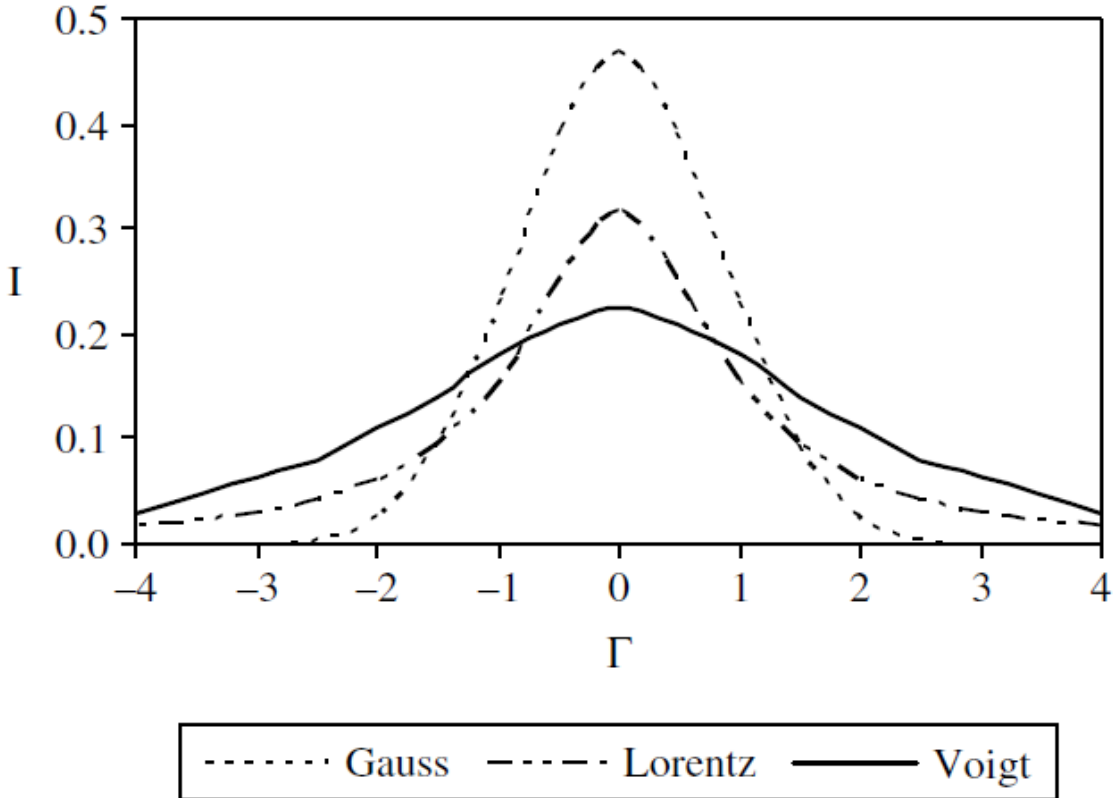

Typically these broadening effects are comparable (Convolution)

Gauss and Lorentz profiles of equal half widths.

3. STARK BROADENING (IN A PLASMA) [asymmetric shifted line]

Approximate expressions (Griem, 1974)

Measured half-width at half-maximum (HWHM) and peak shift

$$w_{\text{total}} \sim [1 + 1.75\,A(1 - 0.75r)](n_e/10^{16})w$$

$$d_{\text{total}} \sim [1 \pm 2.00\,A(1 - 0.75r)](n_e/10^{16})d$$

- w and d are parameters depending on the transition
– the ionic contribution (second term with constants A and r) is typically smaller than electron contribution, and usually neglected $A = \pi r^2$

FOR LIBS PLASMA USUALLY DOPPLER AND STARK ARE DOMINANT

$$\Delta\lambda_D = 7.2 \times 10^{-7}(T/M)^{1/2}\lambda_o$$ Doppler (FWHM)

$$\Delta\lambda_s \approx 2w\left(\frac{n_e[cm^{-3}]}{10^{16}}\right)$$ Stark (FWHM)

Table 2.1 Doppler and Stark widths for lines of some elements of interest in LIBS experiments. Widths are calculated full-width at half maximum intensity (FWHM), for a plasma temperature of 10 000 K and an electron density of $10^{17}/cm^3$, except where noted

Element	λ (nm)	Atomic mass	Temperature (K)	Doppler FWHM (nm)	Stark width coefficient[a] (HWHM in Å at $10^{16}/cm^3$)	Stark width (FWHM in nm at $10^{17}/cm^3$)
Hydrogen	656.3	1	11 000	0.047		0.4440[b]
Hydrogen	656.3	1	20 000	0.067		
Hydrogen	656.3	1	50 000	0.106		
Hydrogen	486.1	1		0.035		0.8300[c]
Deuterium	656.0	2	10 000	0.033		
He	587.5	4	10 000	0.021	0.1700	0.3400
Li	670.7	6.9	10 000	0.018	0.0138	0.0276
Li	610.3	6.9	10 000	0.017	0.2140	0.4280
Li	460.2	6.9	10 000	0.013	1.2700	2.5400
Li	413.2	6.9	10 000	0.011	3.4100	6.8200
Be	234.9	9	10 000	0.006	0.0009	0.0018
Be (II)	313.1	9	10 000	0.008	0.0537	0.1074
C	193.1	12	10 000	0.004	0.0022	0.0044
C	247.9	12	10 000	0.005	0.0036	0.0072
O	777.3	16	10 000	0.014	0.0315	0.0630
Na	589.2	23	10 000	0.009	0.0157	0.0314
Mg	285.2	24	10 000	0.004	0.0041	0.0082
Al	309.2	27	10 000	0.004	0.0260	0.0520
Si	288.1	28	10 000	0.004	0.0064	0.0128
Si	390.5	28	10 000	0.005	0.0117	0.0234
S	181.4	32.1	10 000	0.002	0.0022	0.0044
K	766.5	39.1	10 000	0.009	0.0415	0.0830
Ca	422.6	40	10 000	0.005	0.0063	0.0126

[a] Coefficients from Appendix 4 (neutrals) or 5 (ions) of Griem (Griem, 1974).
[b] Experimental, at $T \sim 11\,000$ K and $n_e = 2 \times 10^{16}/cm^3$ (Parigger *et al.*, 2003). If this scales linearly with electron density, the approximate value at $n_e = 10^{17}/cm^3$ would be 2.2 nm.
[c] Experimental, at $T \sim 11\,000$ K and $n_e = 9.2 \times 10^{15}/cm^3$ (Parigger *et al.*, 2003). If this scales linearly with electron density, the approximate value at $n_e = 10^{17}/cm^3$ would be 10 nm.

Typical natural linewidhts for $\Delta t \approx 10$ ns and $\Delta E \approx 1$-3 eV are $\Delta\lambda \approx 10^{-3}$ nm (@ $\lambda \approx 500$ nm)

When using LIBS at atmospheric pressure, ambient background species densities of molecular oxygen and nitrogen are on the order of $2 \times 10^{19}/cm^3$. Electron densities measured by Stark broadening are often $10^{18}/cm^3$ at less than a microsecond into the plasma, and $10^{16}/cm^3$ at 5 to 10 μs after the laser pulse.

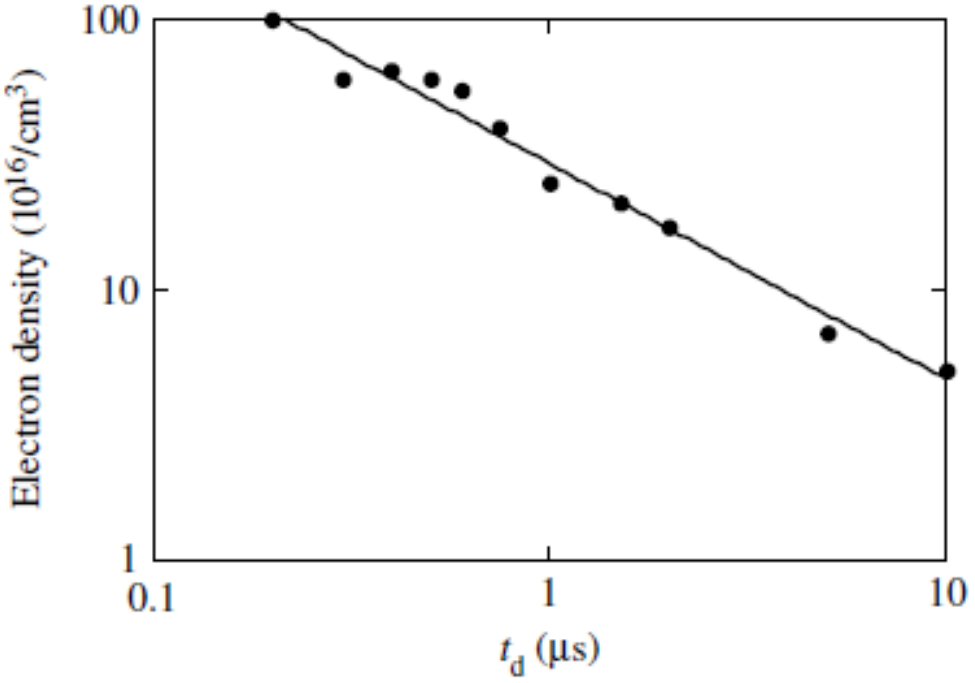

Figure 2.4 Electron densities measured in some LIBS experiments. Data abstracted from Stark widths of F, Ar, N and Cl lines

Stark broadening can be used to measure electron density in the plasma

Why electron density is so important in LIBS plasma?

We want an **ideal plasma** and that **Equilibrium Boltzmann statistics** holds.
BUT we typically have a transient plasma, then we resort to

LOCAL THERMODYNAMIC EQUILIBRIUM (LTE)

For a local temperature equilibrium (LTE) in an optically thin plasma, the probability of a collision-induced transition is much greater than the probability of a radiating transition. This condition is fulfilled, if the following relation holds for all energy levels of an atom with a principal quantum number greater or equal n [8.5]:

$$n_e \geq 7 \times 10^{18} \frac{(z+1)^7}{n^{17/2}} \left(\frac{k_B T_e}{E_H}\right)^{1/2} \text{cm}^{-3}, \qquad (8.17)$$

where z is the ionization stage, $z = 0$ for neutral particles, $z = 1$ for singly ionized particles, etc., n is the principal quantum number, E_H is the ionization energy of hydrogen.

Relation (8.17) is valid exactly only for the hydrogen atom. For transitions of iron atoms studied, e.g., in Sect. 8.2, we have $n \geq 3$ and $z = 0$. All experimentally found electron temperatures of the material plasma were less than $T_e = 11,000\,\text{K}$ (cf. Figs. 8.15, 8.16, 8.19–8.21, 8.23). Relation (8.17) yields then: $n_e \geq 2 \times 10^{14}\,\text{cm}^{-3}$.

There are conditions where LTE condition is fulfilled

Fig. 8.38 Local temperature equilibrium condition (LTE) according to relation (8.17) and plasma trajectory in a $n_e - T_e$ diagram (data points are taken from Fig. 8.16). The *bar* alongside the plasma trajectory indicates exemplarily the integration time window for quantitative LIBS analysis

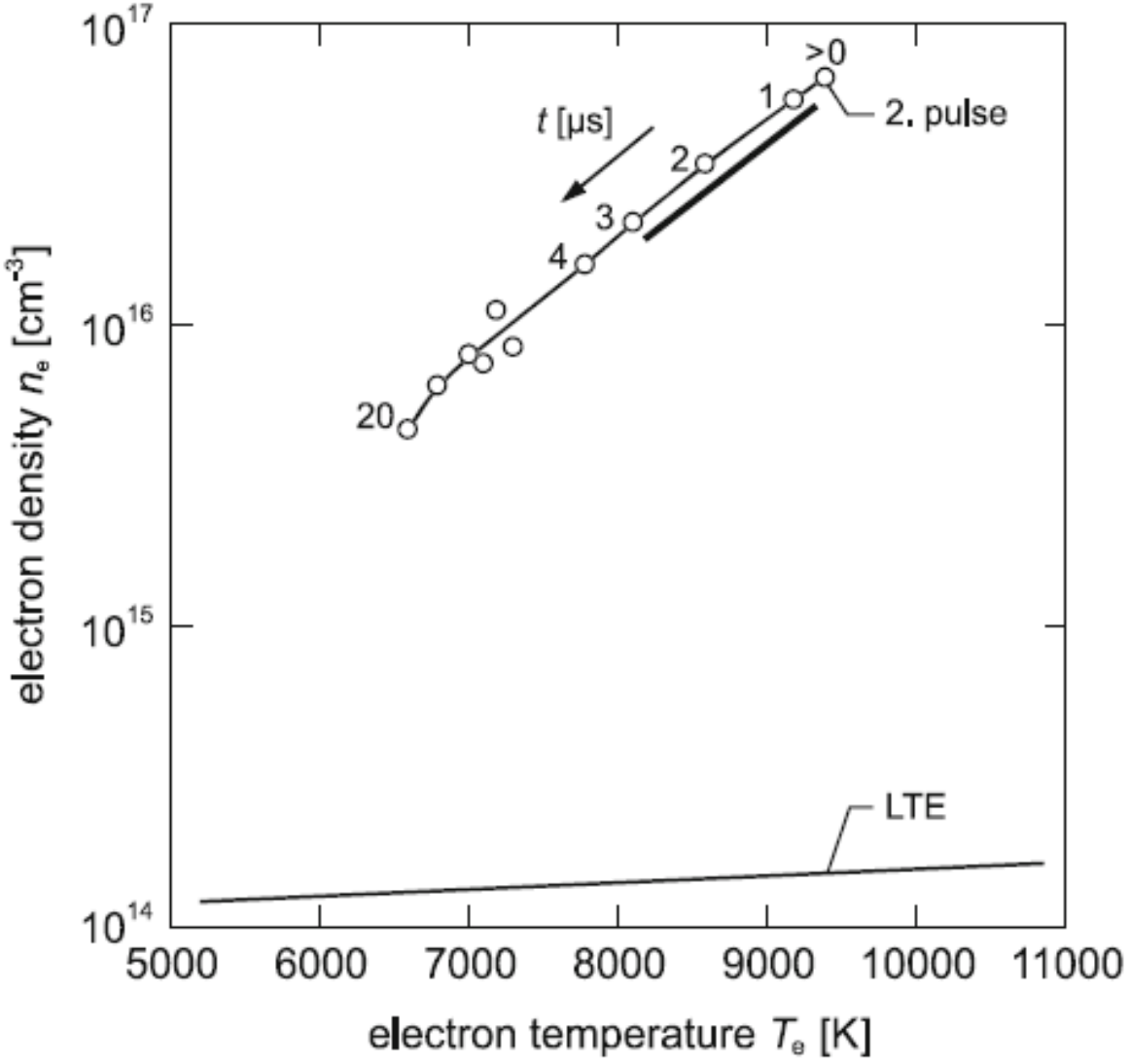

Ideal and classical plasma when the interaction energy between charged particles is small compared with the kinetic energy

We skip here all the analysis of the conditions for ideal plasma. Laser plasma, being transient, can generally reach such conditions in a part of their evolution or specific strategies can be exploited for that!

ALSO ELECTRON TEMPERATURE T_e IS IMPORTANT

T_e can be measured in different ways, one related to spectral analysis is the ***BOLTZMANN PLOT METHOD***

Going back….

Spectral line radianti intensity *I* (W/sr)

$$I = h\nu\, gA\, N/4\pi = (hcN_o gA/4\pi\,\lambda Z)\exp(-E/kT)$$

For each spectral line we evaluate a new quantity y related to the line characteristics (A,g, λ), the measured emission intensity (I) and instrumental response constant (c_B)

$$y = \ln\left(\frac{I\lambda}{A_{nm}g_n}c_B\right)$$

Table 8.1 Wavelength λ, excitation energy E_n, Einstein coefficient A_{nm}, and statistical weight g_n of the upper level n of the selected iron lines for the determination of the electron temperatures from Boltzmann plots

λ (nm)	E_n (eV)	A_{nm} ($10^8 s^{-1}$)	g_n
532.418	5.54	0.15	9
532.804	3.24	0.0115	7
537.150	3.27	0.0105	5
538.337	6.62	0.59	13
539.713	3.21	0.00259	9
540.578	3.28	0.0109	9

The width of the Fe line at 538.34 nm caused by Stark broadening is used to evaluate the electron density [8.6, 8.7]

Tabulated line characteristics [from Handbooks, NIST, literature,….]

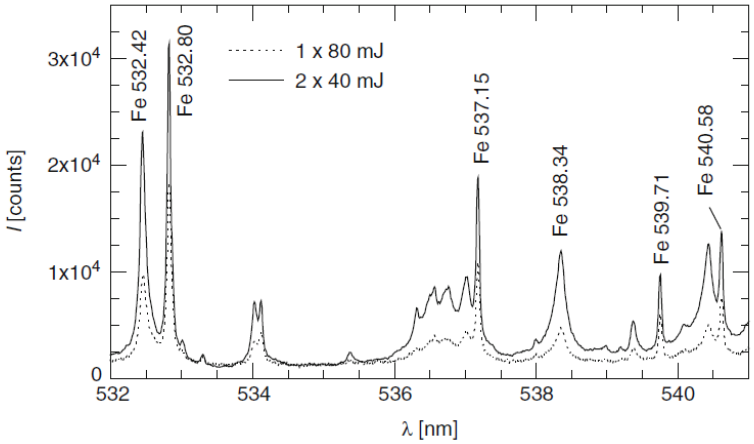

$$y \propto -\frac{E_n}{k_B T_e}$$

Linear fit
y=mx+n

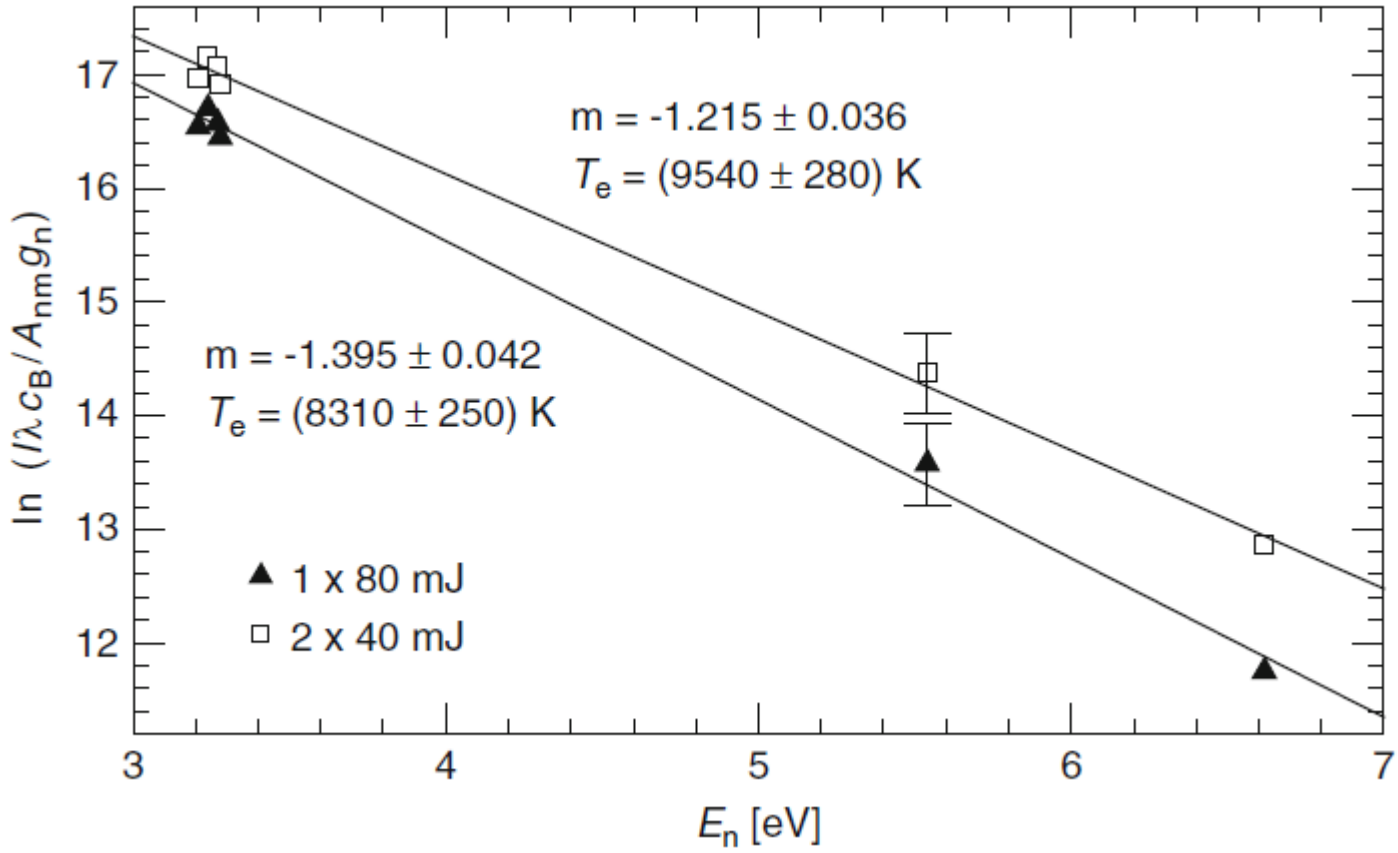

Another example

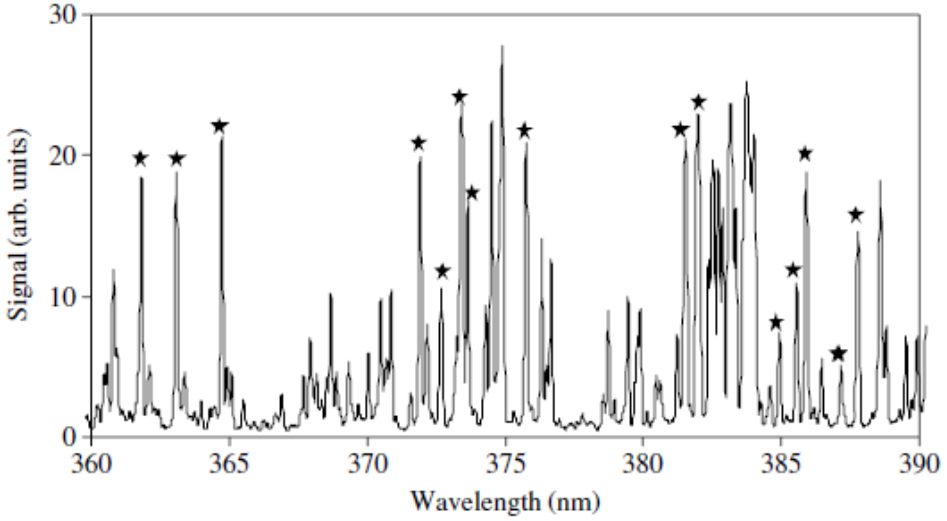

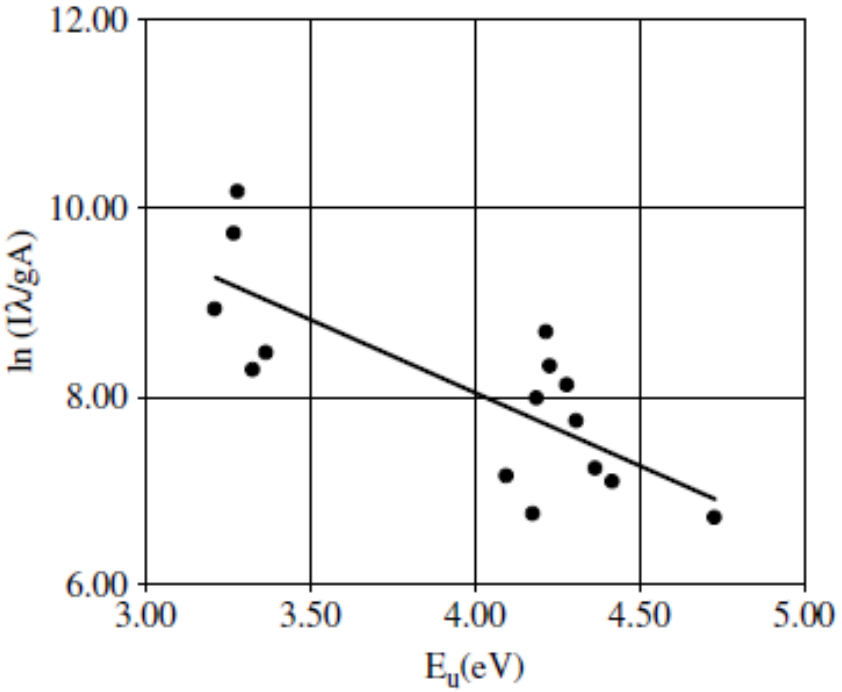

Table 2.2 Neutral Fe [Fe(I)] parameters for a Boltzmann temperature determination (see Figure 2.8)[a]

Wavelength (nm)	E_u (eV)	gA^b	Wavelength (nm)	E_u (eV)	gA^b
361.877	4.42	5.1	382.043	4.10	6.01
363.146	4.37	4.65	384.044	4.22	1.41
364.784	4.31	3.21	384.997	4.23	0.61
371.994	3.33	1.78	385.637	3.27	0.23
372.762	4.28	1.12	385.991	3.21	0.87
373.487	4.18	9.92	387.250	4.19	0.53
373.713	3.37	1.28	387.857	3.28	0.2
381.584	4.73	9.1			

[a] Data from: http://physics.nist.gov/PhysRefData/ASD/index.html
[b] In units of 10^8/s.

PLASMA OPACITY

Having introduced the concepts of line profile and line width, we can now discuss the opacity of a plasma. Fundamentally, a plasma is optically thin when the emitted radiation traverses and escapes from the plasma without significant absorption or scattering. The intensity of radiation emitted from a plasma is given by:

$$I(\lambda) = [\varepsilon(\lambda)/\alpha(\lambda)]\{1 - \exp[-\alpha(\lambda)L]\} \quad (2.8)$$

where $\varepsilon(\lambda)$ is the emissivity, $\alpha(\lambda)$ is the absorption coefficient (/cm), and L is the plasma length along the line of sight to the observer. Note that when α is small:

$$I(\lambda) = [\varepsilon(\lambda)/\alpha(\lambda)][\alpha(\lambda)L)] \sim \varepsilon(\lambda)L \quad (2.9)$$

which is the condition for the plasma to be optically thin.

Some ways to check if plasma is optically thin:

- Relative intensity ratio of well-known lines
- Strong lines spectral profiles (flattened top, dip formation on the peak, etc…)
- ……..

Self-absorption is very subtle and must be avoided to get reliable results!

INSTRUMENTATION

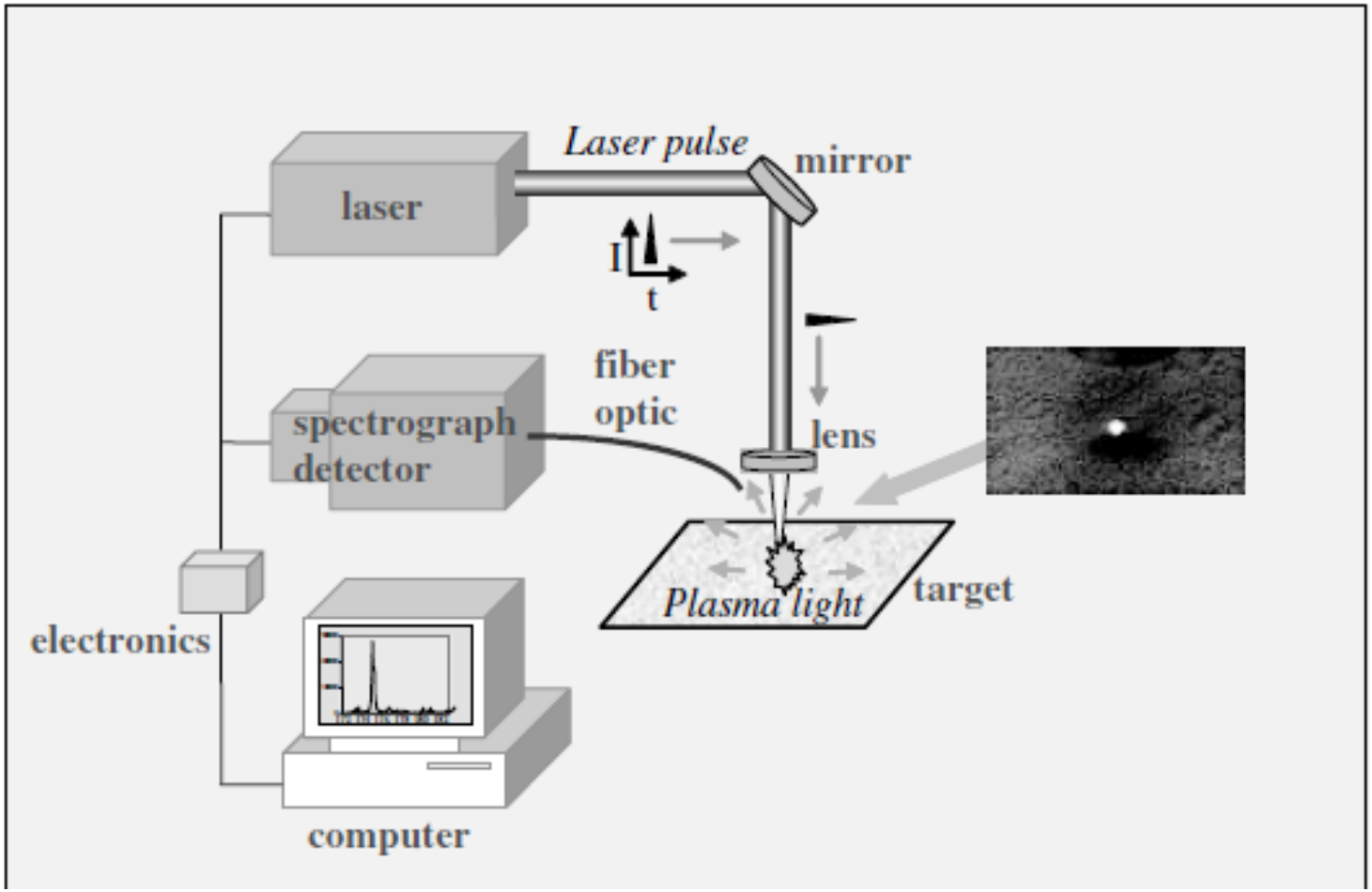

Lasers (many types)

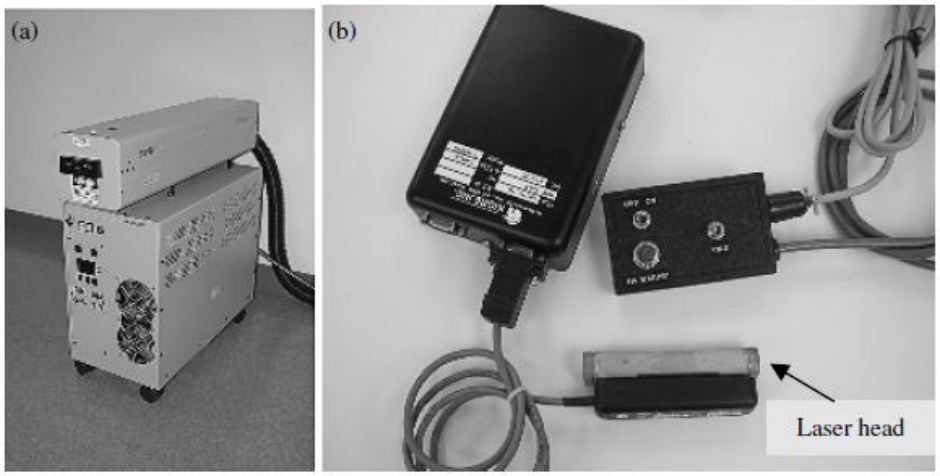

Figure 3.3 (a) Typical laboratory Nd:YAG laser (Surelite laser; photo courtesy of Continuum, Inc.); (b) compact Nd:YAG laser (MK-367; photo courtesy of Kigre Laser, Inc.)

From large laboratory sources to compact systems depending on applications

Typically ns laser source are used, but in the last decade many experiments and system regard the use of shorter pulses (ps, fs).

Table 3.2 Specifications of the laboratory and compact Nd:YAG lasers of Figure 3.3

Parameter	Laboratory	Compact
Pulse energy (mJ) max.	450	25
Pulse width (ns)	5–8	4
Repetition rate (Hz)	10	1
Energy stability (±%)	2	<10
Beam diameter (mm)	<10	3
Beam divergence (mrad)	0.5	1.1
Flashlamp lifetime (10^6 shots)	10	0.3
Mass (kg)	71	1.2
Cooling	water	air
Power requirements	220 V AC; 12 A	12 V DC; 1.2 A

AC, alternating current; DC, direct current

Table 3.1 Specifications of lasers used for LIBS

Type	Wavelength (nm)	Pulse width (ns)	Rep. rate (Hz)	Comments related to LIBS applications
Nd:YAG (s)	Fundamental: 1064	6–15	ss to 20	(1) Fundamental wavelength easily shifted to provide harmonic wavelengths (2) Available in very compact form for small instrumentation (3) Good beam quality possible (4) Dual-pulse capabilities in single unit (5) Flashlamp or diode-pumped available
	Harmonics: 532, 355, 266	4–8		
Excimer (g)	XeCl: 308	20 ns	ss to 200	(1) Requires periodic change of gases (2) Beam quality less than Nd:YAG laser (3) Provides UV wavelengths only
	KrF: 248			
	ArF: 194			
CO_2 (g)	10 600	200 (with 1000 ns trailing edge)	ss to 200	(1) Requires periodic change of gases or gas flow (2) Does not couple well into many metals (3) Beam quality less than Nd:YAG laser
Microchip	1064	<1 ns	1–10 k	(1) Good mode and beam quality (2) High shot-to-shot pulse stability (3) High rep. rates ~10 kHz

s, solid state laser; g, gas laser; ss, single shot.

GOOD and **BAD** must be considered when selecting the laser source

An exemplificative table of comparison

Many more lasers are available!

OPTICAL SYSTEMS

FOCUSING AND LIGHT COLLECTION

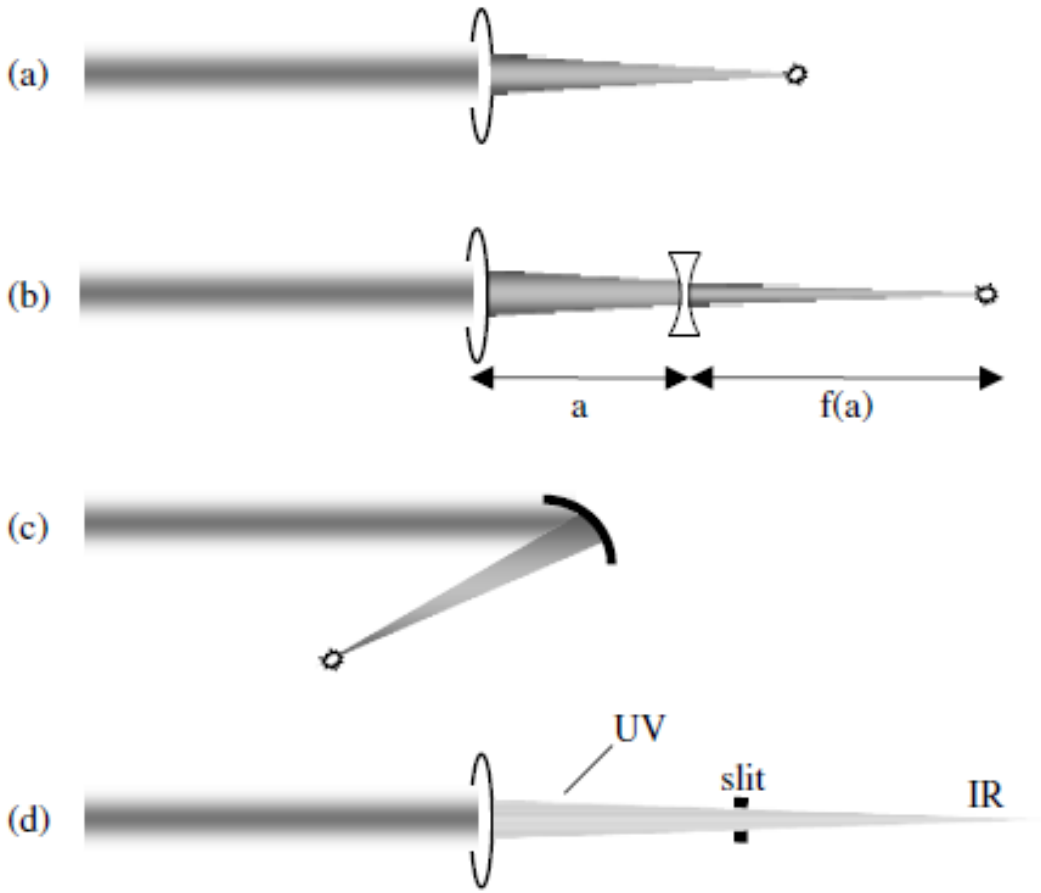

Figure 3.7 Different arrangements for focusing laser pulses to generate a plasma

Usually simple lenses are OK
but more complex focussing system can be designed for specific purposes

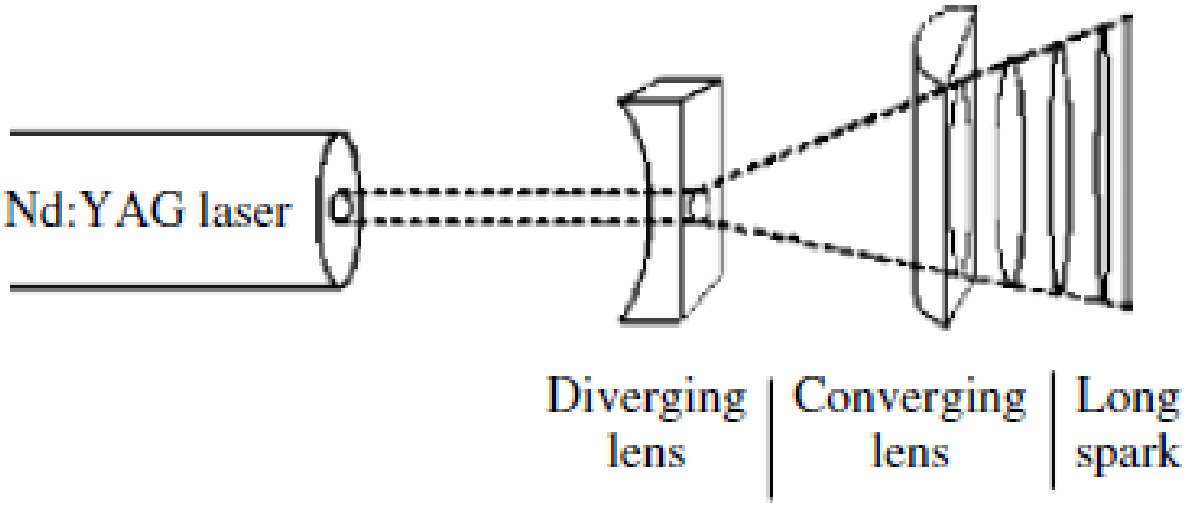

Figure 3.8 Lens system used to form a long spark on a sample

Optical fibers for light collection

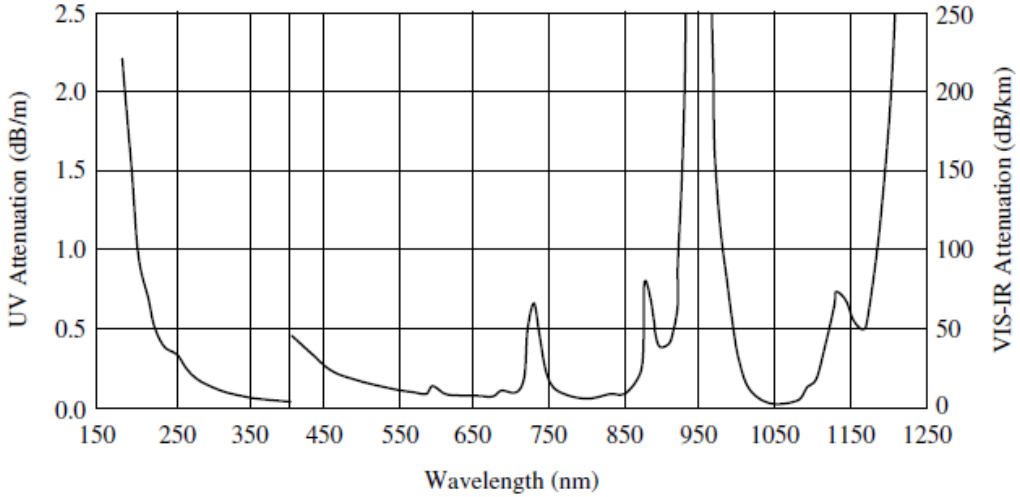

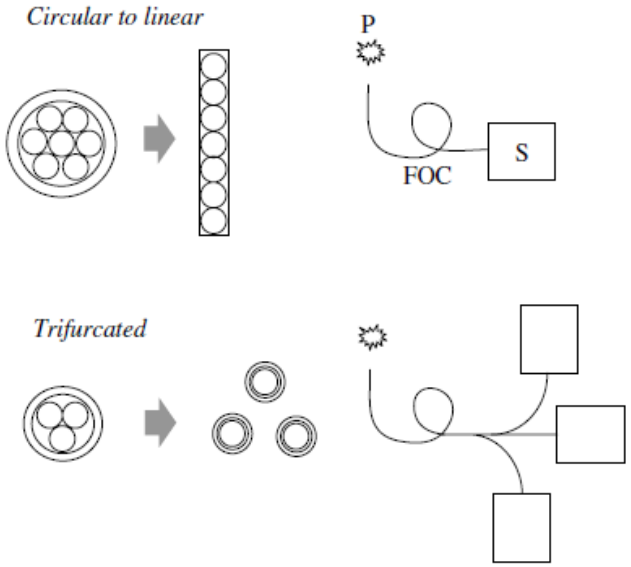

In various cases also simple lens, system of lenses or objectives are used (e.g. in imaging systems).

Figure 3.14 Custom FOC configurations

DETECTORS

Table 3.7 Comparison of some detectors used for LIBS

Detector	Characteristics
Photomultiplier tube (PMT)	Measure instantaneous light intensity; temporal responses < 1 ns; useful to map out decay response of plasma light; spectral response tailored to spectral region; inexpensive; compact; used with line filter or monochromator to provide single wavelength detection
Avalanche photodiode (APD)	Solid-state detector; high gain; fast response; rugged; compact; high signal-to-noise ratio; high quantum efficiency; fabrication as an array
Photodiode array (PDA)	Provides one-dimensional spatial information about light intensity along array; light intensity integrated with temporal response determined by readout time; used with spectrograph to provide simultaneous detection over a certain spectral range
Intensified PDA (IPDA)	PDA characteristics plus time-resolved detection down to few ns; more expensive than PDA
Charge coupled device (CCD)	Provides two-dimensional spatial information about light intensity on array; light intensity integrated with temporal response determined by readout time; used with spectrograph to provide simultaneous detection over a certain spectral range through vertical binning of pixel signals; intensity distribution along vertical dimension can be used in certain applications (e.g. long spark) or multiple FOC input at entrance slit to monitor spectra from different regions simultaneously
Intensified CCD (ICCD)	CCD characteristics plus time-resolved detection down to few ns; more expensive than CCD

METHODS OF SPECTRAL RESOLUTION

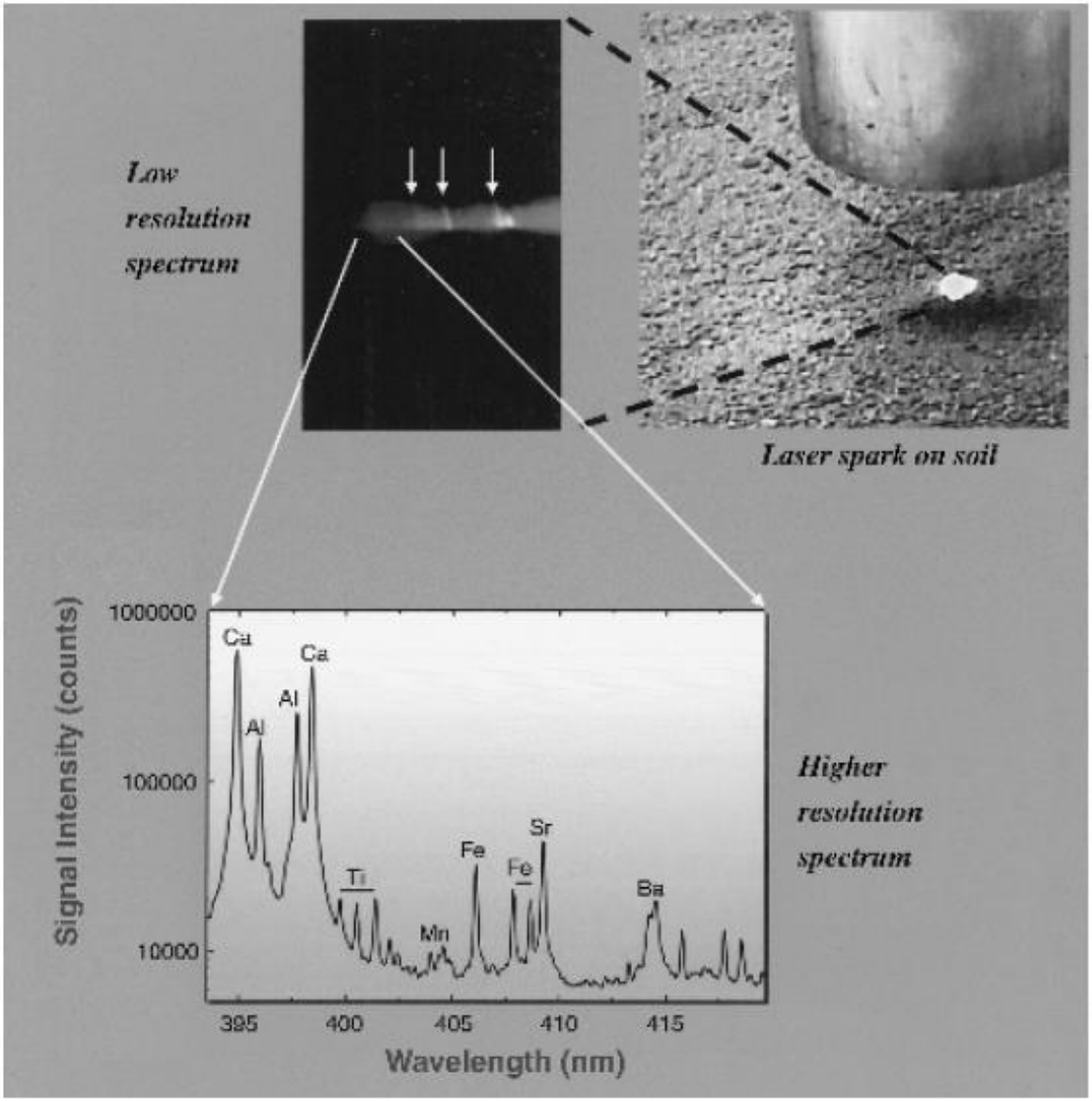

- Spectral range
- Signals intensity level
- Spatial resolution
- Temporal resolution & gating
- Known/unknown samples
- Portability
- Possibility of remote sampling
- Costs
- …….

Figure 3.16 LIBS spectrum produced by a simple transmission diffraction grating from the plasma formed at the right on soil. Here only strong lines of nitrogen from air are observed. Higher resolution of the spectrum shows emissions from major, minor and trace elements in the soil (see Plate 4)

Spectral selection and imaging possibilities

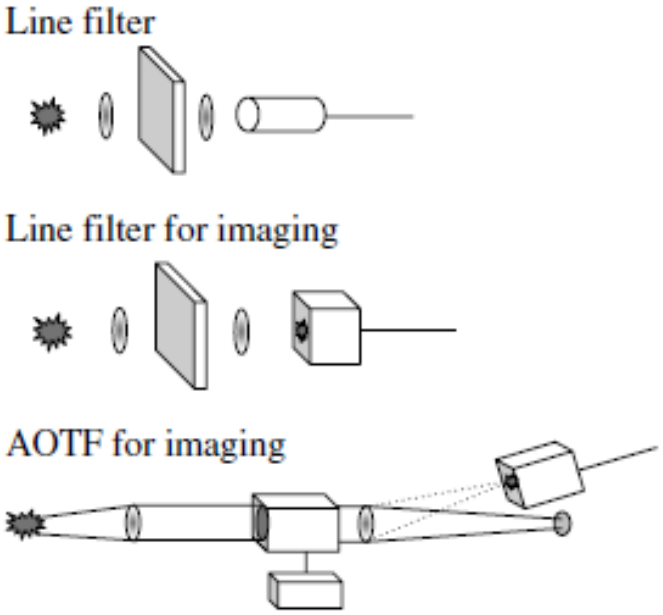

spectrograph

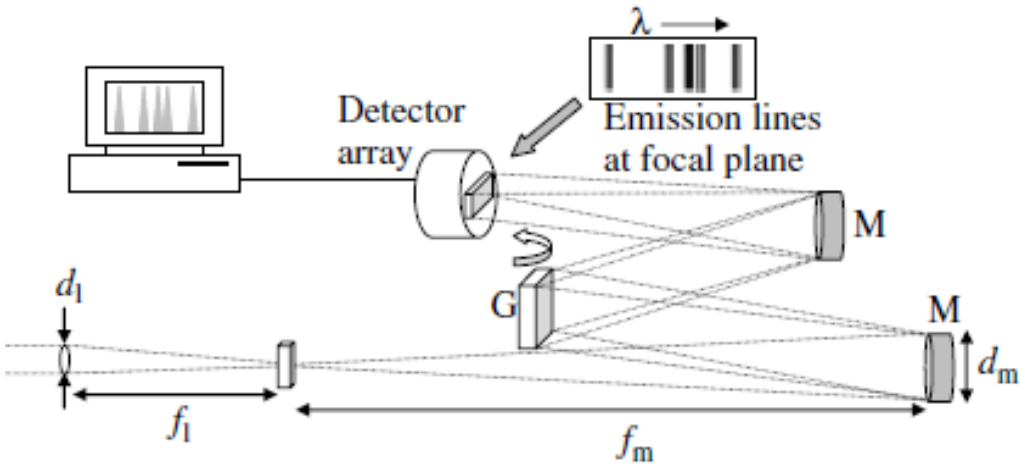

Table 3.4 Comparison of methods of spectral resolution

Method	Characteristics
Spectral filter	Single fixed wavelength, small, inexpensive, useful for imaging
AOTF*	Single wavelength, tunable wavelength, useful for imaging
Grating monochromator	Single wavelength, high resolution, tunable, f#∼4
Echelle spectrograph	High resolution, broadband spectral coverage, alignment more critical, typical f#>9, requires two-dimensional detector array
Grating spectrograph	Wide spectral coverage, high resolution, tunable, different gratings offers ability to tailor spectral resolution, f#∼4

*Acousto-optic tunable filter

AOTF for imaging

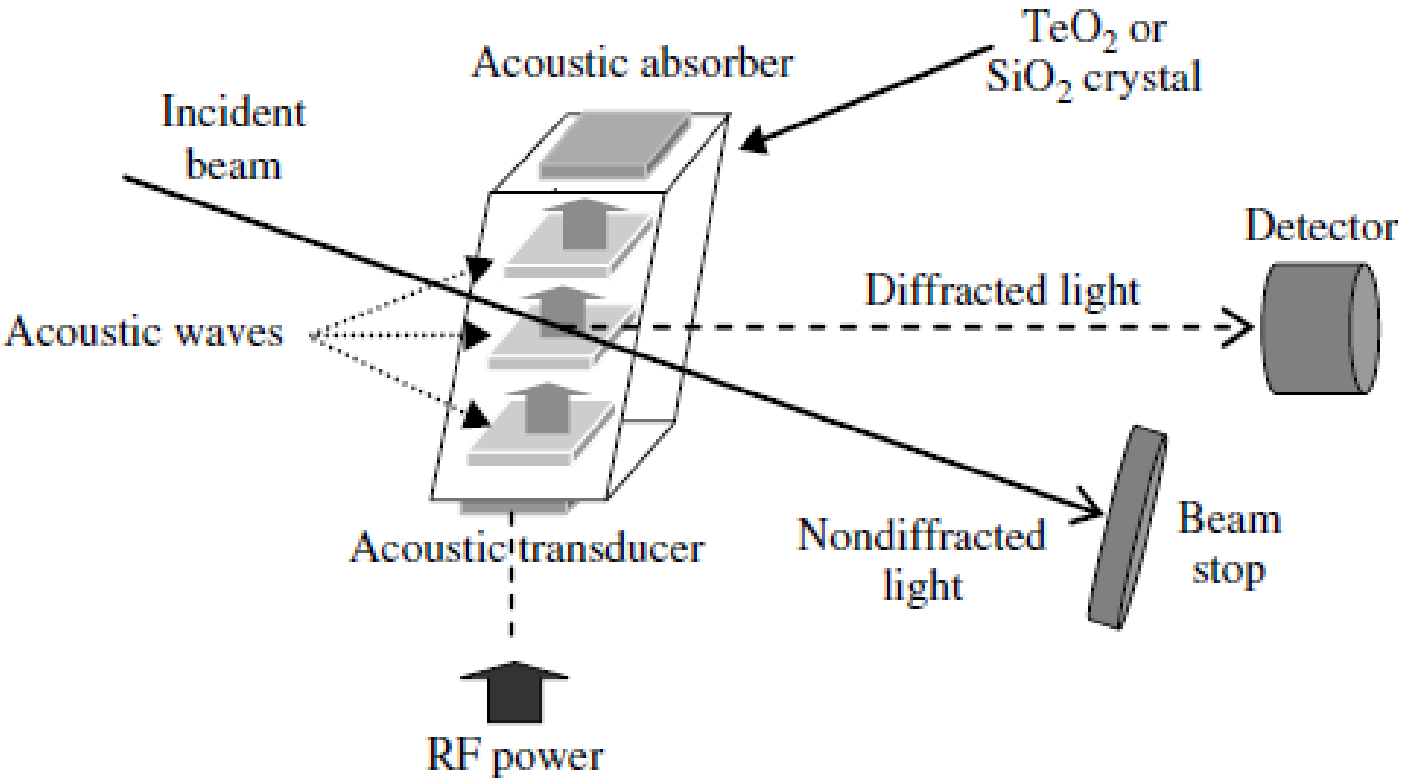

Figure 3.19 Diagram of the operation of an AOTF device

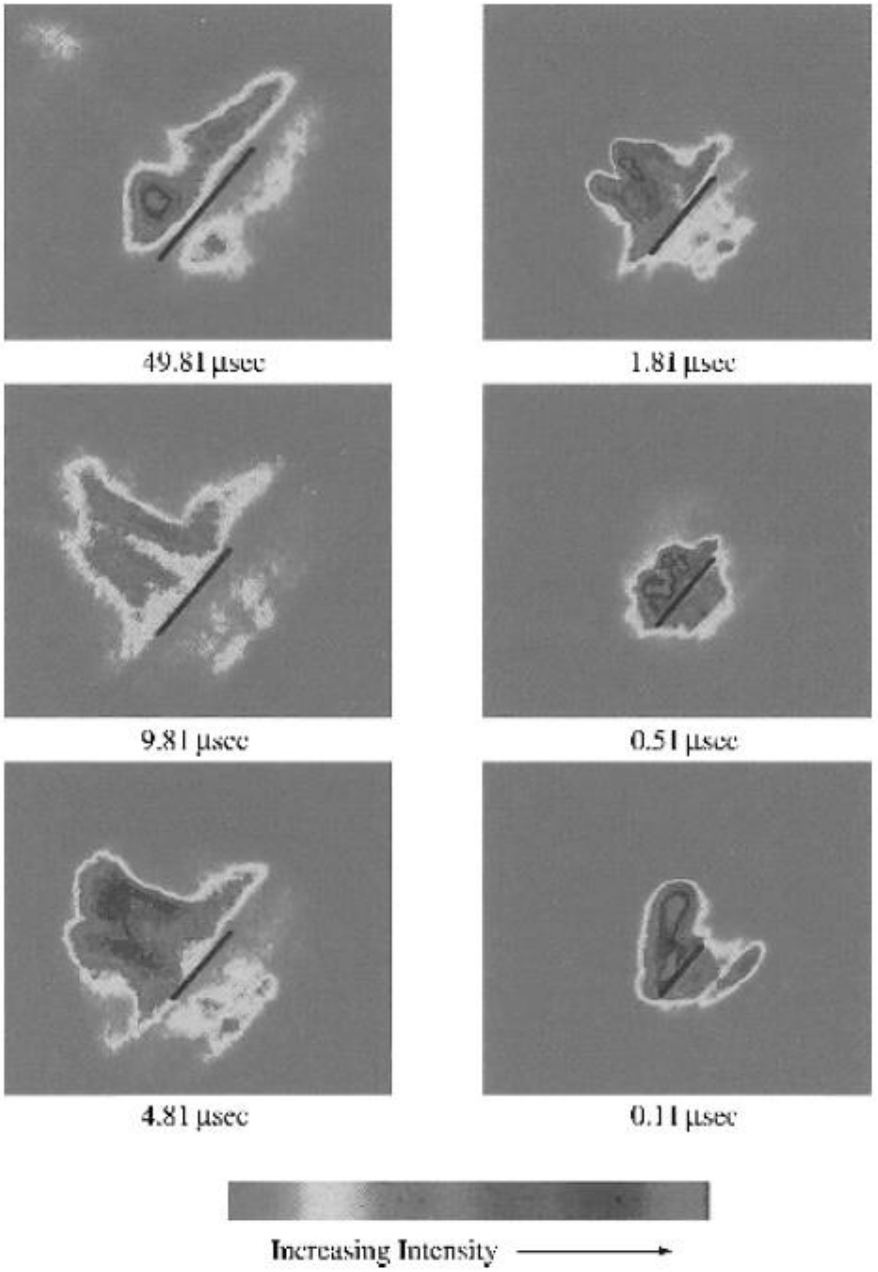

Figure 3.20 Cr emission observed using the AOTF with an ICCD. (Reproduced from Multari and Cremers, Copyright 1996 IEEE) (see Plate 5)

Czerny-Turner Imaging spectrograph

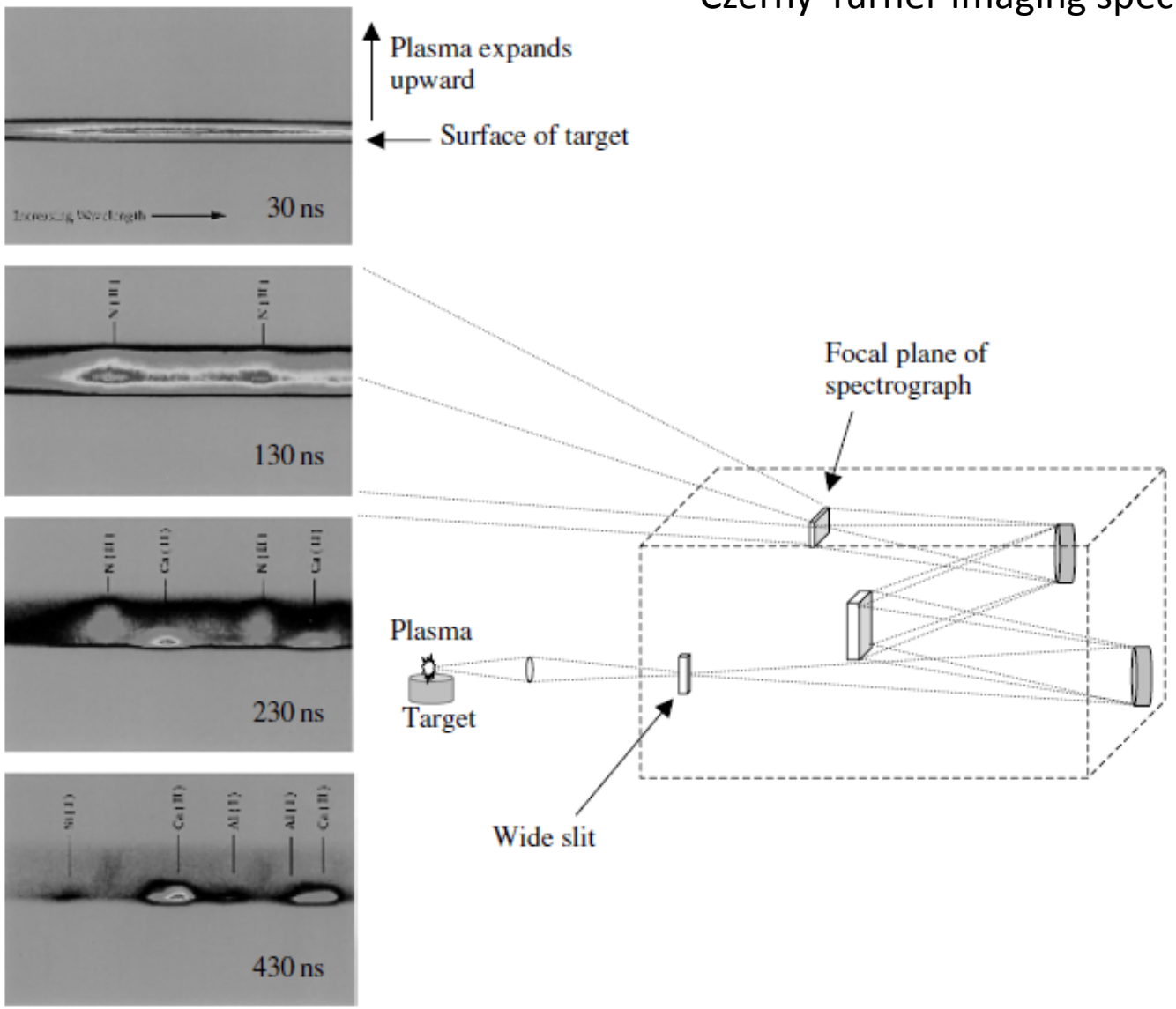

Figure 3.21 (a) Detection of LIBS spectrum using a Czerny-Turner spectrograph and array detector. (b) Examples of LIBS spectra recorded at the focal plane of a spectrograph. (Multari *et al.*, 1996, with permission from Society for Applied Spectroscopy) (see Plate 6)

Time gated 1D imaging of laser ablation plasma produced by ns laser pulses

Imaging and spectrally resolved diagnostics for laser ablation plasmas and pulsed laser deposition (PLD)

Analysis of the ablation of $LaAlO_3$

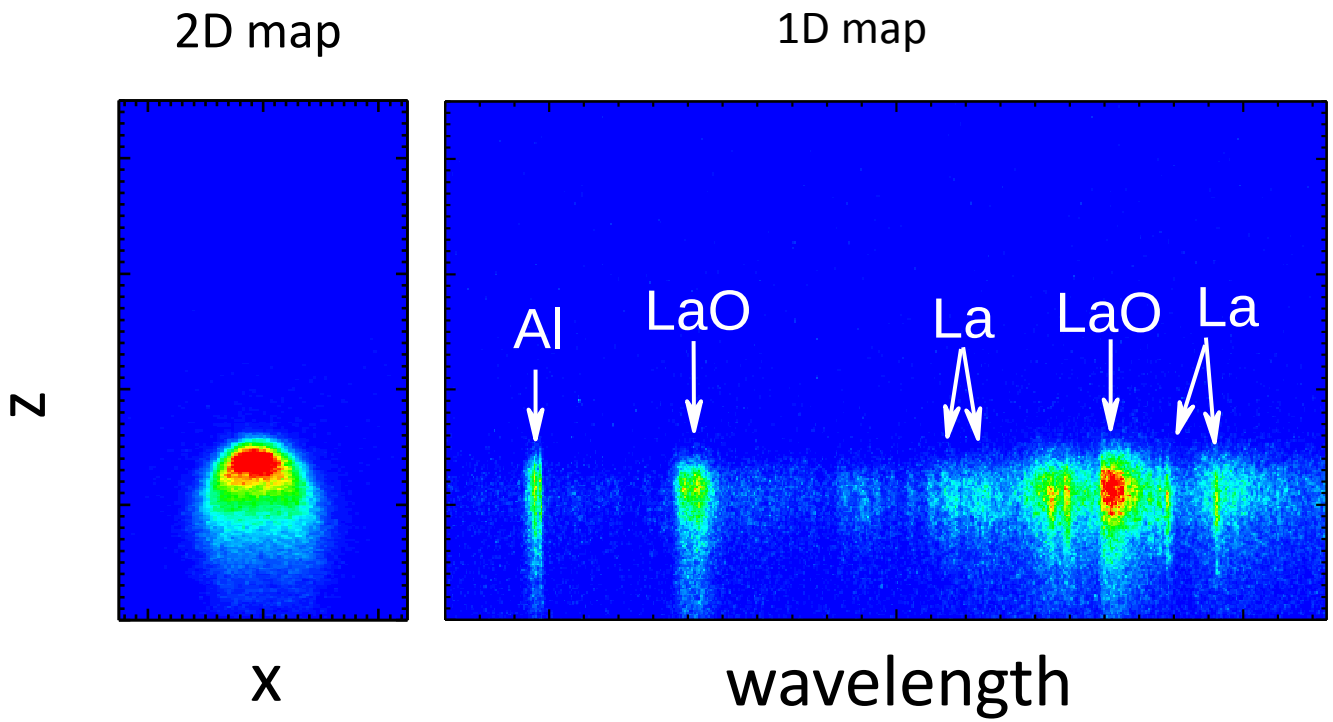

- **Nanosecond excimer laser**
- High vacuum and background gas (10^{-6} – 1 mbar)

(Laser Ablation Group)

Time gated 1D imaging of laser ablation plasma produced by fs laser pulses

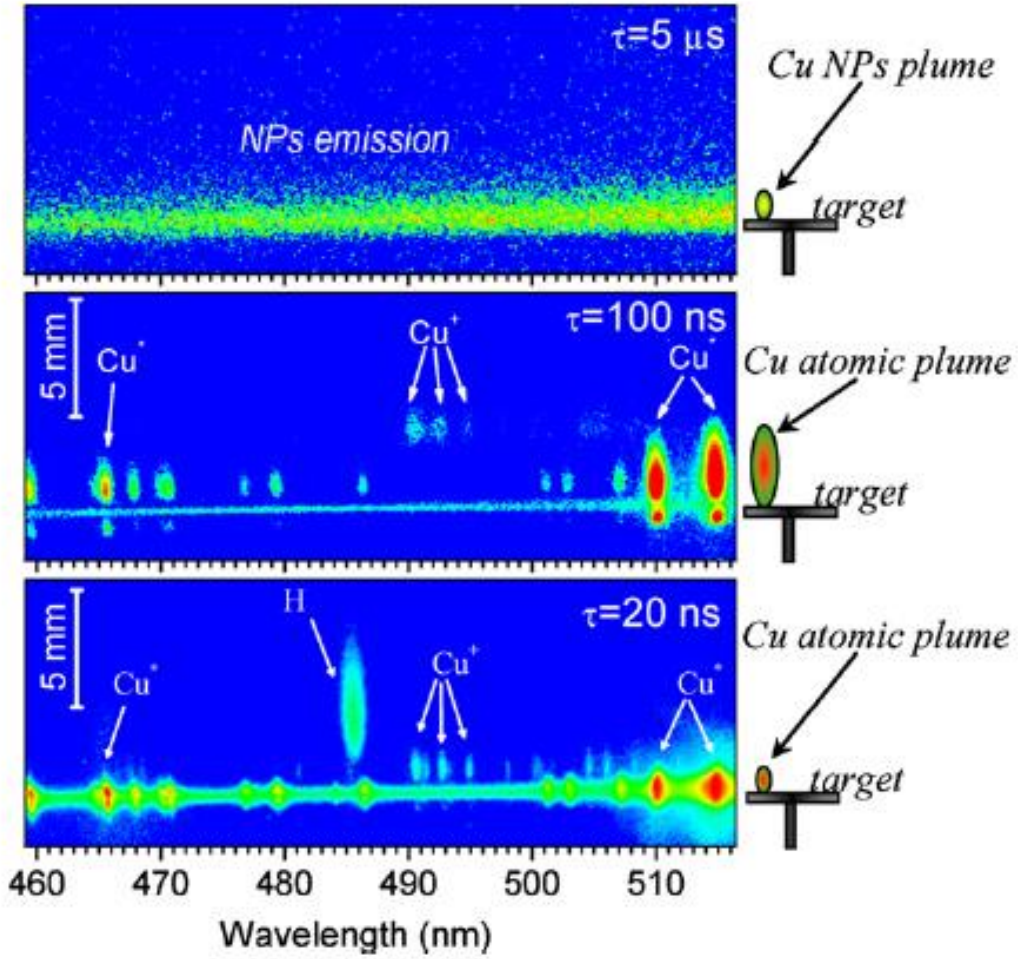

Fig. 1. Time-gated 1D spectrally resolved images of the copper plasma plume in the spectral window (459–518) nm, at three different time delays τ with respect to the laser pulse. The gate width is 20 ns for the two lower panels and 500 ns for the upper panel. A logarithmic intensity scale is used to compensate for the differences in the emission intensities of the various species. Each image is normalized to its own maximum intensity. The drawing on the right side of each panel schematically shows the experimental conditions.

Femtosecond pulses

↓

Atoms and nanoparticles

Ultrafast laser ablation

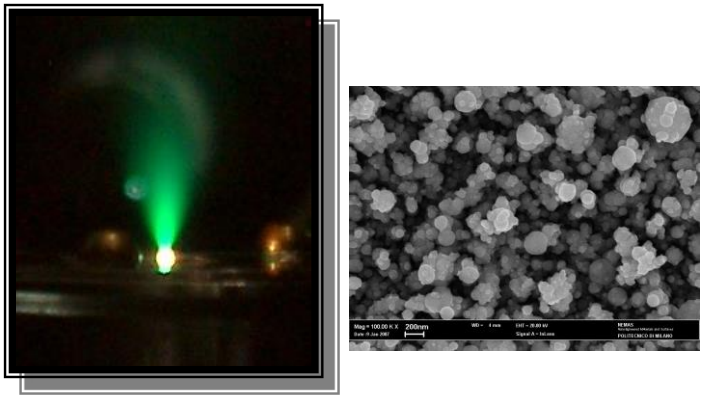

Photo of a fs plume for a silver target in a vacuum and a NPs-assembled film produced by ULA

Spectrally resolved analysis with a spectral filtering

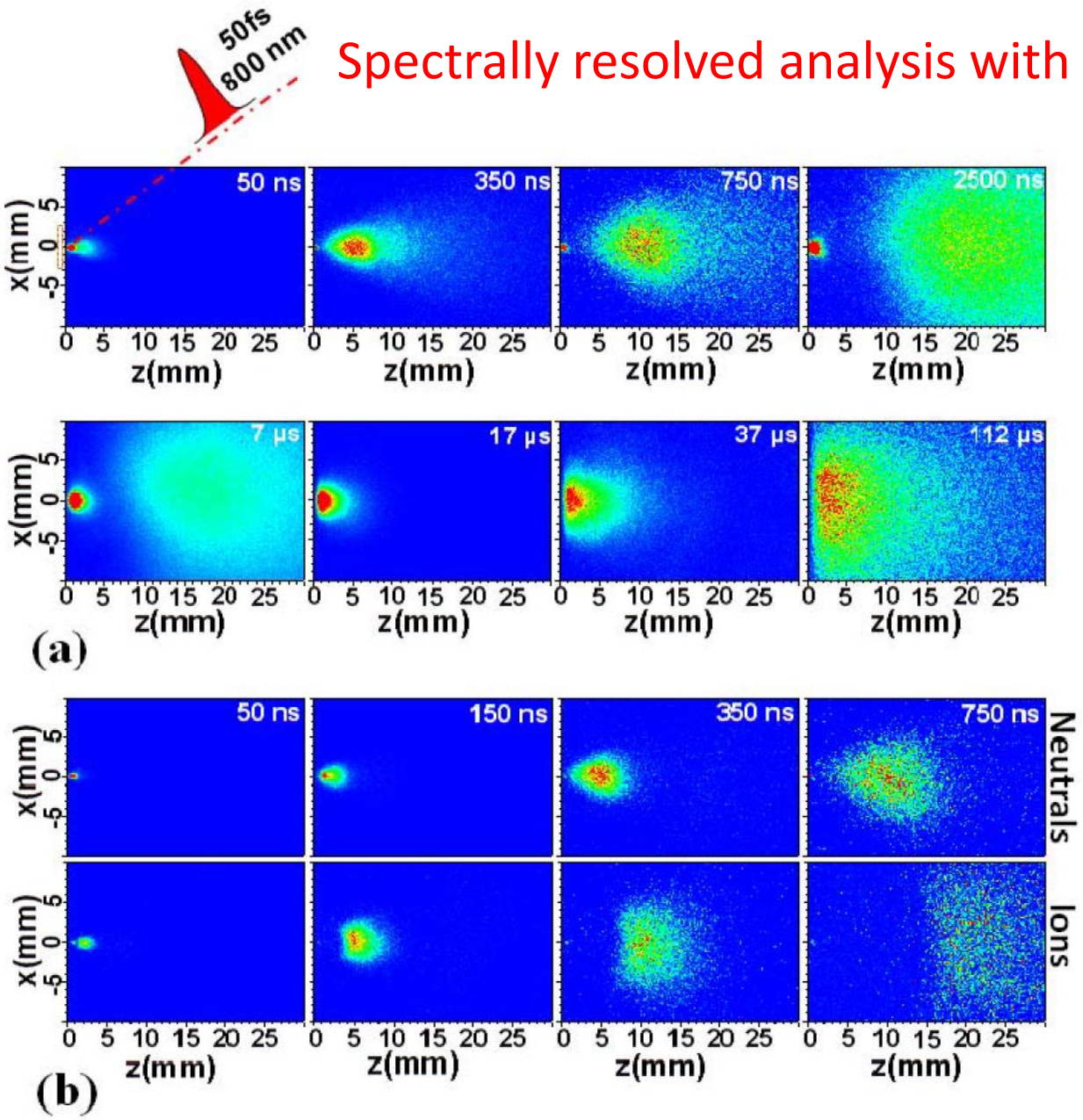

Atomic plume

Nanoparticles plume

Time gated 2D imaging of the atomic plume
Using specie selective optical interferential filters

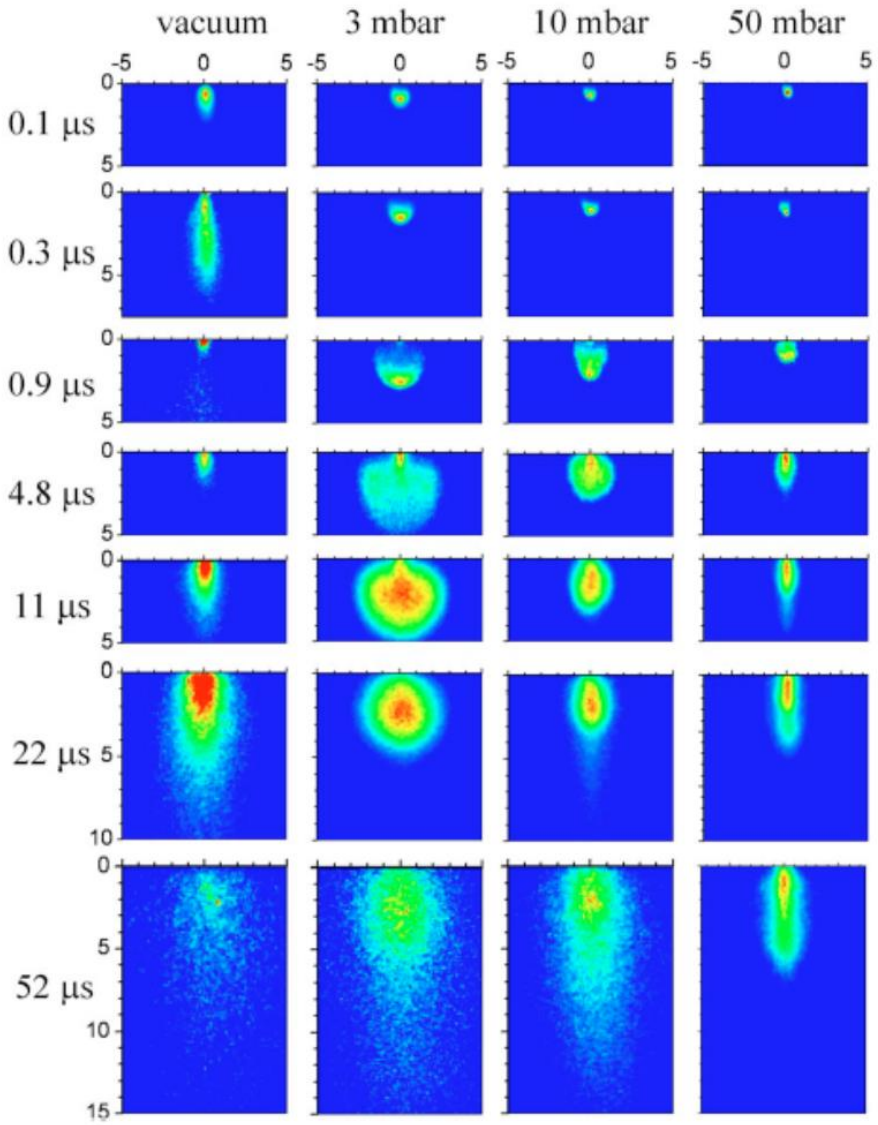

FIG. 1. (Color online) Temporal sequences of the plume self-emission at different background gas pressure. The time on the left side of the snapshots corresponds to the delay τ after the laser pulse. The axes of the images report a scale in millimeters. Each ICCD image is obtained from a different laser shot and is normalized to its own maximum intensity.

Ambient gas confinement

fs pulses
an example from our lab.

Effect of ambient pressure on a Fe plasma produced by fs laser pulses from high vacuum to tens of mbar

Importance of confinement effects on the spatial evolution and intensity

Polychromator

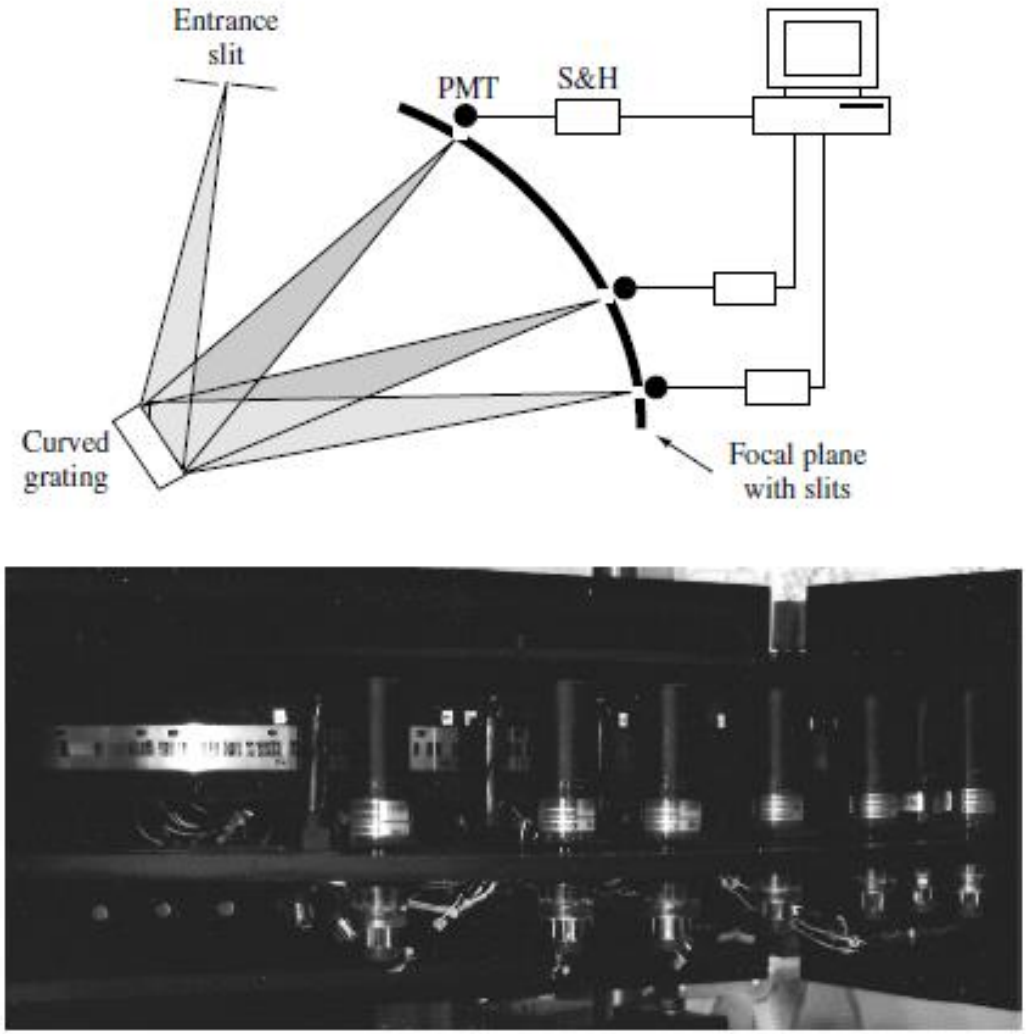

Figure 3.22 Polychromator system with PMTs positioned behind slits in the focal plane. The PMT signal is processed, for example, using a sample-and-hold circuit (S & H). PMT = photomultiplier tube detector

Compact spectrograph (scarse temporal resolution)

- 150 × 94 × 44 mm
- 510 gm
- Power: 100 mA at +5 VDC
- Symmetric crossed Czerny-Turner
- f# = 4, 60 mm fl
- Resolution down to 0.1 nm
- Light integration times down to 1 ms

Figure 3.23 Compact, fiber-optic-coupled spectrograph. (Source: Stellar-Net www.StellarNet.us)

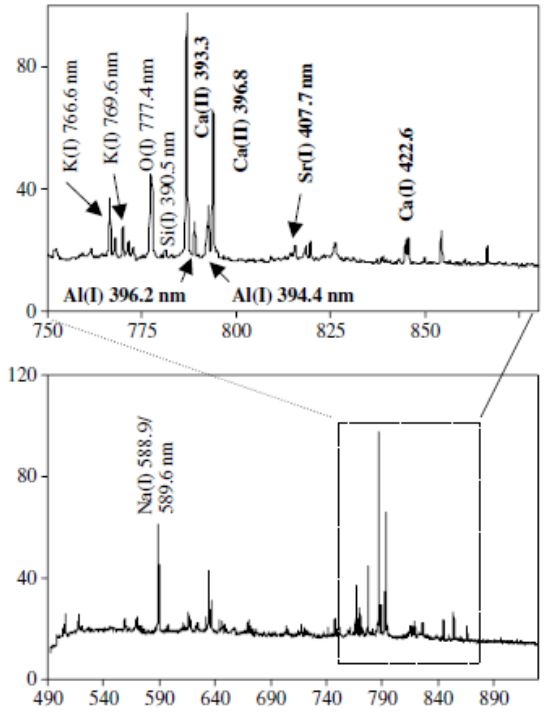

Figure 3.24 Spectrum obtained using a spectrograph similar to that shown in Figure 3.23

Echelle spectrograph (very high spectral resolution, very complex)

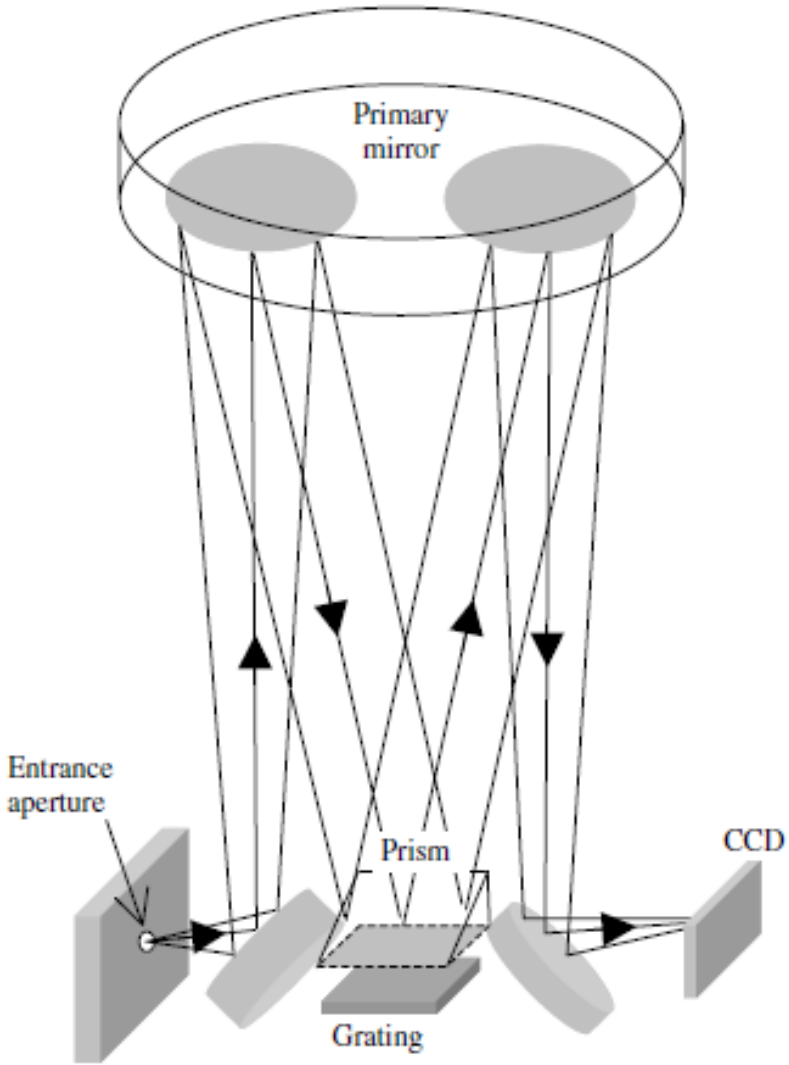

Figure 3.25 Diagram of an echelle spectrograph. (Designed and Manufactured by Optomechanics Research Inc.)

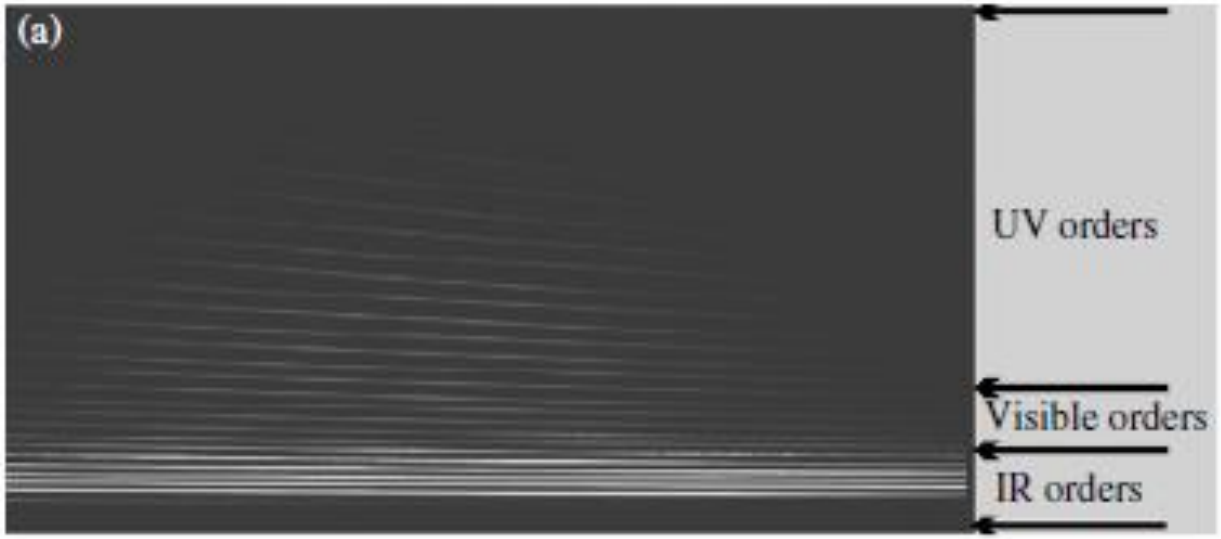

(a) Arrangements of diffraction orders in the focal plane

(a) Emission lines of an Hg calibration lamp

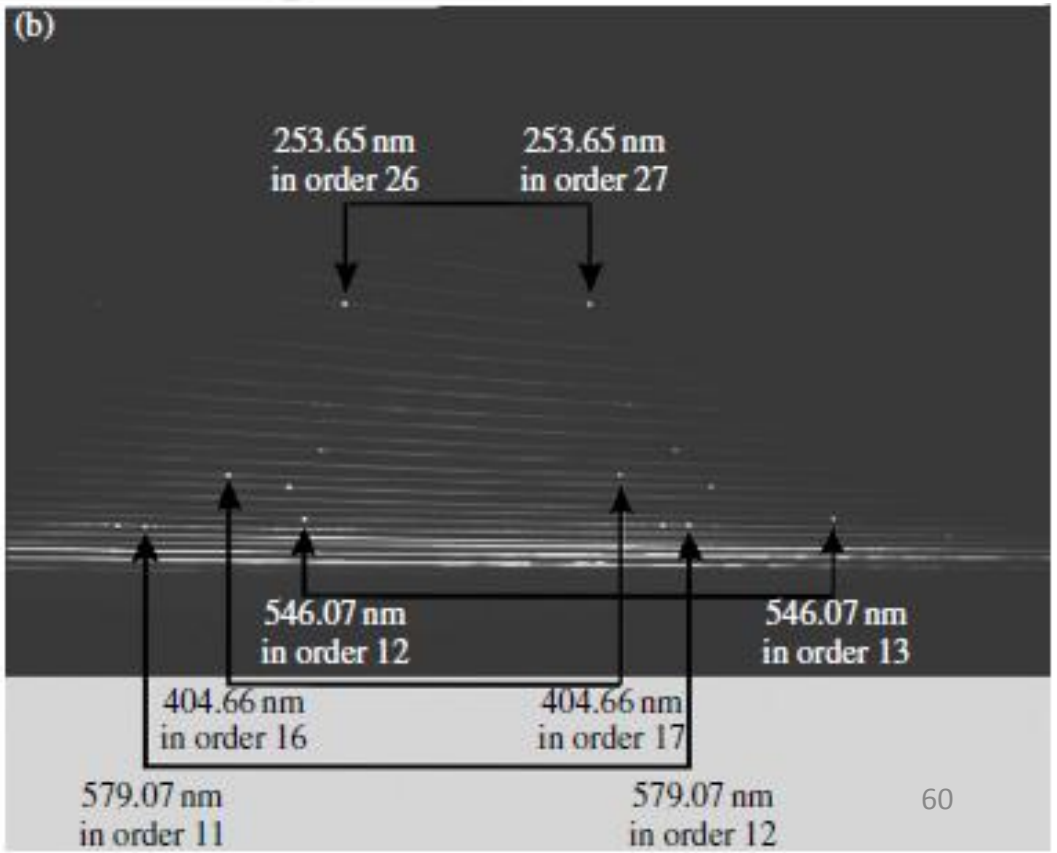

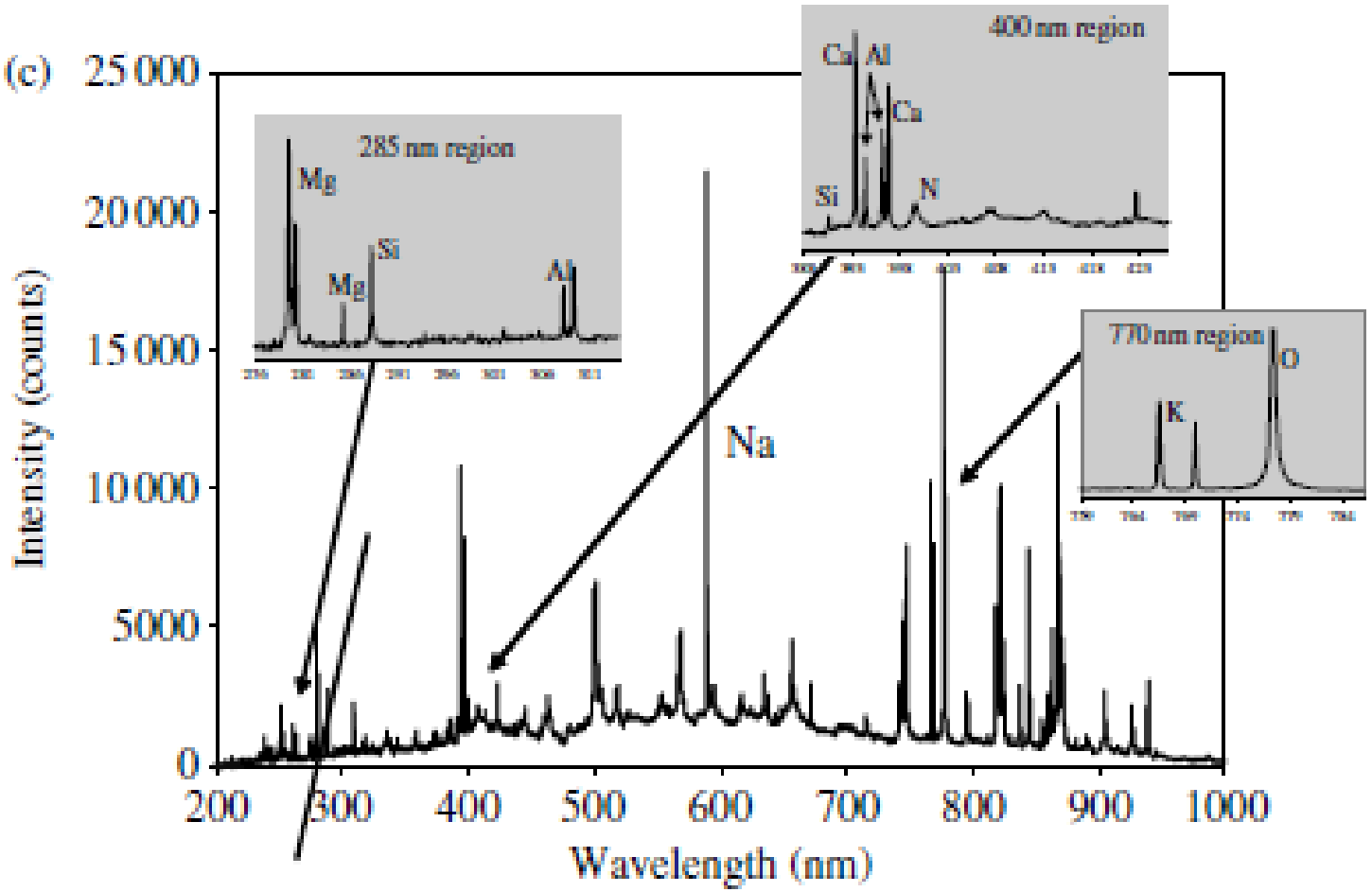

LIBS spectrum of a soil recorded with an Echelle spectrograph couple to an ICCD

DETECTION SYSTEM CALIBRATIONS

WAVELENGTH CALIBRATION

Table 3.9 Hg calibration spectrum (Data sourced from Sansonetti *et al.*, 1996, with permission from Optical Society of America)

Wavelength (nm)	Intensity[a]
253.6521	300 000
289.3601	160
296.7283	2600
302.1504	280
312.5674	2800
313.1655	1900
313.1844	2800
334.1484	160
365.0168	5300
365.4842	970
366.2887	110
366.8284	650
404.6565	4400
407.7837	270
434.7506	34
435.8385	10 000
546.0750	10 000
576.9610	1100
579.0670	1200

[a] Relative units with the measured value of the 436 nm line arbitrarily set to 10 000.

CALIBRATION LAMPS ….

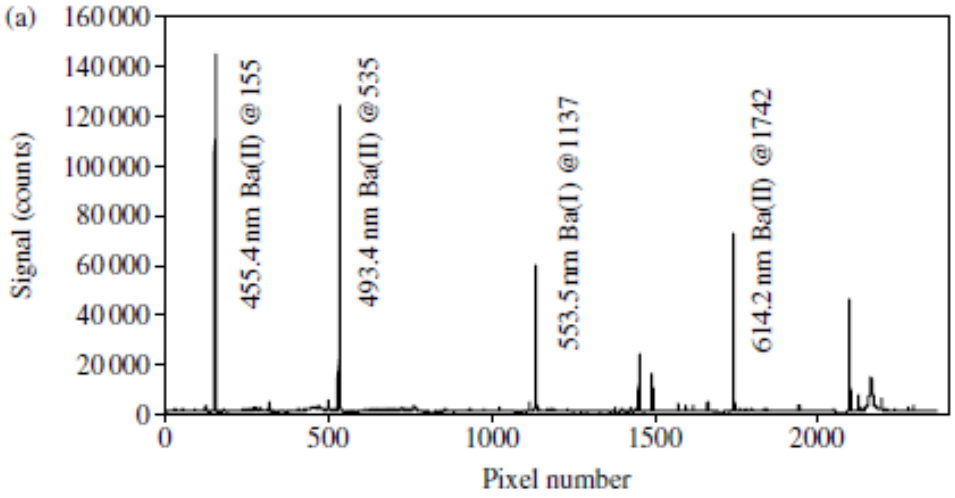

…. OR IDENTIFYBLE SPECTRAL LINES

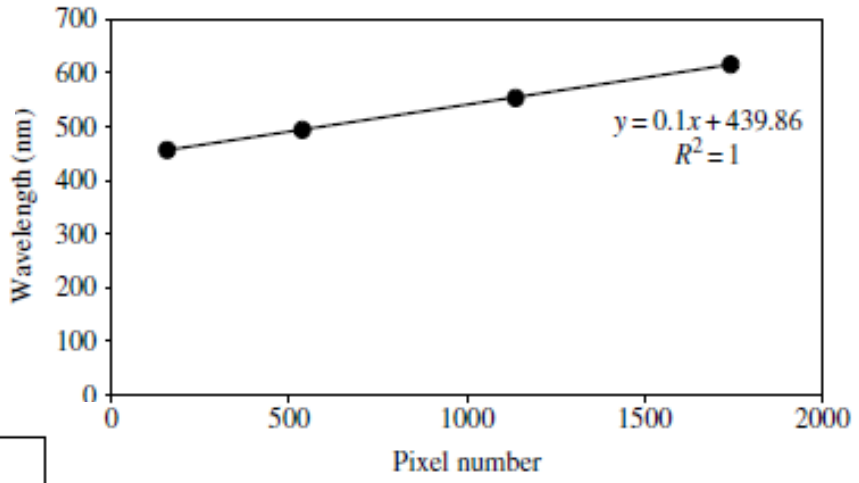

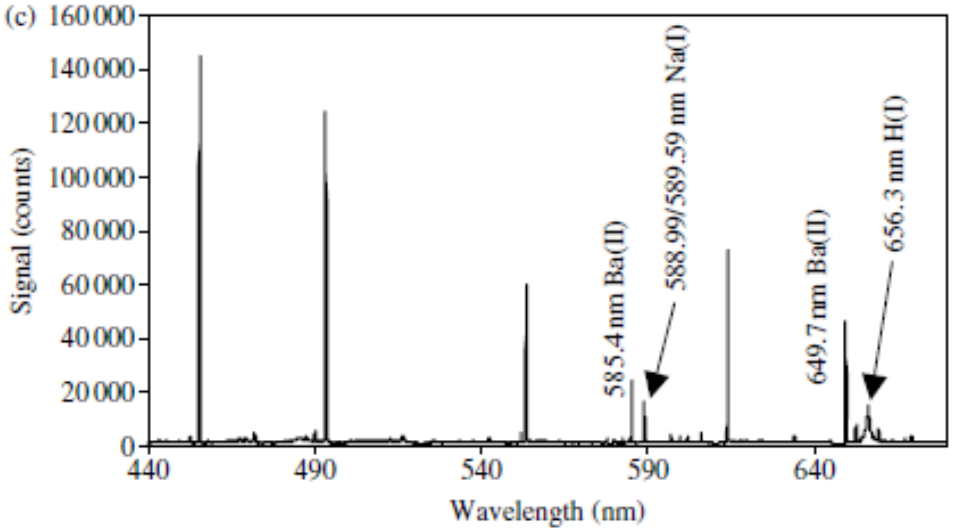

SPECTRAL RESPONSE CALIBRATION

Each component of a LIBS detection system has a certain spectral response curve associated with it $r(\lambda)$. That is, the response depends on wavelength such that not all wavelengths are transmitted through or reflected off optical components with the same transfer efficiency. In addition, the detector used to record the light has a response function that is wavelength dependent. The end result is that the complete detection system (fiber optic, spectrograph, detector, lenses, etc.) will show a sensitivity that is wavelength dependent. In some cases it may be important to know how the response of the detection system varies with wavelength. As an example, the relative intensities of emission lines in different regions of the spectrum may be compared independent of the detection system response. In principle, the total response of a detection system may be computed from the separate response curves of the different components. Consider Figure 3.34 which shows response curves for the spectrograph, detector, and fiber optic cable. The responses have been normalized to 100 as most often it is the relative response of the system that must be computed with absolute response seldom used. By multiplying the different response curves, the total response $r_{TOT}(\lambda)$ can be determined:

$$r_{TOT}(\lambda) = r_{FOC}(\lambda) \times r_{SPEC}(\lambda) \times r_{DET}(\lambda). \quad (3.6)$$

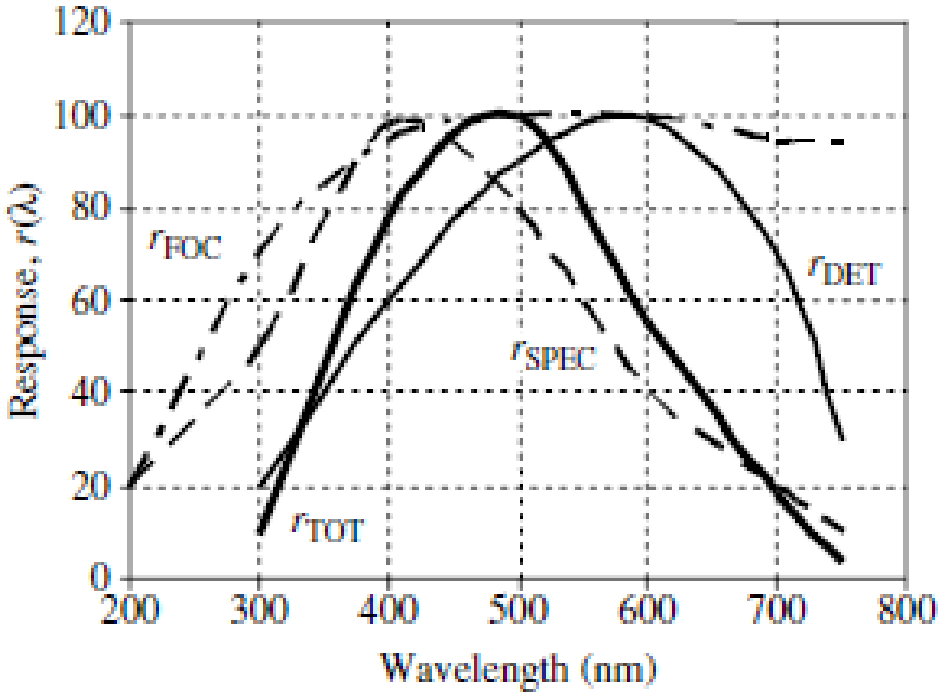

Figure 3.34 Response curves for different components of a LIBS detection system along with the total response curve

$$r_{\mathrm{TOT}}(\lambda) = r_{\mathrm{FOC}}(\lambda) \times r_{\mathrm{SPEC}}(\lambda) \times r_{\mathrm{DET}}(\lambda)$$

TIMING CONSIDERATIONS

TIME GATED METHODS ARE USUALLY MUCH BETTER

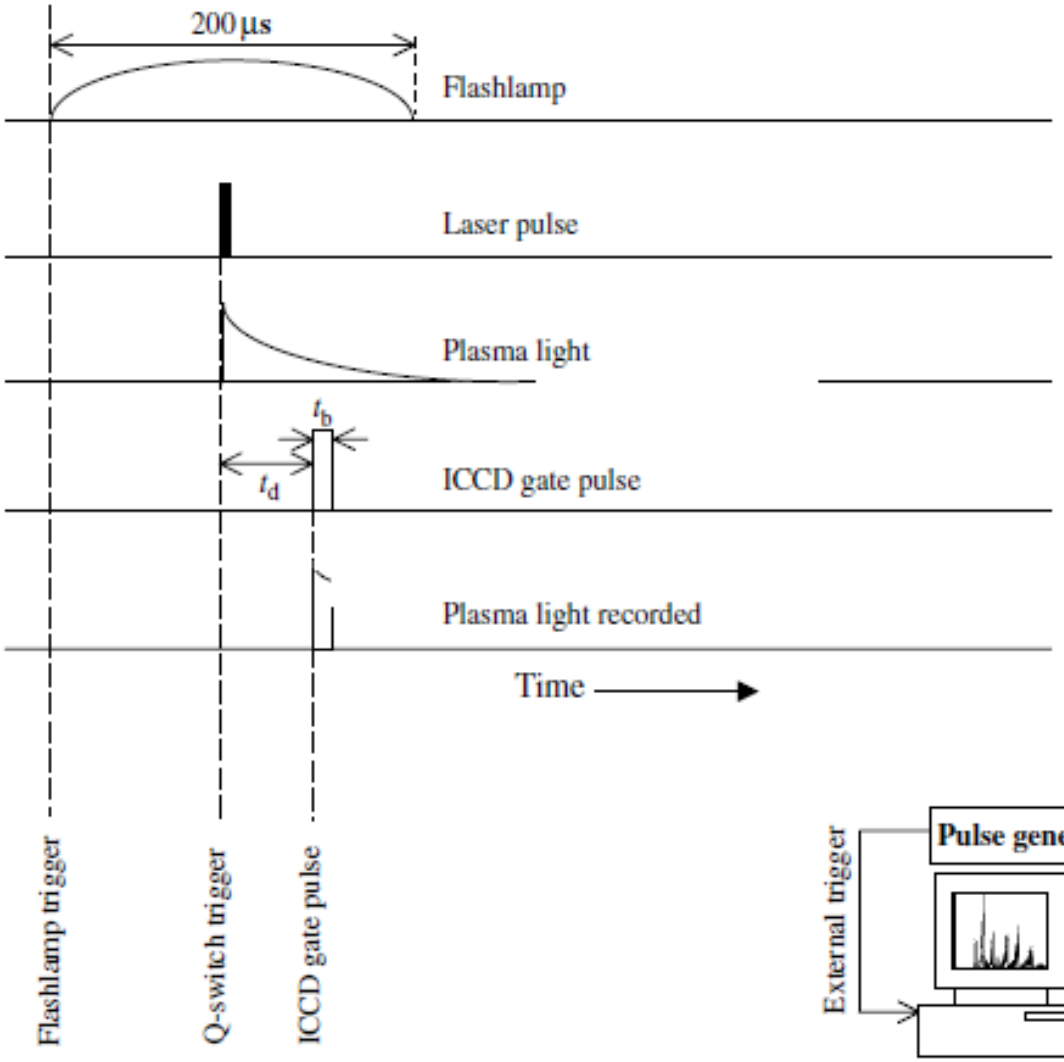

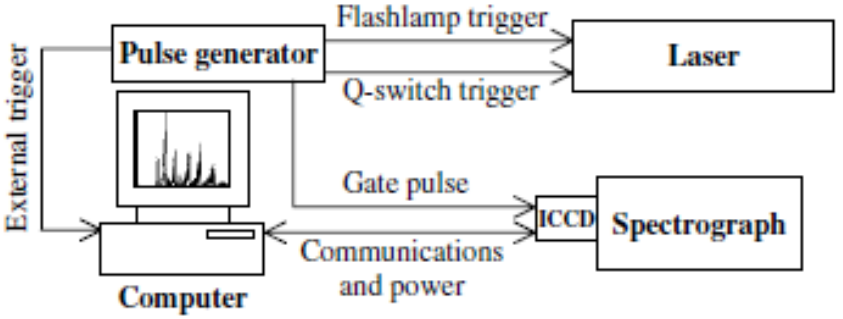

gure 3.35 Typical timing used in a LIBS experiment

METHODS OF LIBS DEPLOYMENT

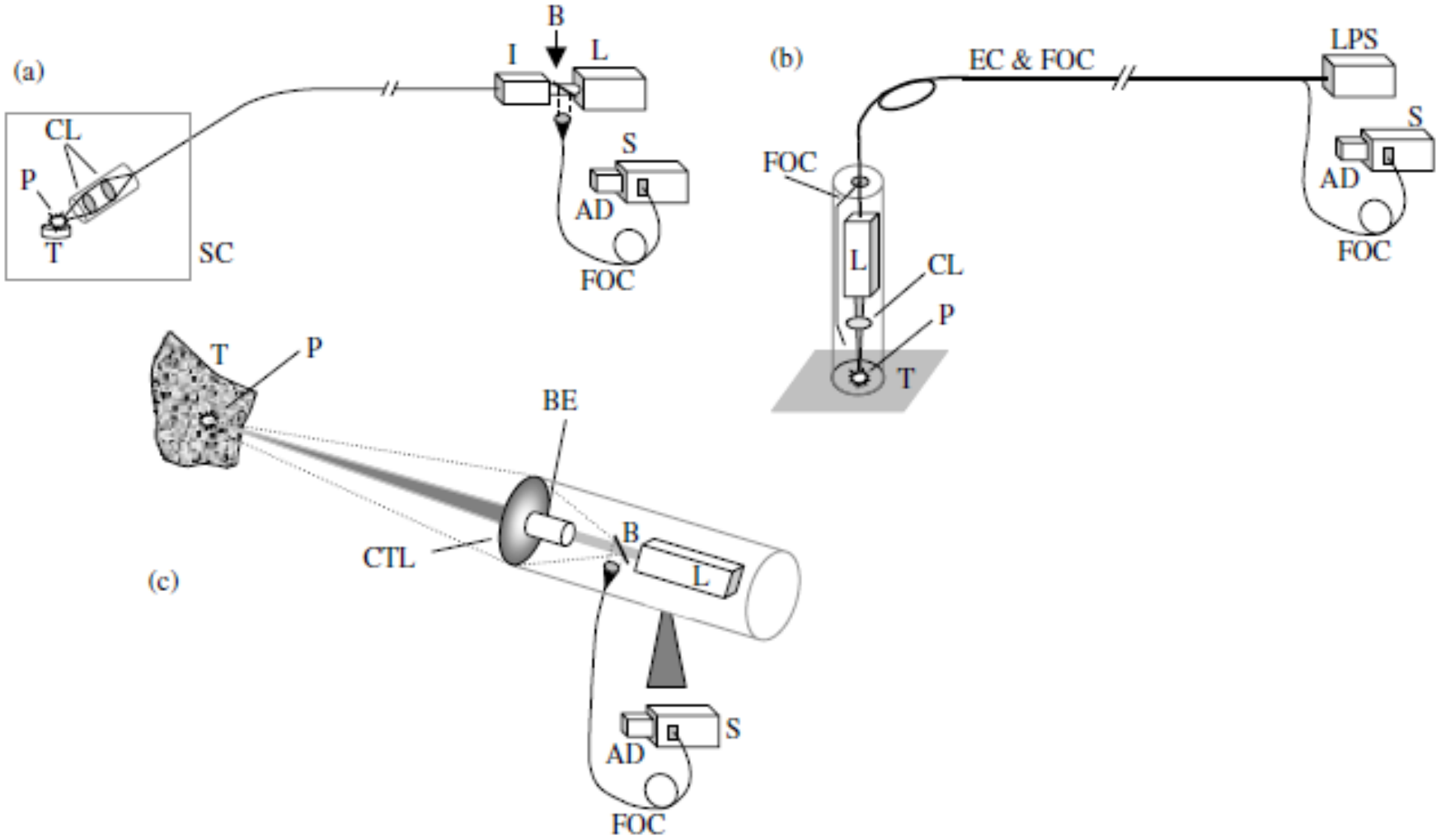

Figure 3.36 Three possible configurations (a–c) for LIBS analysis in addition to direct analysis (Figure 3.1). L, laser; B, beamsplitter; FOC, fiber optic cable; I, pulse injector for FOC; CL, lens; T, target; P, plasma; S, spectrograph; AD, array detector; CTL, collection lens; EC, electrical cables; LPS, laser power supply; BE, beam expander

LIBS methods extension

Double and multiple pulses

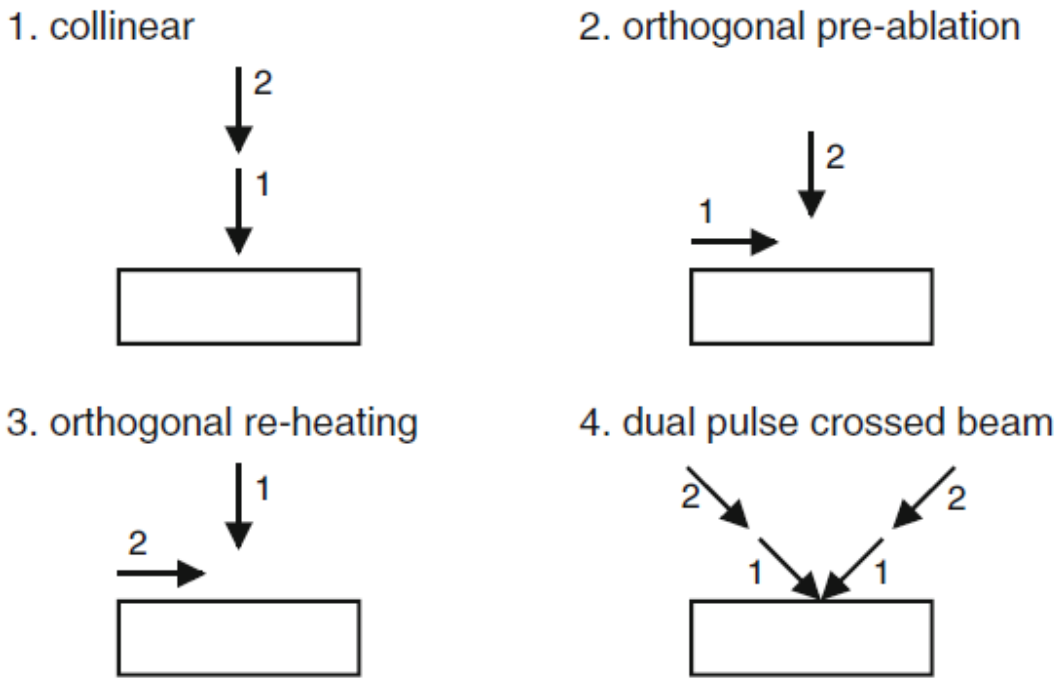

Fig. 6.1 Double-pulse configurations studied for LIBS. The *arrows* depict the laser pulses and their direction of propagation and the *numbers 1, 2* their temporal sequence

In Ambient Air

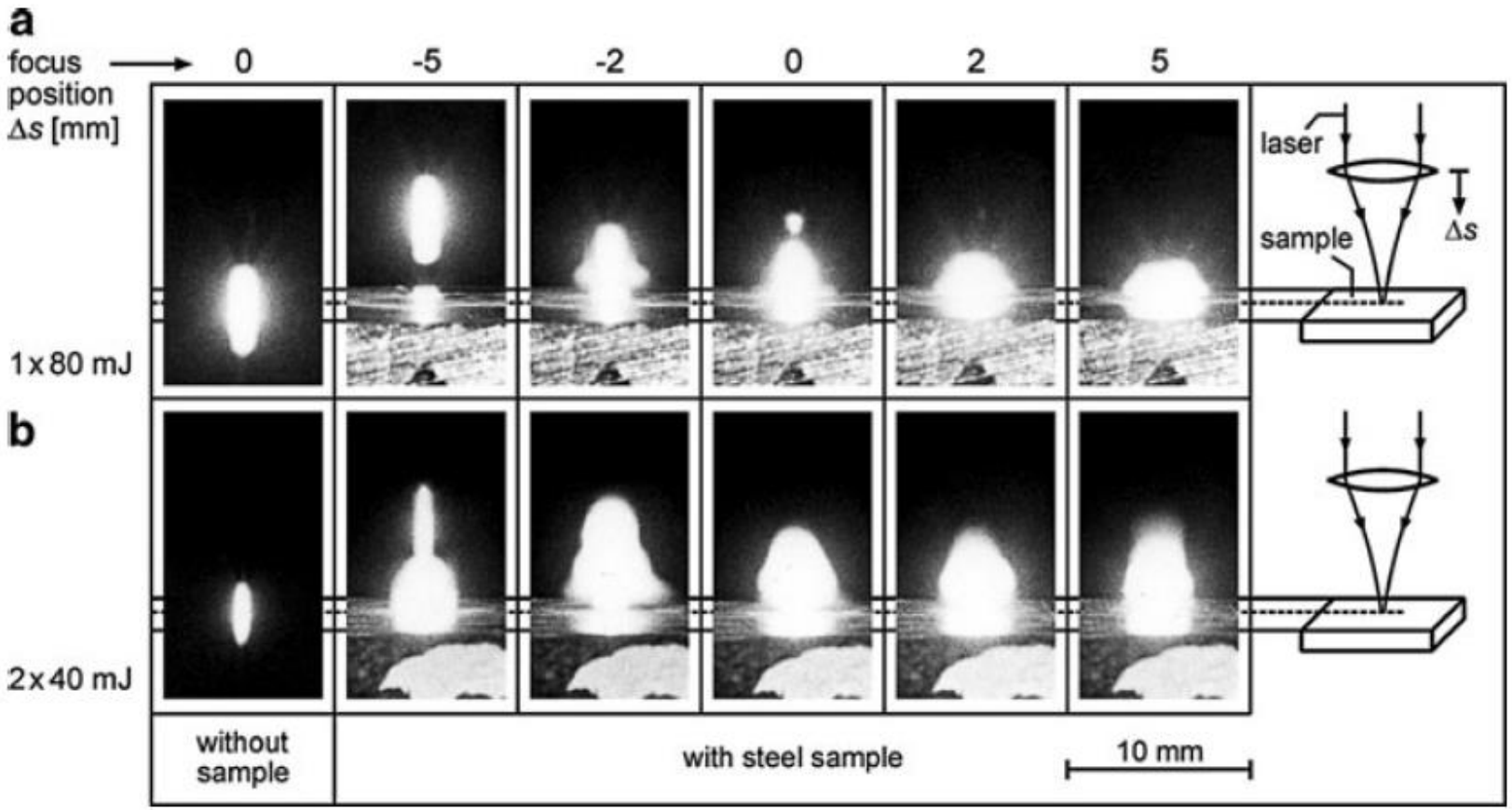

Fig. 6.2 Time-integrated photographs of the plasmas in the visible spectral range induced in the atmosphere and on a steel surface by single and double laser pulses of 80 mJ burst energy. The distance between the focal plane of the laser beam and the surface of the sample is denoted by Δs, see text for details

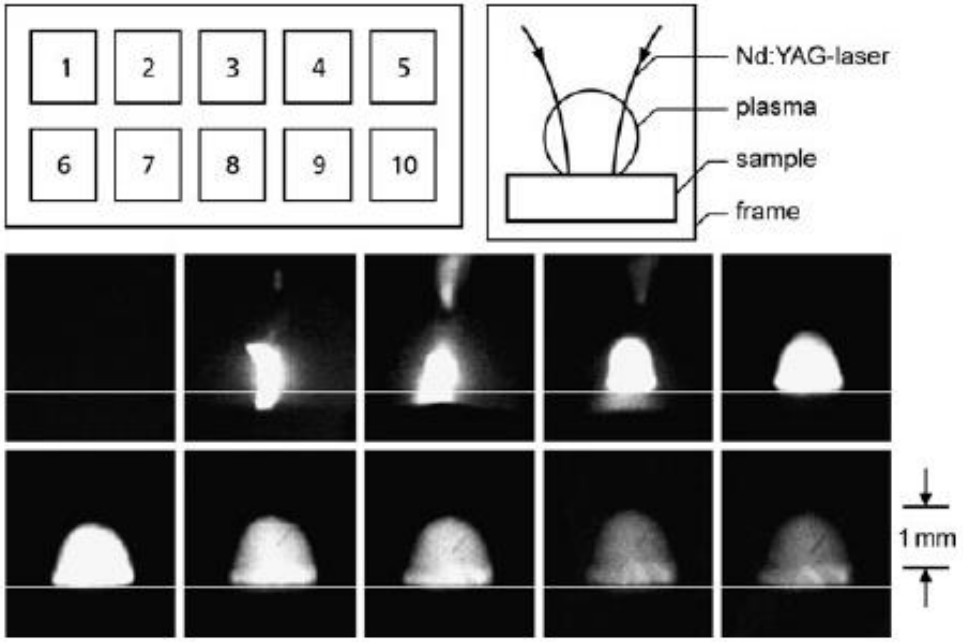

In Ambient Air

Single pulse

Fig. 8.3 Framing images of the laser-induced plasma after the first pulse of a double pulse. Exposure time 10 ns per frame, time between subsequent frames 50 ns. The time sequence of the frames is shown on the *top left* with the *numbers 1–10*. The view detected by the frames is illustrated schematically on the *top right*. The *white horizontal line* in each frame indicates approximately the position of the sample surface. Laser parameters: 2×40 mJ, interpulse separation 6 µs

Double pulse

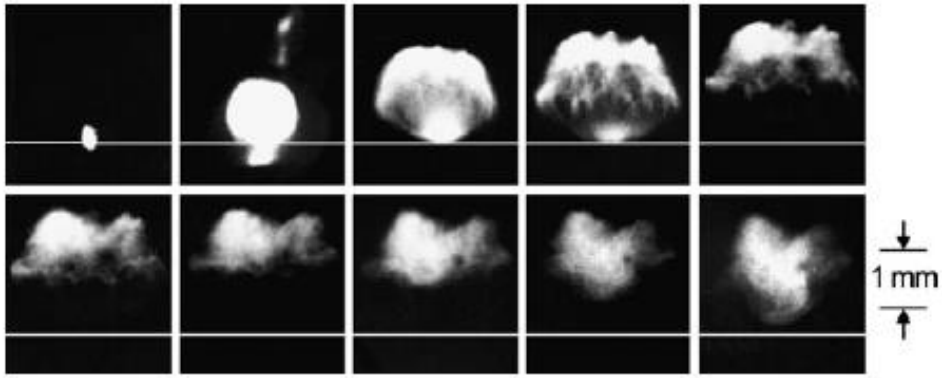

Fig. 8.4 Framing images of the laser-induced plasma after the second pulse of a double pulse. Experimental settings and arrangement of frames are the same as for Fig. 8.3

fs pulses
another example
from our lab.

Double pulse approach

vacuum environment

Various time lags between the two pulses in the 0-2 ns range can change the emission intensity of the atomic and NPs components

Optical delay line is needed

Long delays not easily achievable

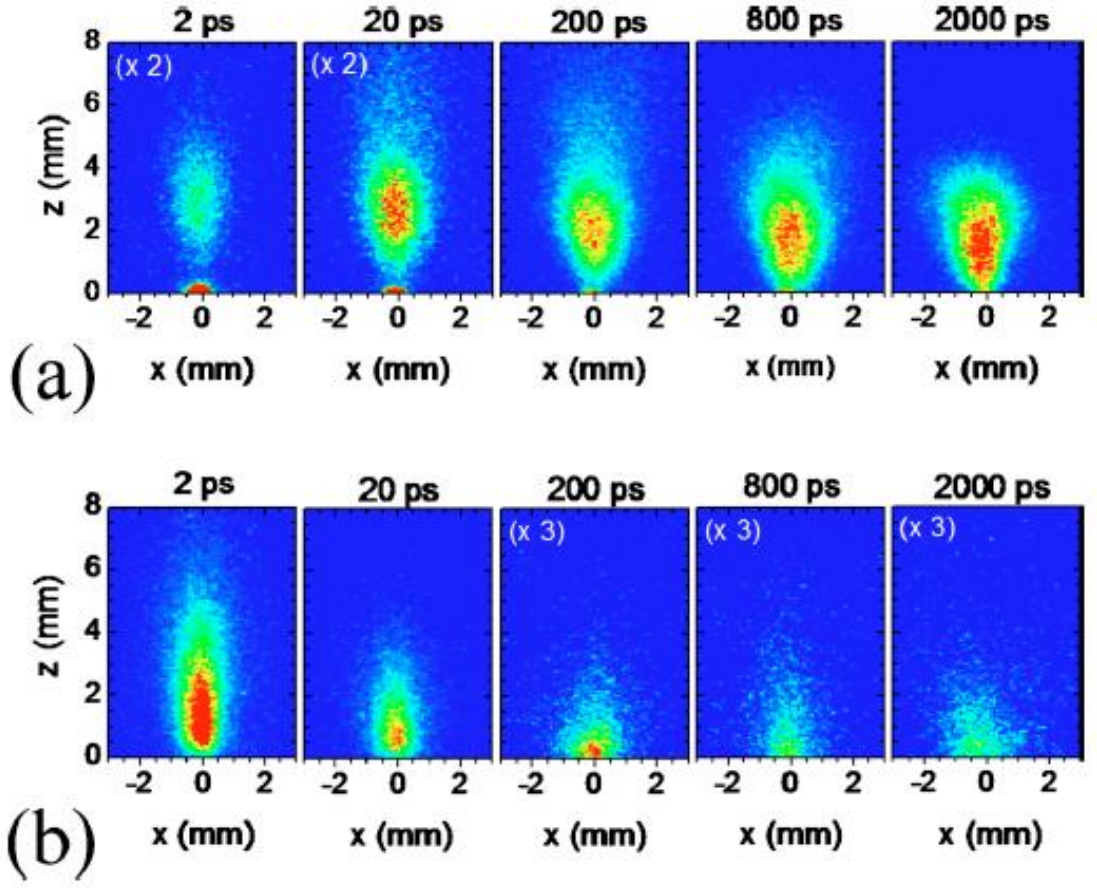

FIG. 7. (Color online) (a) Snapshots of the atomic plume emission at different delays Δt, acquired 200 ns after the ablating laser pulse with a gate width of 50 ns. (b) Snapshots of the NP plume emission at different delays Δt, acquired $\approx$10 μs after the ablating laser pulse with a gate width of 5 μs. The delay Δt is reported on the top of each image. The number in parenthesis in the top-left corner of the image indicates that the intensity has been multiplied by that factor. z=0 marks the position of the target surface. The intensity is plotted in linear scale.

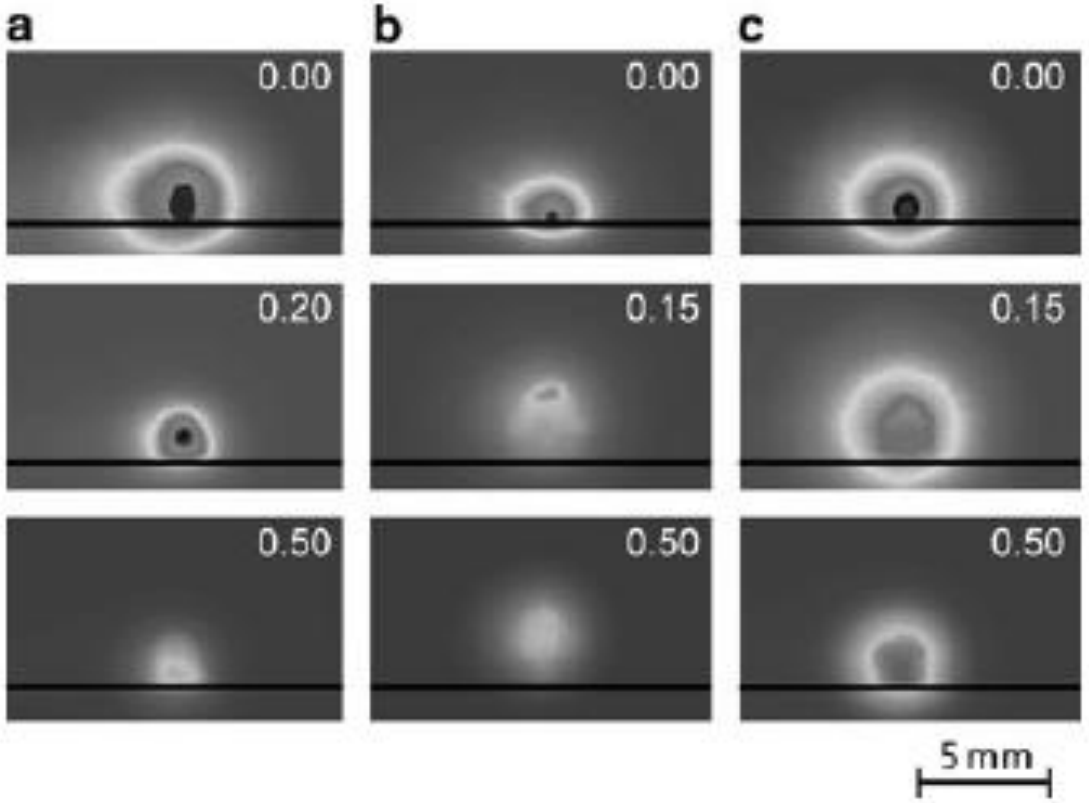

Fig. 8.12 Comparison of the plasma emission for (a) a single pulse of 80 mJ, (b) a symmetric double pulse with 2×40 mJ, and (c) an asymmetric double pulse with $E_1 = 10$ mJ and $E_2 = 70$ mJ. The *numbers* in the *upper right corner* of each image show the delay time t_{delay} in microseconds of the start of the exposure with respect to the last pulse irradiated

Electrical delay
with synchronization
or
special DP laser sources

Time lag between the two pulses Δt=6 μs
Exposure time Δt_{int}=50 ns

Appropriate time lag and energy ratio between the two pulses can improve the emission intensity

Applications

Due to its potential to handle samples in the solid, liquid and gaseous (including aerosols) form, which may or may not be conductive, LIBS has been applied both for qualitative and quantitative purposes in a multitude of matrices of interest to many areas. Some of these applications are unique to LIBS and make use of the intrinsic attributes of the technique, such as its microanalyses capability, possibility of remote analyses and quasi-non-destructive nature.

J. Braz. Chem. Soc., Vol. 18, No. 3, 463-512, 2007.
Printed in Brazil - ©2007 Sociedade Brasileira de Química
0103 - 5053 $6.00+0.00

Review

Laser Induced Breakdown Spectroscopy

Celio Pasquini, Juliana Cortez, Lucas M. C. Silva and Fabiano B. Gonzaga*

Instituto de Química, Universidade Estadual de Campinas, CP 6154 13084-971 Campinas-SP, Brazil

The following section does not intend to be an extensive overview, but provides the most significant, representative and recent analytical applications of LIBS, as reported in the literature.

Alloys and metallurgic samples

Archaeological materials and art objects

Use in pottery and ceramic analysis

LIBS for determination of pigments and inks

Medical and biological applications

Environmental applications

Aerosol measurements by LIBS

LIBS for analysis in space

Forensic analysis

Military and homeland-security applications

Application to pharmaceutical products

Chemometrics applications

Miscellaneous applications

ARTICLE

JAAS
www.rsc.org/jaas

***In situ* interferometric depth and topography monitoring in LIBS elemental profiling of multi-layer structures†**

Dimitris G. Papazoglou, Vassilis Papadakis and Demetrios Anglos*

Institute of Electronic Structure and Laser, Foundation for Research and Technology – Hellas, P.O. Box 1527, GR 71110 Heraklion, Crete, Greece. E-mail: anglos@iesl.forth.gr; Fax: 30 2810 391318; Tel: 30 2810 391154

Elemental depth profiling of semiconductor wafers

Elemental depth profiling of daguerreotype

Many other examples of interest are present in the literature

Principles of Optical Emission Spectroscopy and Laser Induced Plasma/Breakdown Spectroscopy

Salvatore Amoruso

Lectures for the course of Atomic and Molecular Physics and Laser Spectroscopy

Laser Induced Fluorescence

- Introduction
- General principles
- Example of applications

Adapted from a presentation of the

COMBUSTION ENERGY FRONTIER RESEARCH CENTER

PRINCETON UNIVERSITY

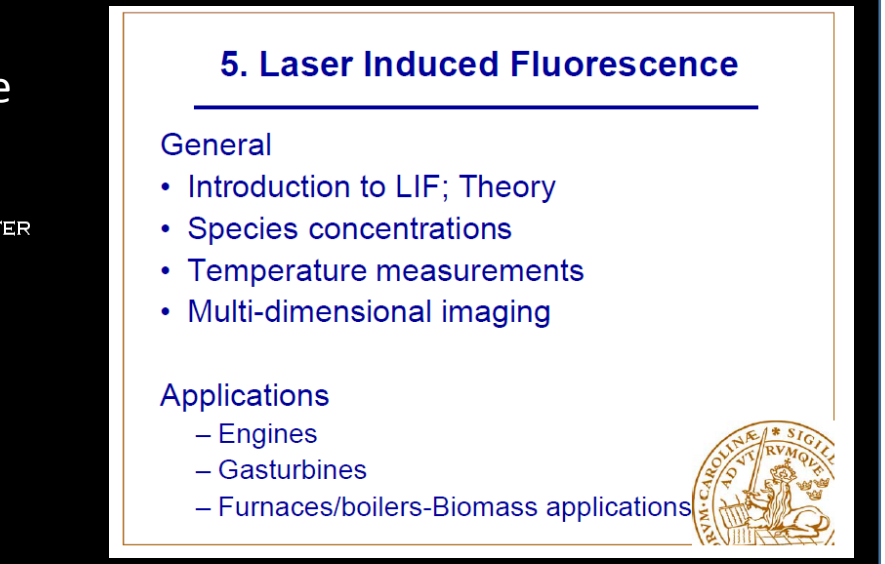

Laser-induced fluorescence

LIF:

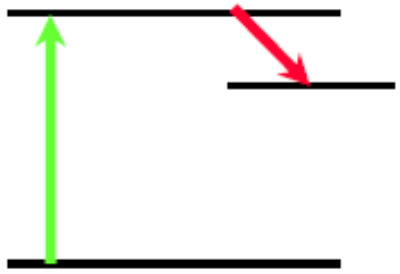

Measures e.g, NO, OH,
CH, CN, C_2, O_2, fuel-tracer

General features

- High sensitivity
- 2D imaging capabilities
- Measure temperature and concentration
- Quantification problem

Fluorescence spectrum

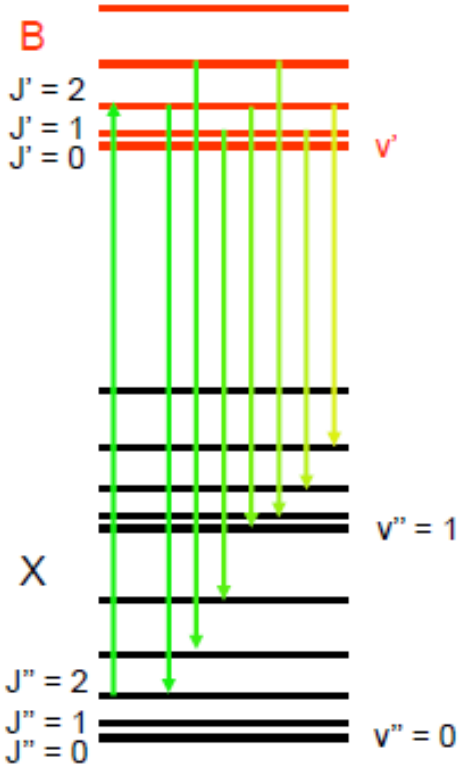

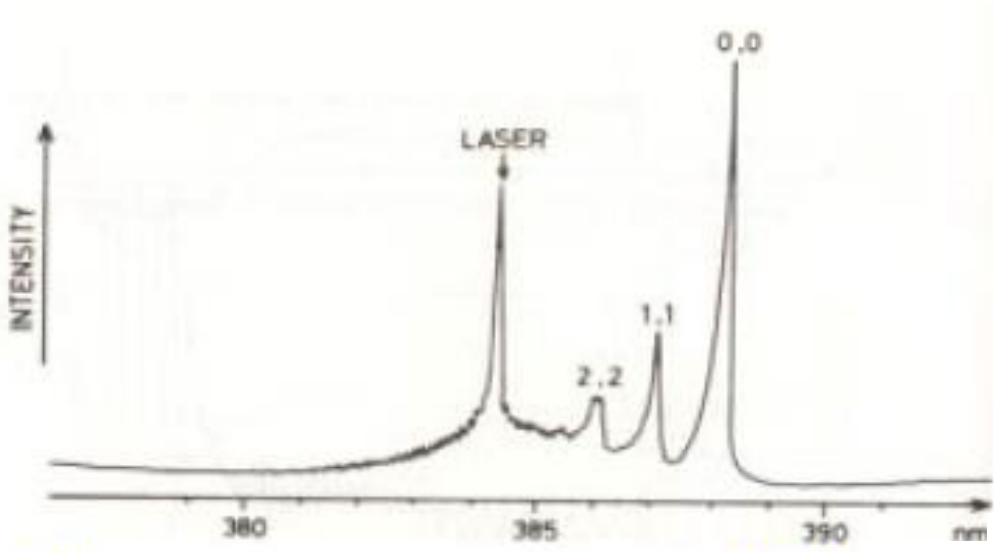

Fluorescence spectrum of CN

Laser tuned to a specific absorption line and the spectrometer is scanned

Important molecules detected by LIF

Molecule	Abs. wavelength (nm)
OH	~306
C_2	~516
CH	~431
CN	~388
NH	~336
NO	~226
CH_2O	~320-360
NO_2	450-470

LIF Theory

S ~ $A_{21}N_2$, How is N_2 related to N_{tot} ?

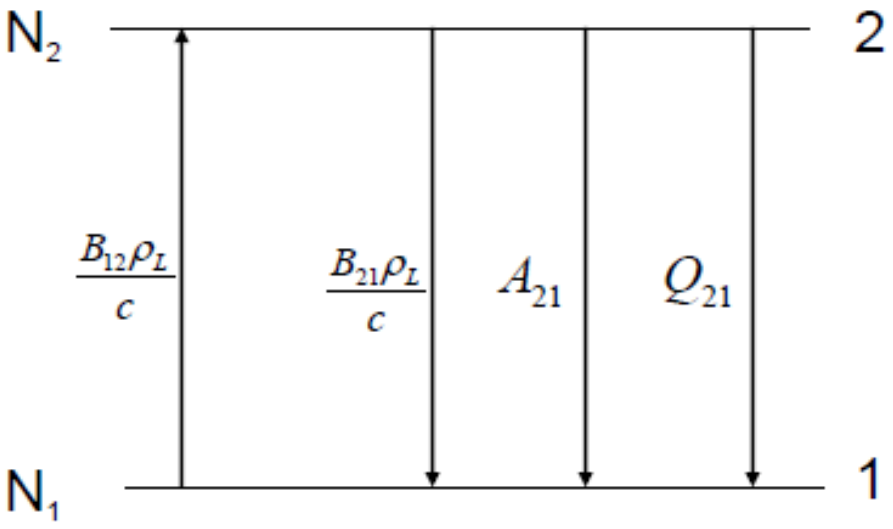

Rate equation analysis

$$\frac{\partial N_1(t)}{\partial t} = -N_1(t)\frac{B_{12}\rho_L}{c} + N_2(t)\left(A_{21} + Q_{21} + \frac{B_{21}\rho_L}{c}\right)$$

$$\frac{\partial N_2(t)}{\partial t} = N_1(t)\frac{B_{12}\rho_L}{c} - N_2(t)\left(A_{21} + Q_{21} + \frac{B_{21}\rho_L}{c}\right)$$

$N_{tot} = N_1 + N_2$ and assume steady state; dN/dt=0

$b_{ij}=B_{ij}/c$

$A_{21}/B_{21}=8\pi h/\lambda^3$

$$N_2 = \frac{N_{tot} b_{12} \rho_L}{A_{21} + Q_{21} + (b_{21} + b_{12}) \rho_L}$$

$$S = A_{21} \frac{N_{tot} b_{12} \rho_L}{A_{21} + Q_{21} + (b_{12} + b_{21}) \rho_L}$$

Fluorescence power versus laser irradiance

$$S = \rho_L \frac{A_{21} N_{tot} b_{12}}{(b_{12} + b_{21})\rho_L + (A_{21} + Q_{21})}$$

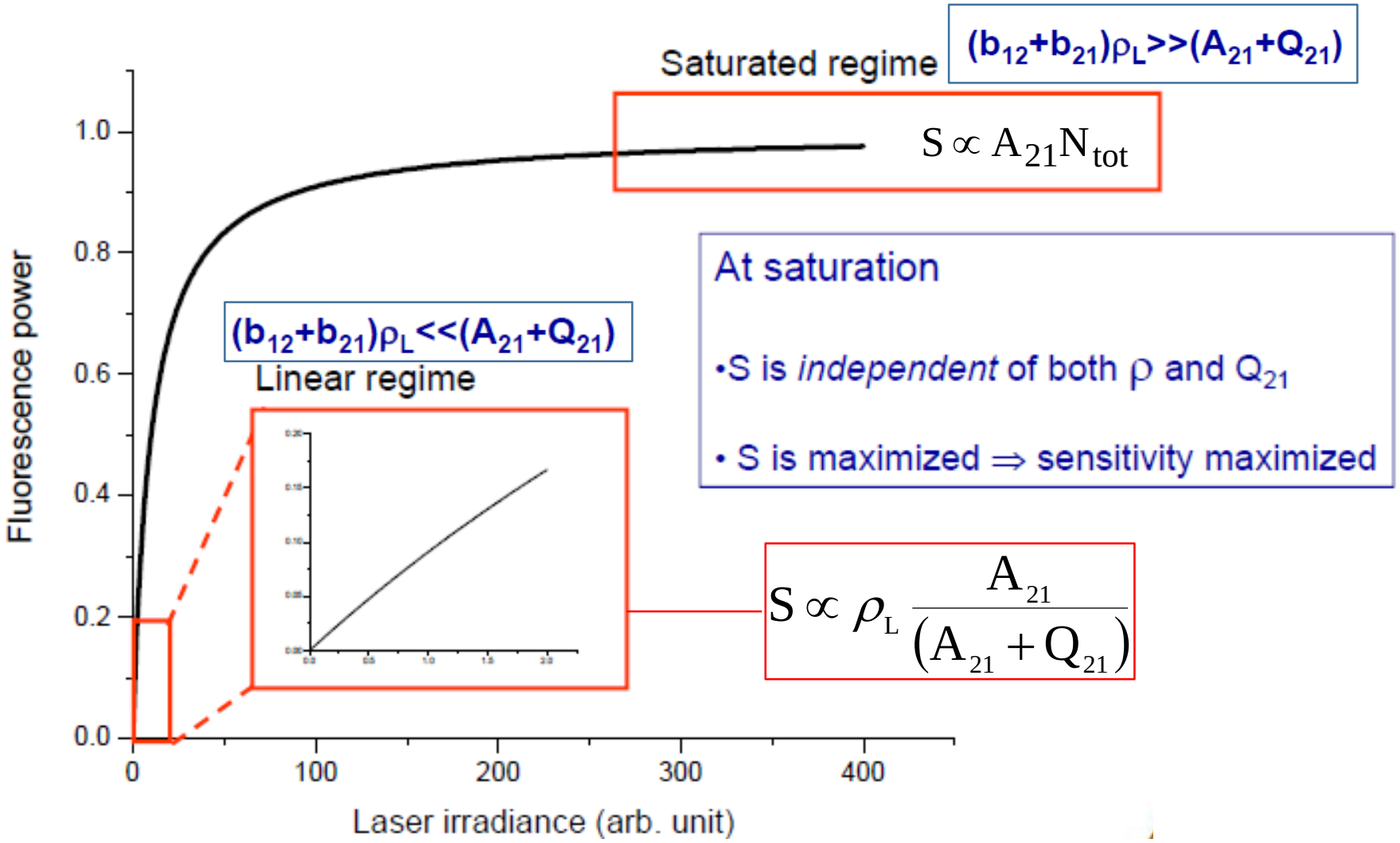

LIF in the linear regime

Fluorescence efficiency

$$S \propto \rho_L \frac{A_{21}}{(A_{21} + Q_{21})}$$

- The fluorescence is linearly proportional to the input laser irradiance
- Since most often $A_{21} << Q_{21}$, the fluorescence efficiency is generally <<1, which diminishes the sensitivity
- For quantitative measurements usually Q_{21} has to be evaluated
- Q_{21}(p,T,composition) $\Rightarrow$ difficult to obtain quantitative data

For quantitative measurements it is critical to measure/estimate Q !!

Applications

- Engines
- Gasturbines
- Furnaces/boilers

LIF set-up: 0D

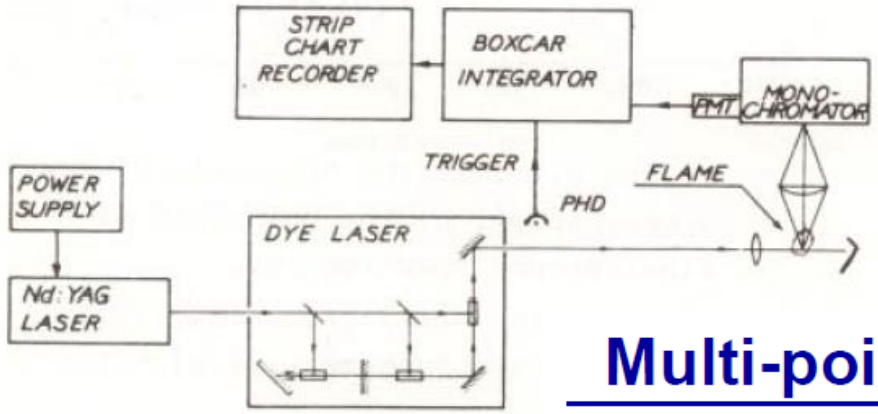

Multi-point visualization: 1D

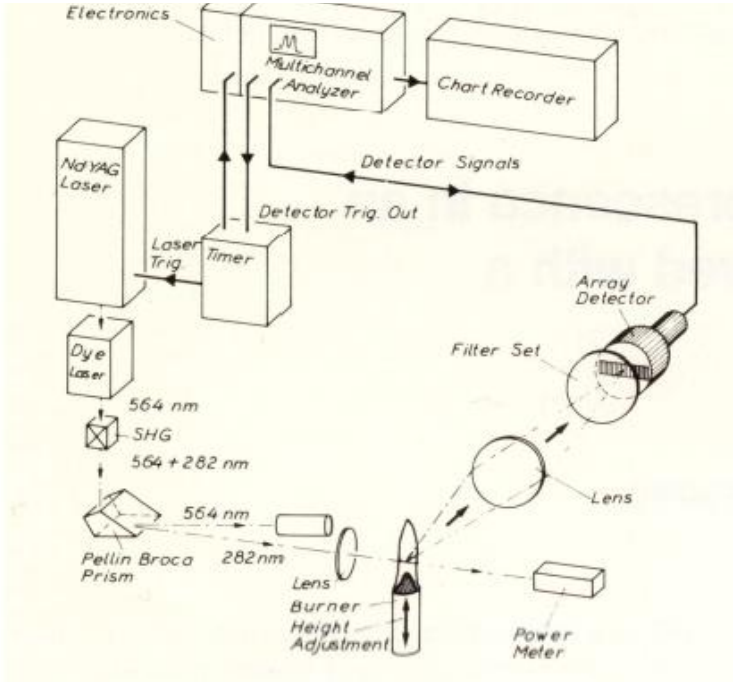

Two-dimensional measurements

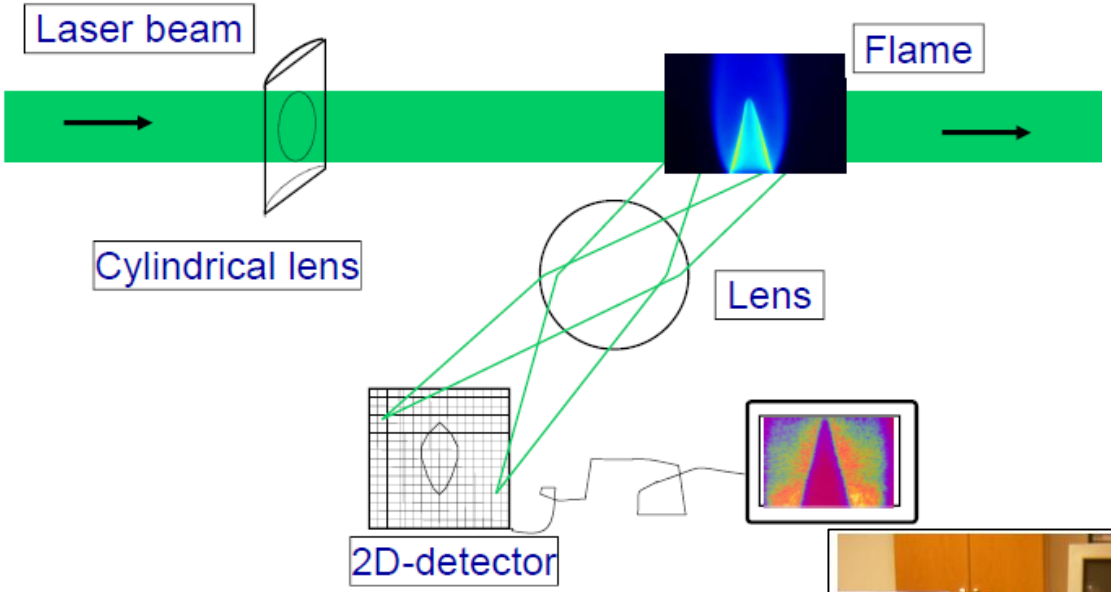

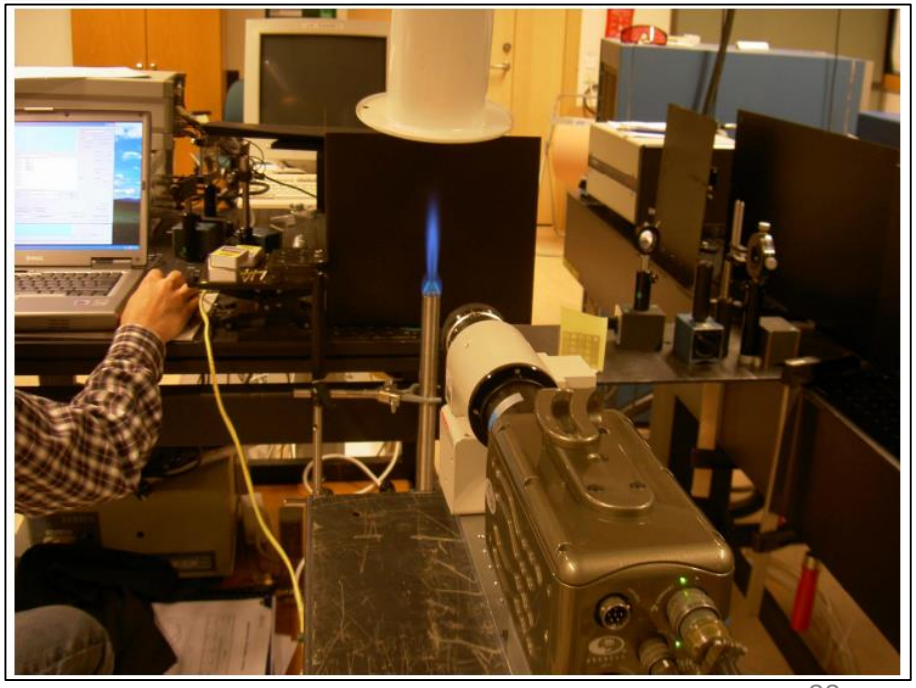

CH visualization in a turbulent flame

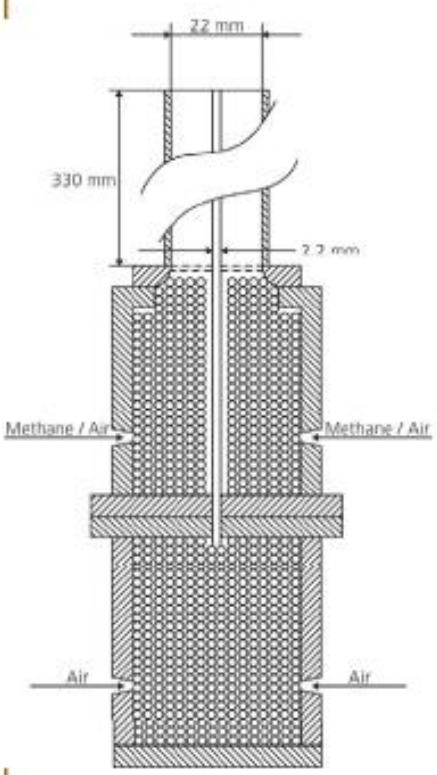

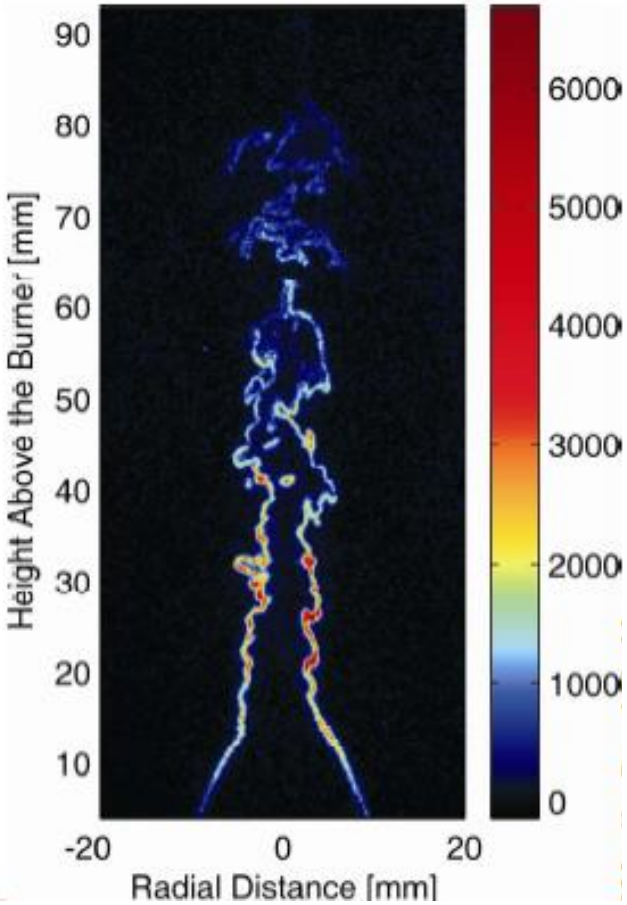

Kiefer et al, 31st Comb. Symp

Multi species visualization CH, OH

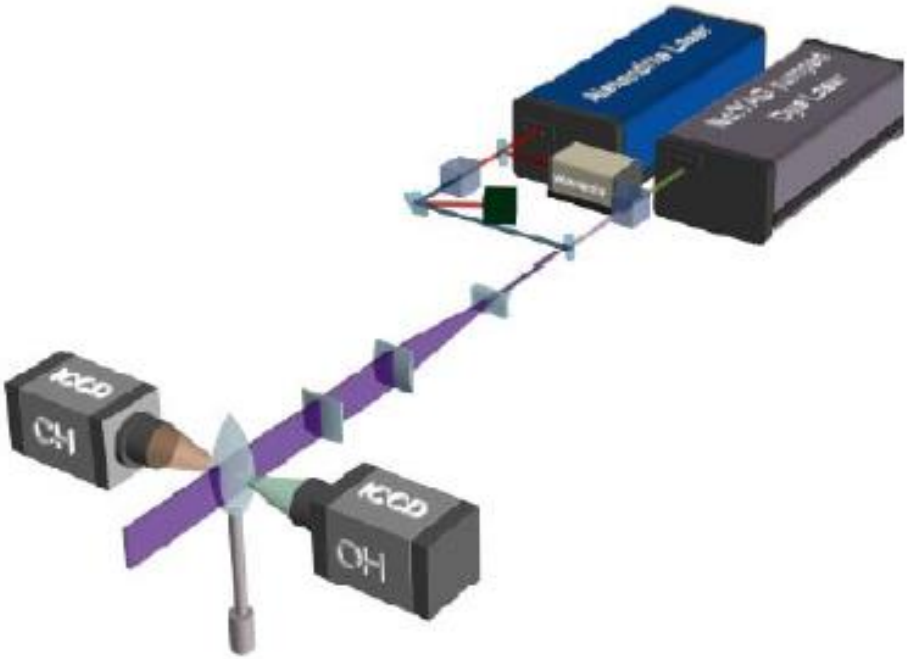

Kiefer et al, Comb.Flame 2008

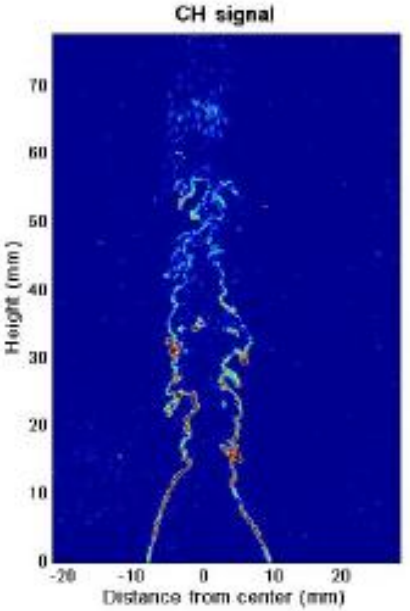

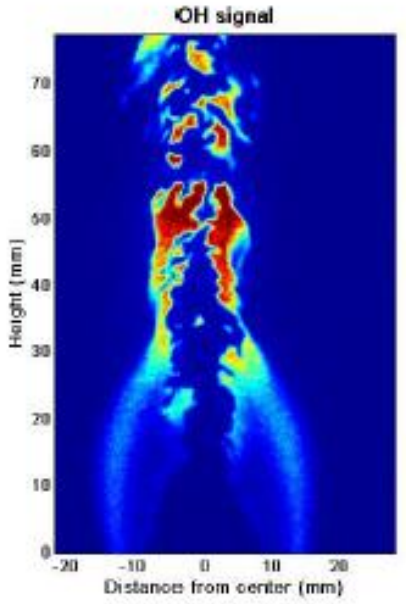

Multi-Species Measurements

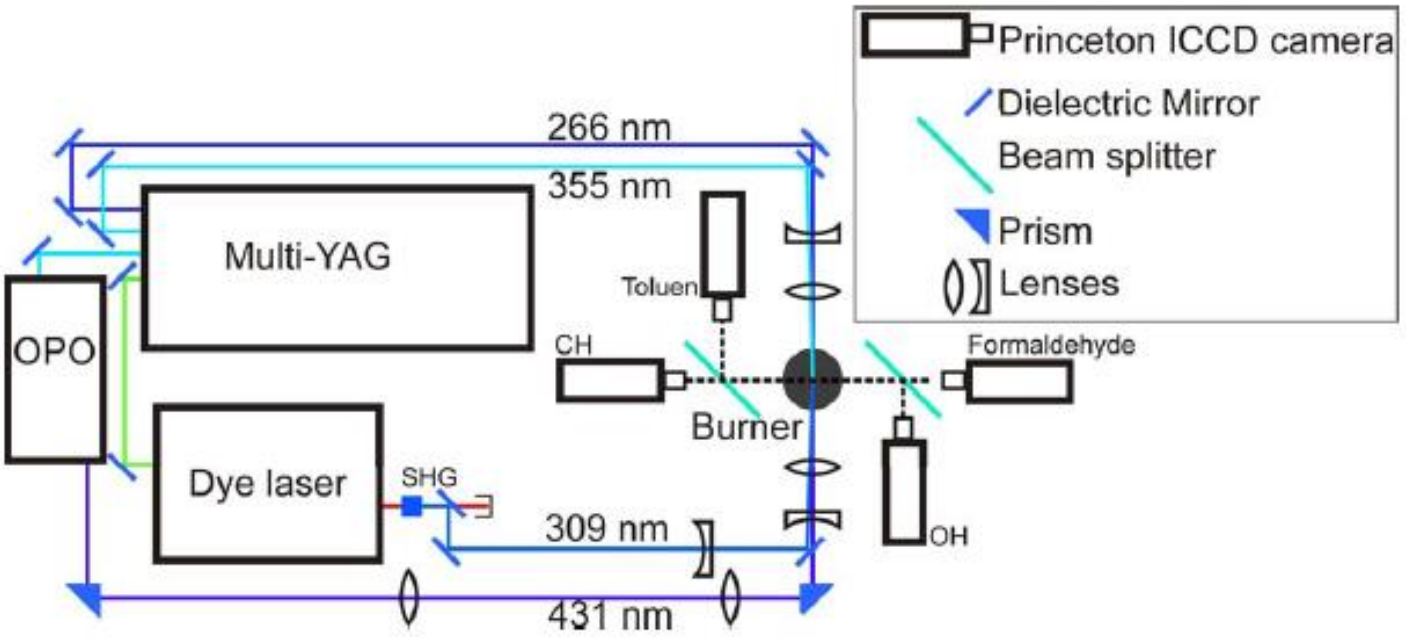

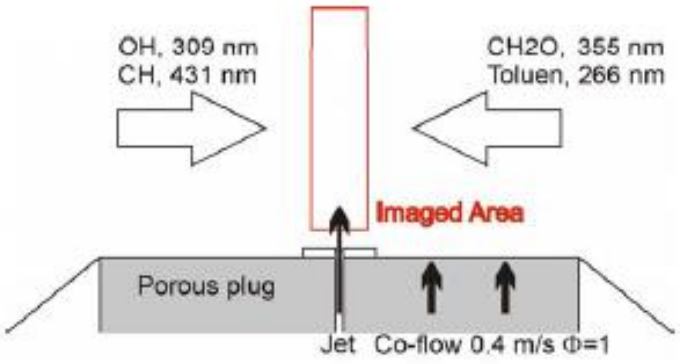

Multi-Species Measurements

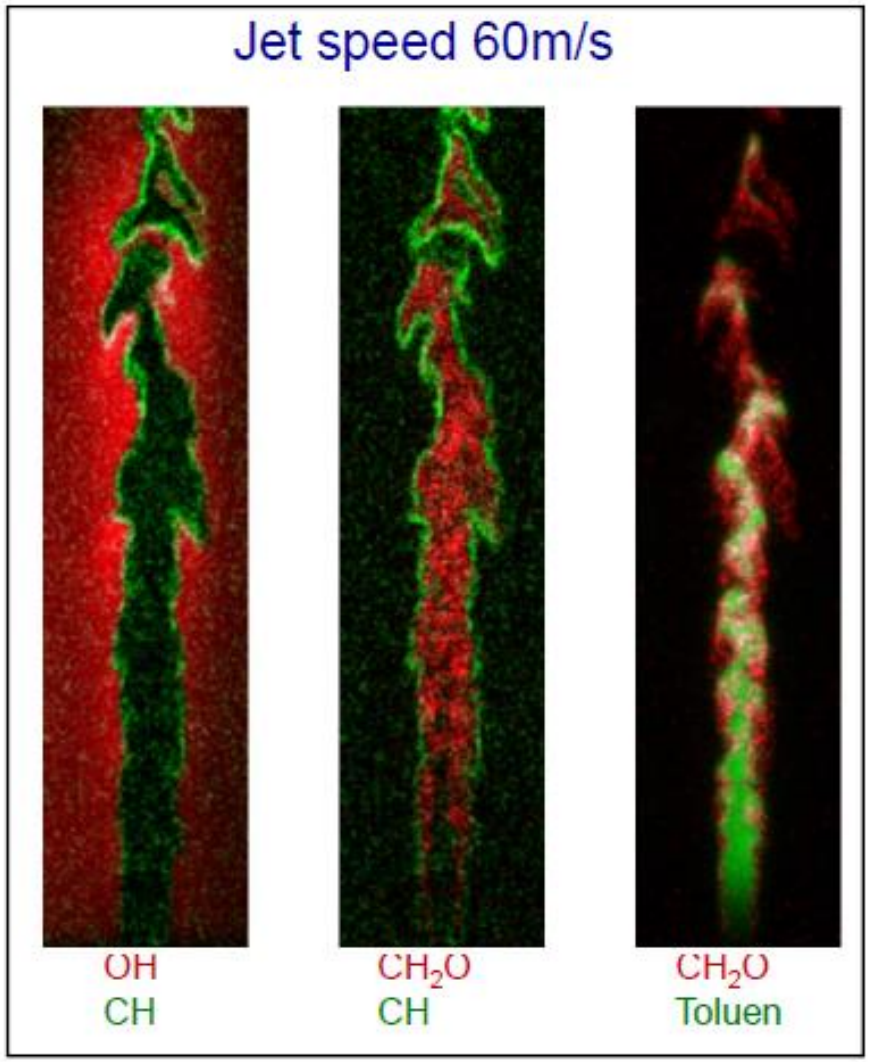

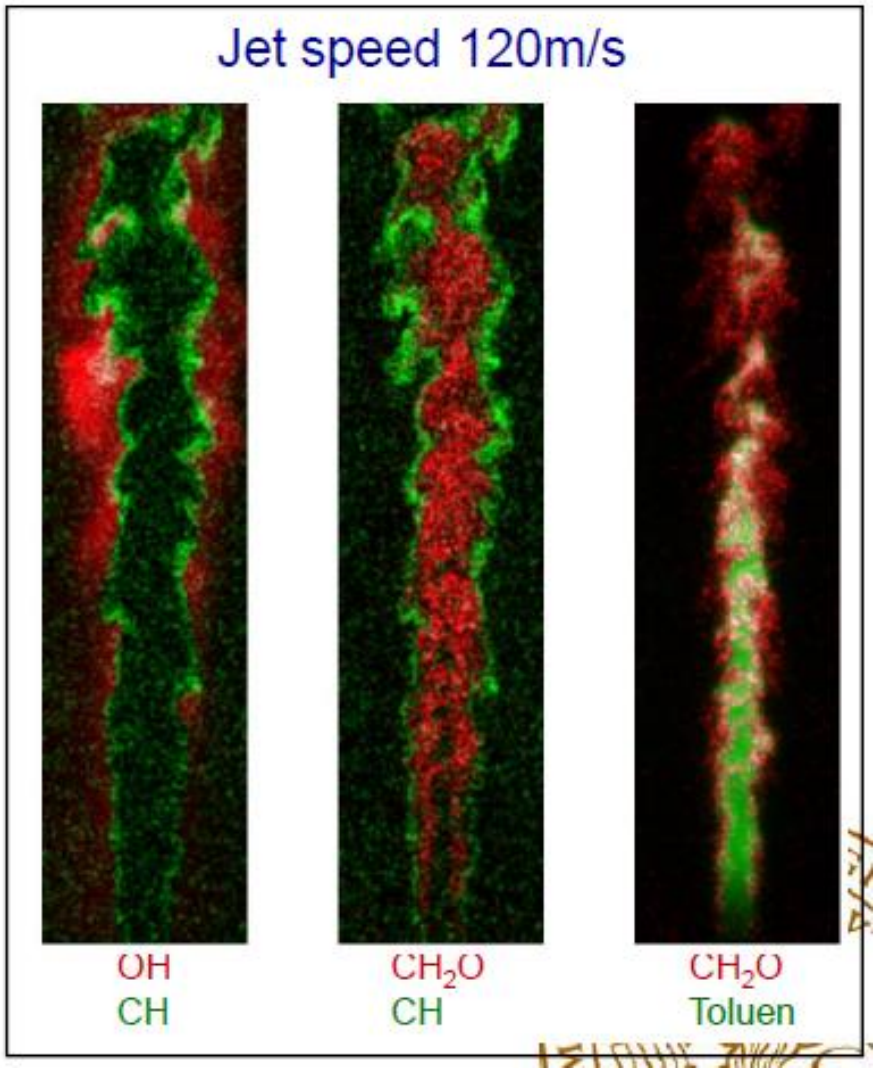

LIF to measure the temperature

LIF thermometry

- Any method that reflects the distribution of population over two or more individual vibrational rotational states can in principle be used for temperature measurement. LIF is such a method.
- LIF thermometry restricted to high temperatures if molecular radicals are employed. For OH temperatures above ~1500 K are needed.
- If atomic species, such as metal atoms, are used, these have to be seeded into the flame or flow.
- If LIF was used for concentration measurements it is definitely convenient to apply it for thermometry too.

Temperature masurements

$$n_j = \frac{(2J+1)N_{tot}Exp(-\frac{E_j}{kT})}{Q_{vib}Q_{rot}}$$

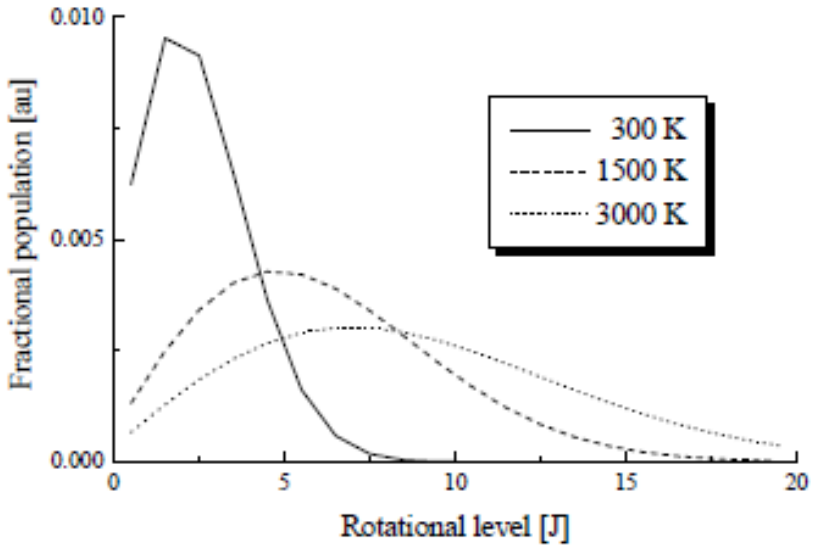

Two-line LIF thermometry

Basic idea:

To measure the relative population of two states ⇒ T from Boltzmann expression

Excitation to the same upper state ⇒ F_{21} and F_{20} are equally affected by quenching and energy transfer processes

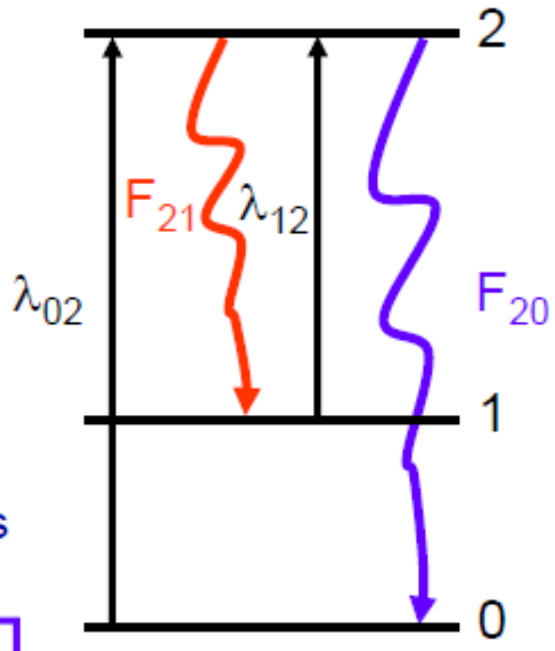

$$T = \frac{(E_1 - E_0)/k}{\ln\frac{F_{21}}{F_{20}} + \ln\frac{I_{12}}{I_{02}} + 4\ln\frac{\lambda_{21}}{\lambda_{20}} + \ln C}$$

C non-dimensional system dependent calibration constant

Summary: LIF

- Can measure 2D temperatures and species distributions
- Measure preferably atoms (O, H, N, C) and diatomic molecules (NO, OH, CH, CN, C_2, O_2, CO, H_2). Some polyatomic species (NH_3, H_2O, HCO, CH_2O)
- High sensitivity (ppm)
- Mainly used for one species detection
- Accuracy; concentration: ~10% (stationary flame, all quenching parameters known)
  ~30% (turbulent flame, no quenching corrections)
  temperature: ~2% (point measurement)
  ~8 % (2D measurement)

- Resonant excitation ⇒ Tunable laser needed
- Incoherent non-elastic scattering ⇒ Signal emitted in all directions
- Suffers from quenching, i.e. collisional deexitation ⇒ quantitative species concentration measurements not trivial
- Problem with separation of multi-atomic species, e.g. PAH's
- Outlook: Further 3D visualization, high speed imaging (>kHz), velocity visualization without molecule seeding